ISSN 0016-7029, Geochemistry International, 2006, Vol. 44, No. 11, pp. 1053–1104. © Pleiades Publishing, Inc., 2006.
Original Russian Text © E.M. Galimov, L.A. Kodina, O.V. Stepanets, G.S. Korobeinik, 2006, published in Geokhimiya, 2006, No. 11, pp. 1139–1191.

Biogeochemistry of the Russian Arctic. Kara Sea: Research Results under the SIRRO Project, 1995–2003

E. M. Galimov, L. A. Kodina, O. V. Stepanets, and G. S. Korobeinik

Vernadsky Institute of Geochemistry and Analytical Chemistry, Russian Academy of Sciences, ul. Kosygina 19, Moscow, 119311 Russia

Received April 11, 2006

Abstract—The Kara Sea is an area uniquely suitable for studying processes in the river–sea system. This is a shallow sea into which two great Siberian rivers, Yenisei and Ob, flow. From 1995 to 2003, the sea was studied by six international expeditions aboard the R/V *Akademik Boris Petrov.* This publication summarizes the results obtained, within the framework of this project, at the Vernadsky Institute of Geochemistry and Analytical Chemistry, Russian Academy of Sciences. Various hydrogeochemical parameters, concentrations and isotopic composition of organic and carbonate carbon of the sediments, plankton, particulate organic matter, hydrocarbons, and dissolved CO_2 were examined throughout the whole sea area at more than 200 sites. The $\delta^{13}C$ varies from –22 and –24‰ where Atlantic waters enter the Kara Sea and in the North-eastern part of the water area to –27‰ in the Yenisei and Ob estuaries. The value of $\delta^{13}C$ of the plankton is only weakly correlated with the $\delta^{13}C$ of the organic matter from the sediments and is lower by as much as 3–4‰. The paper presents the results obtained from a number of meridional river–sea profiles. It was determined from the relations between the isotopic compositions of plankton and particulate matter that the riverwaters carry material consisting of 70% detrital–humus matter and 30% planktonogenic material in the river part, and the material contained in the offshore waters consists of 30% terrigenous components, with the contribution of bioproducers amounting to 70%. The carbon isotopic composition of the plankton ranges from –29 to –35‰ in the riverine part, from –28 to –27‰ in the estuaries, and from –27.0 to –25% in the marine part. The relative lightness of the carbon isotopic composition of plankton in Arctic waters is explained by the temperature effect, elevated CO_2 concentrations, and long-distance CO_2 supply to the sea with riverwaters. The data obtained on the isotopic composition of CO_2 in the surface waters of the Kara Sea were used to map the distribution of $\delta^{13}C_{CO_2}$. The complex of hydrocarbon gases extracted from the waters included methane, C_2–C_5, and unsaturated $C_{2=}$–$C_{4=}$ hydrocarbons, for which variations in the concentrations in the waters were studied along river–estuary–sea profiles. The geochemistry of hydrocarbon gases in surface fresh waters is characterized by comparable concentrations of methane (0.3–5 μl/l) and heavier hydrocarbons, including unsaturated ones. Microbiological methane with $\delta^{13}C$ from –105 to –90‰ first occurs in the sediments at depths of 40–200 cm. The sediments practically everywhere display traces of methane oxidation in the form of a shift of the $\delta^{13}C$ of methane toward higher values and the occurrence of autogenic carbonate material, including ikaite, enriched in the light isotope. Ikaite ($\delta^{13}C$ from –25 to –60‰) was found and examined in several profiles. The redox conditions in the sediments varied from normal in the southern part of the sea to highly oxidized along the Novaya Zemlya Trough. Vertical sections through the sediments of the latter exemplify the complete suppression of the biochemical activity of microorganisms. Our data provide insight into the biogeochemistry of the Kara Sea and make it possible to specify the background values needed for ecological control during the future exploration operations and extraction of hydrocarbons in the Kara Sea.

DOI: 10.1134/S0016702906110012

1. INTRODUCTION

The Arctic Basin is an active link in the global circulation of matter and the processes controlling the Earth's climate. The low temperatures, predominantly oxidized conditions in the waters and surface sediments, unusual biological production, and an ice cover are unique features of Arctic seas. The Arctic Basin is particularly important for Russia. The resources of this basin, its ecological conditions, and the factors controlling its climate directly affect the economics and life conditions over the vast territory of Russia adjacent to the Arctic Basin.

The Kara Sea is of particular interest in the context of these problems. First of all, it is a unique area suitable for studying processes in the river–sea system. The Kara Sea receives a vast river runoff: the total annual runoff of the Ob, Yenisei, and some other medium-sized and small rivers amounts to 1350 km^3, which is comparable with the overall riverine runoff to all other Russian Arctic seas: Barents, White, Laptev, East Siberian, and Chukchi (close to 1420 km^3/yr). The Kara Sea is shallow: its average depth is 110 m, with 40% of the area of this sea having depths of less than 50 m. The only deep parts of the basin are troughs bordering the

sea: the Novaya Zemlya Trough (along the eastern shore of Novaya Zempla, 200 to 400 m deep), St. Anna Trough (along the eastern shore of Franz Josef Land, 620 m deep), and Voronin Trough (along the western shore of Severnaya Zemlya, 450 m deep).

Biogeochemical and radioecological investigations in the Kara Sea are also of prime interest. Russia's Arctic seas contain significant reserves of hydrocarbons. The future development of the fuel potential of the country is currently considered to be dependent on the development of hydrocarbon resources in the Arctic shelf, including that of the Kara Sea. In this context, the possibility that the ecologically delicate northern seas can be polluted with oil is potentially hazardous.

The radioecological problems of the Kara Sea are also known to be quite unusual. Novaya Zemlya was utilized as a testing ground for nuclear weapons in the 1960s. In some harbors of the Kola Peninsula are house bases of navy and civilian ships equipped with nuclear power-generating systems and the related infrastructures: storages for a diversity of nuclear wastes and spent nuclear fuel, graveyards of attrition vessels, which are to be relieved of their nuclear fuel and are awaiting further utilization. Radioactive-waste containers and shipboard nuclear reactors were dumped at the eastern shore of Novaya Zemlya. In case of accidents at large radiochemical plants within the drainage areas of the Ob and Yenisei rivers in western Siberia, the artificial radionuclides can be carried by these rivers to the sea.

Studies under the SIRRO International Project were launched at the Vernadsky Institute of Geochemistry and Analytical Chemistry, Russian Academy of Sciences, with the aim of elucidating the impact of the runoff of Siberian rivers on the biogeochemical and radioecological conditions in the Kara Sea. The six international expeditions conducted under this project aboard the R/V *Akademik Boris Petrov* were attended by Russian and German researchers on a parity basis. The pivoting investigations were conducted by scientists from the Vernadsky Institute of Geochemistry and Analytical Chemistry (GEOKhI), Russian Academy of Sciences, in Moscow, Russia, and the Alfred Wegener Institute for Polar and Marine Research (AWI) in Bremerhaven, Germany. The preliminary results published in 1996, upon the completion of the first expedition [1], provided a general idea of the biogeochemistry of the Kara Sea, including the carbon isotopic composition, and unique data on the behavior of radionuclides. Materials on other problems and aspects of this research within the scope of the project were published in the proceedings of the project [2, 3] and in separate papers [4–14].

This paper summarizes the principal results of the studies conducted at the Vernadsky Institute of Geochemistry and Analytical Chemistry, Russian Academy of Sciences, on the basis of materials collected by the 1995–2003 expeditions aboard the R/V *Akademik Boris Petrov* in the Kara Sea itself and the lower reaches of the Ob and Yenisei rivers.

2. MATERIALS AND METHODS

Figure 1 shows the location of the research sites examined in various years within the Kara Sea.

Bottom sediments were sampled with gravity corers (5 and 8 m) with plastic inserts, a box corer 50 cm high, and a multicorer equipped with twelve dismountable plastic tubes. Water samples were taken along a geological profile, using a Rozett sampler with 24 bathometers (1.7 l in volume) and a MARK-3B CTD probe for measuring water temperature and salinity. The bottom waters were collected from the tubes of the multicorer. In order to obtain large volumes of deep waters, a 200-l steel bathometer was used.

Aboard the research vessel, the physicochemical characteristics of samples from various layers were measured: their moisture, density, Eh, and pH (by Orion electrodes). Pore waters were cold-squeezed immediately after core lifting aboard, with the simultaneous use of six steel presses exerting a pressure of 1–10 kbar. The major hydrogeochemical parameters (PO_4^{3-}, NO_3^-, NO_2^-, SiO_4^{3-}, SO_4^{2-}) were analyzed by classical hydrochemical methods.

Gas samples for analysis for the molecular and isotopic carbon composition of methane were obtained from 250–500-ml[3] samples of sediments separated from the vessels with a syringe immediately after the core was lifted on board. The sediments were degassed by means of stirring in salt solution and heating to 70°C. The gas phase was collected and put into glass vessels (25–50 ml in volume), which were tightly plugged with rubber stoppers with aluminum caps to be transported to the Vernadsky Institute and then analyzed at its laboratory.

The particulate matter of water suspensions was obtained from a number of water depth levels by vacuum filtration through calcinated and weighted GF/F fiberglass filters with 0.75-μm pores. The concentrations of C_{org} in the particulate matter were determined by wet oxidation with a sulfuric acid–potassium bichromate mixture on a filter, with the subsequent coulometric determination of the CO_2 yield.

The plankton samples obtained from a surface water layer (to a depth of 10 m) with plankton nets (10 and 90 μm) were further utilized to prepare phytoplankton samples for isotopic analysis. For this purpose, zooplankton, chitin fragments, floral detritus, and other microscopically unidentifiable particles were removed from the original sample by means of filtration and selective decantation [9]. The preser-

Fig. 1. Location map of sites in the Kara Sea and the Yenisei and Ob estuaries examined during the cruises of the R/V *Akademik Boris Petrov* in 1995, 1997, 1999, 2000, 2001, and 2002.

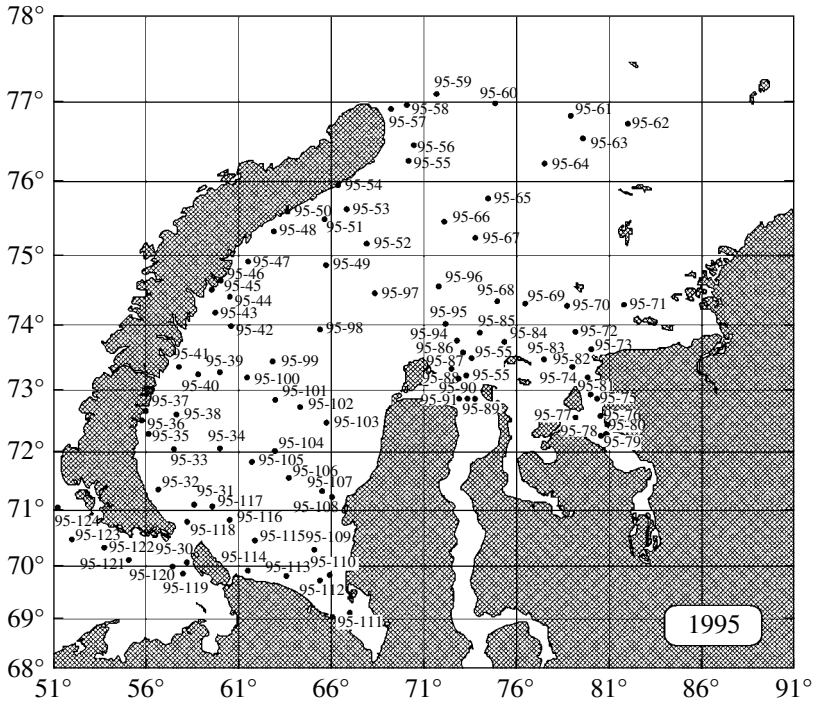
1995

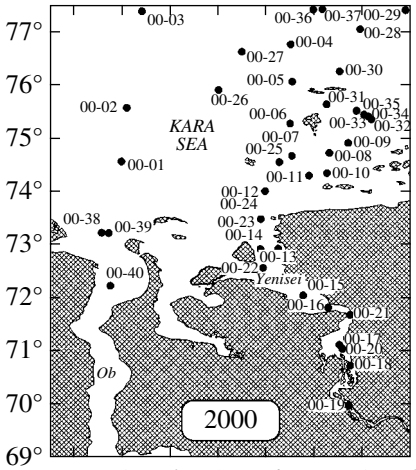
KARA SEA
Yenisei
Ob
2000

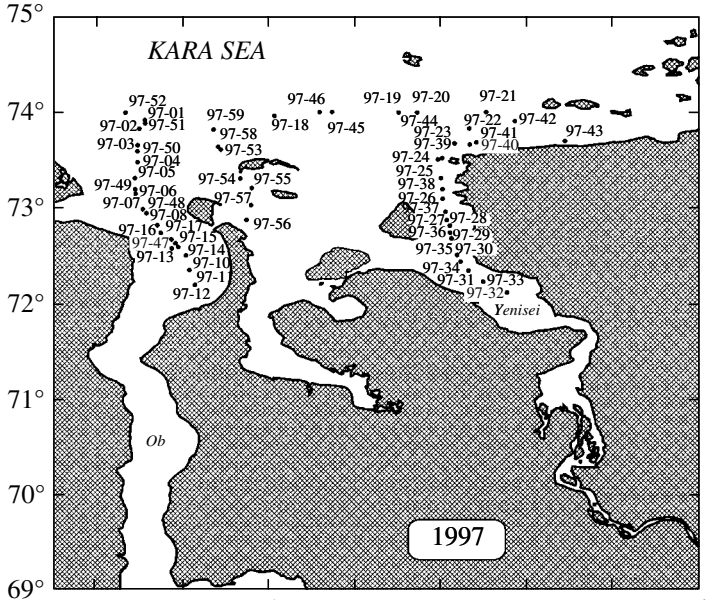
KARA SEA
Yenisei
Ob
1997

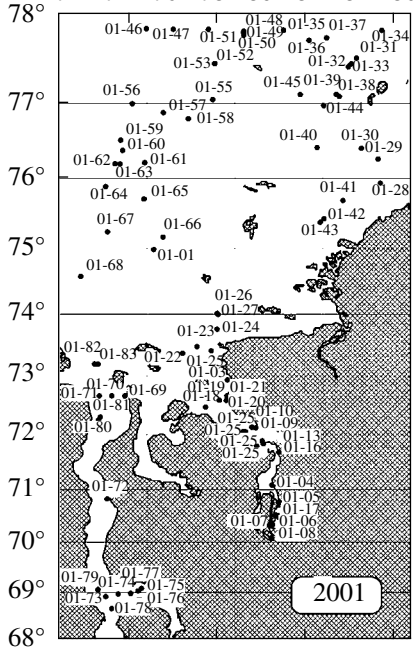
2001

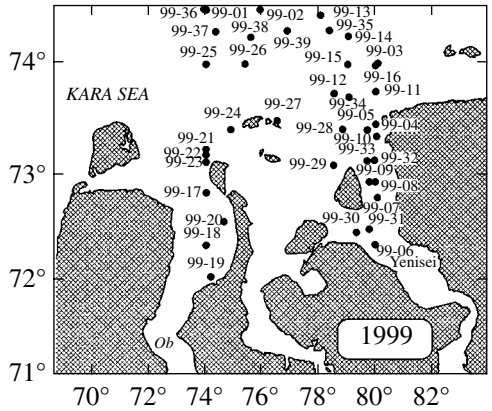
KARA SEA
Yenisei
Ob
1999

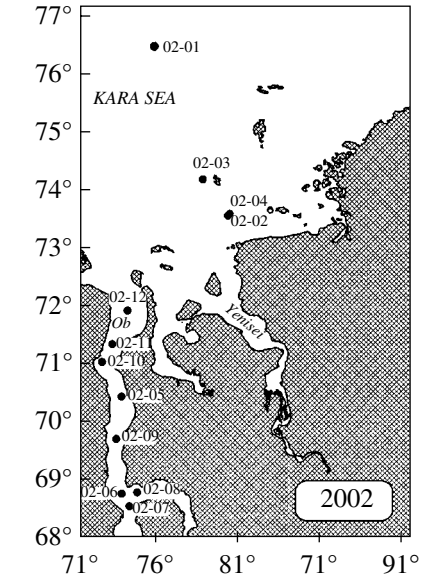
KARA SEA
Yenisei
Ob
2002

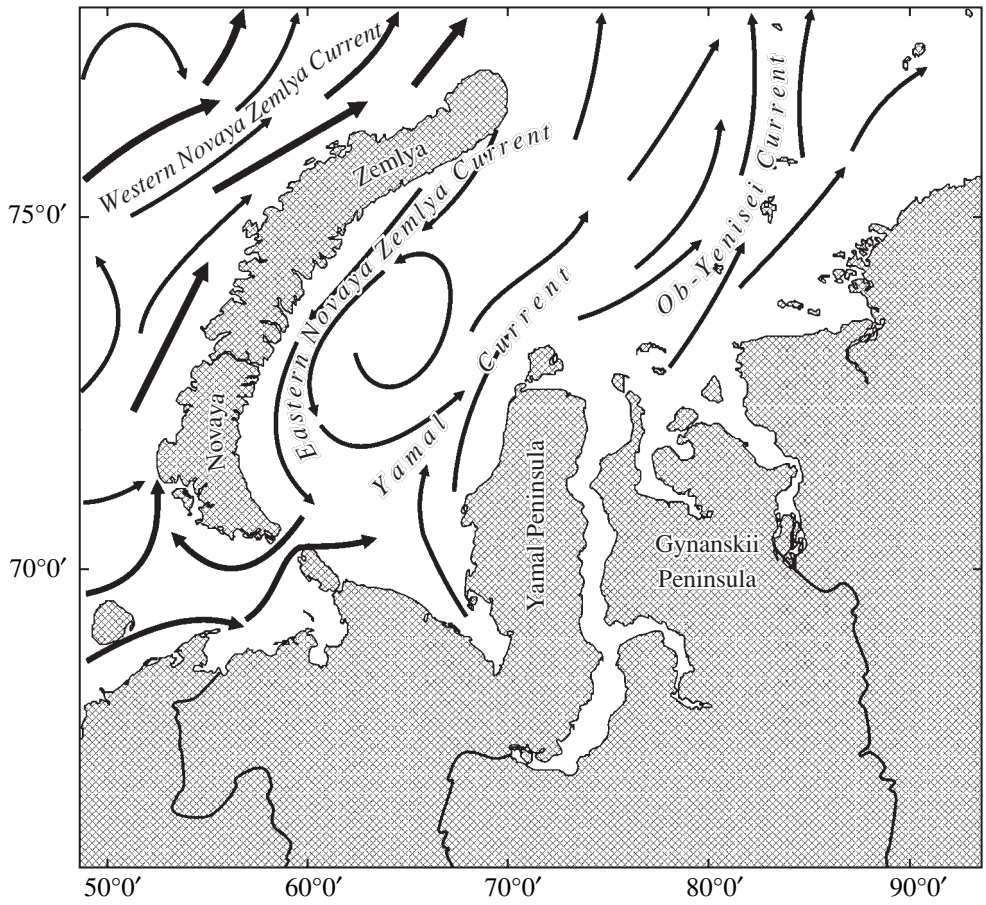

Fig. 2. Structure of currents in the Kara Sea.

vation of the species composition of the phytoplanktonic communities was monitored under a microscope.

The samples transported from the research vessel were examined at the Laboratory of Carbon Geochemistry at the Vernadsky Institute of Geochemistry and Analytical Chemistry, Russian Academy of Sciences.

The concentrations of C_{org} in sediments and the hydrogen (*HI)* and oxygen (*OI*) indices were determined on a Rock-Eval II apparatus. The C_{org} values obtained by this procedure on modern marine sediments are in good agreement with data obtained with a CHN analyzer.

The isotopic composition of organic carbon was carried out on Delta S and Delta Plus mass spectrometers. The samples of sediments were preparatorily crushed in a Reatsch HM 200 ball mill, and the carbonates were removed by treating with diluted HCl. The sample were then washed and dried at 60°C.

Phytoplankton and suspension samples were preparatorily treated with HCl vapors in an desiccator and held for a few days in air. The particulate matter and filter were pulverized in a ball mill, and the samples thus obtained and containing 0.1–0.2 mg of C_{org} were used to determine its isotopic composition on a Delta Plus CHN mass spectrometer (with an instrumental accuracy of ±0.1‰). The precision of the whole cycle, including sampling operations, was at least ±0.3‰ PDB.

The concentrations of C_1–C_5 hydrocarbon gases were determine on a chromatograph with a steel separation column (300 × 0.3 cm) filled with Al_2O_3 that was preliminarily treated by NaOH and activated at 450°C. The gas sample for isotopic analysis was introduced through the chromatographic system of the Delta Plus mass spectrometer to determine composition of methan carbon.

3. HYDROLOGY OF THE KARA SEA

The Arctic Ocean accounts for a little more than 1% of the World Ocean volume and for approximately 10% of the global river runoff [16]. Close to 35% of the freshwater of the Arctic Basin is supplied by three rivers: the Yenisei, Ob (which flow in the Kara Sea) and the Lena (which empties into the Laptev Sea). Both seas are the major freshwater and ice suppliers to the Arctic Ocean [17, 18]. The major water circulation directions of the Kara Sea are shown in Fig. 2.

Atlantic waters come to the Kara Sea in the north, from the Barents Sea, through the strait between Franz

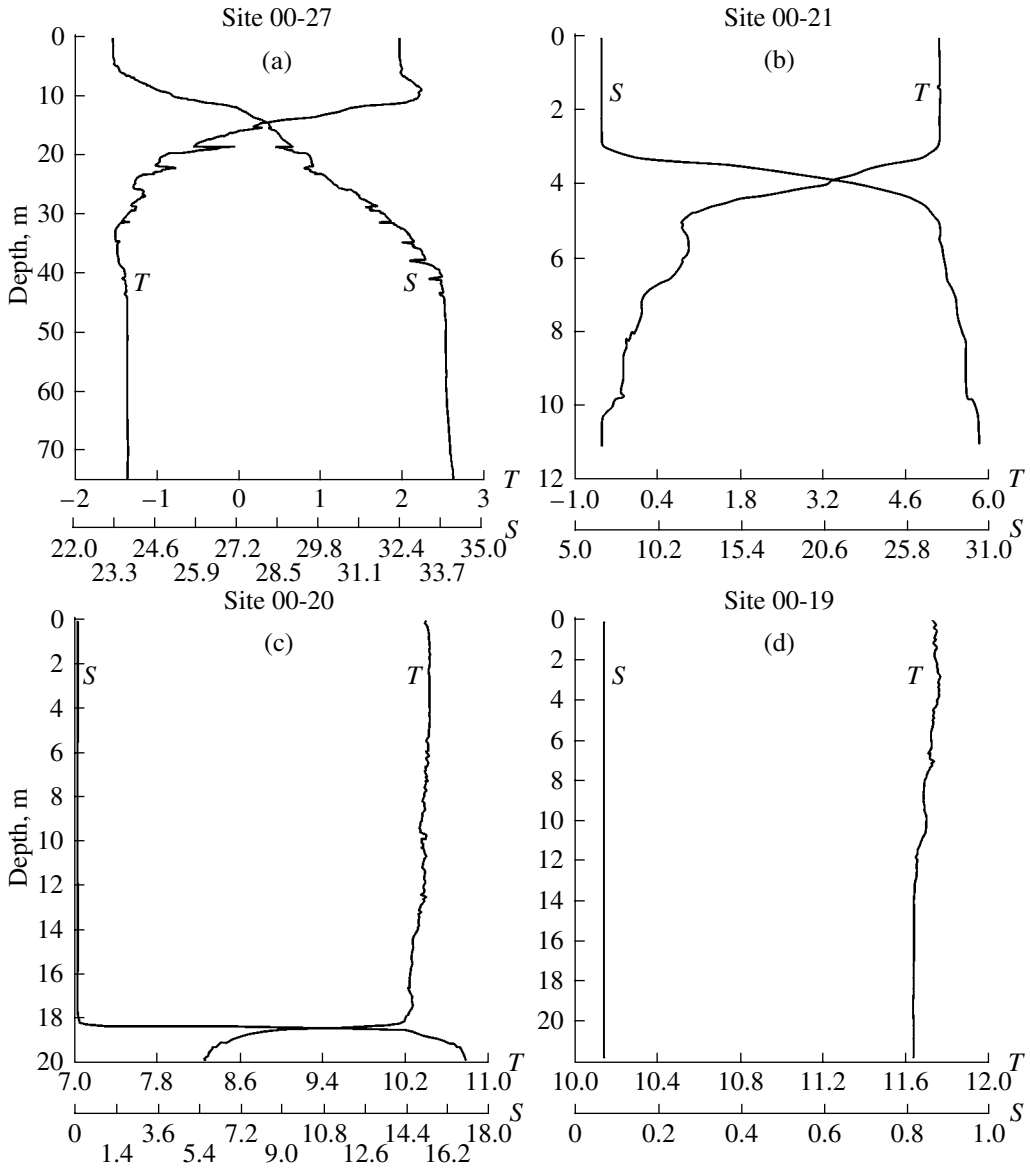

Fig. 3. Distribution of temperature (T°C) and salinity (S, g/l) in waters at sites on the Kara Sea–Yenisei River profile: (a) northern part of the Kara sea; (b) three-layer structure of the water mass in the southern part of the Kara Sea, in the Yenisei estuary mouth; (c) penetration of seawater far (up to 70° N) into the estuary; water with salinity of 18 g/l composes a near-bottom layer; (d) homogeneous freshwater mass in the far southern part of the estuary.

Josef Land and Novaya Zemlya. In the south, Atlantic waters (from the Barents Sea) extend eastward from the Kara Strait [19]. The volume of water coming through the Kara Strait is one order of magnitude greater than the total river discharge to the Kara Sea [20].

Upon arriving through the Kara Strait, Atlantic waters flow to Yamal Peninsula and form the Yamal Current, which is enhanced by the runoff-related Ob–Yenisei Current. The eastern branch of the Yamal Current turns west and, merging with the subsurface Atlantic waters in the St. Anna Trough, forms the Eastern Novaya Zemlya Current, which is directed southward, along the eastern shore of Novaya Zemlya.

Water circulation in the near-estuary area of the Kara Sea is characterized by seasonal variations due to the effect of atmospheric processes. Dominating spring and summer winds enhance northerly and northwesterly currents, whereas western and southwestern winds in wintertime activate northerly and northeasterly currents [21–23].

The interaction of fresh and warm riverwaters with cold and more saline offshore seawaters is the most intense in the estuaries (Obskaya Guba and Yenisei Bay) and in the adjacent southern part of the sea (Fig. 3). The variations in the temperature and salinity are at a maximum in the freshened water layer, whose effect is discernible over hundreds of kilometers south

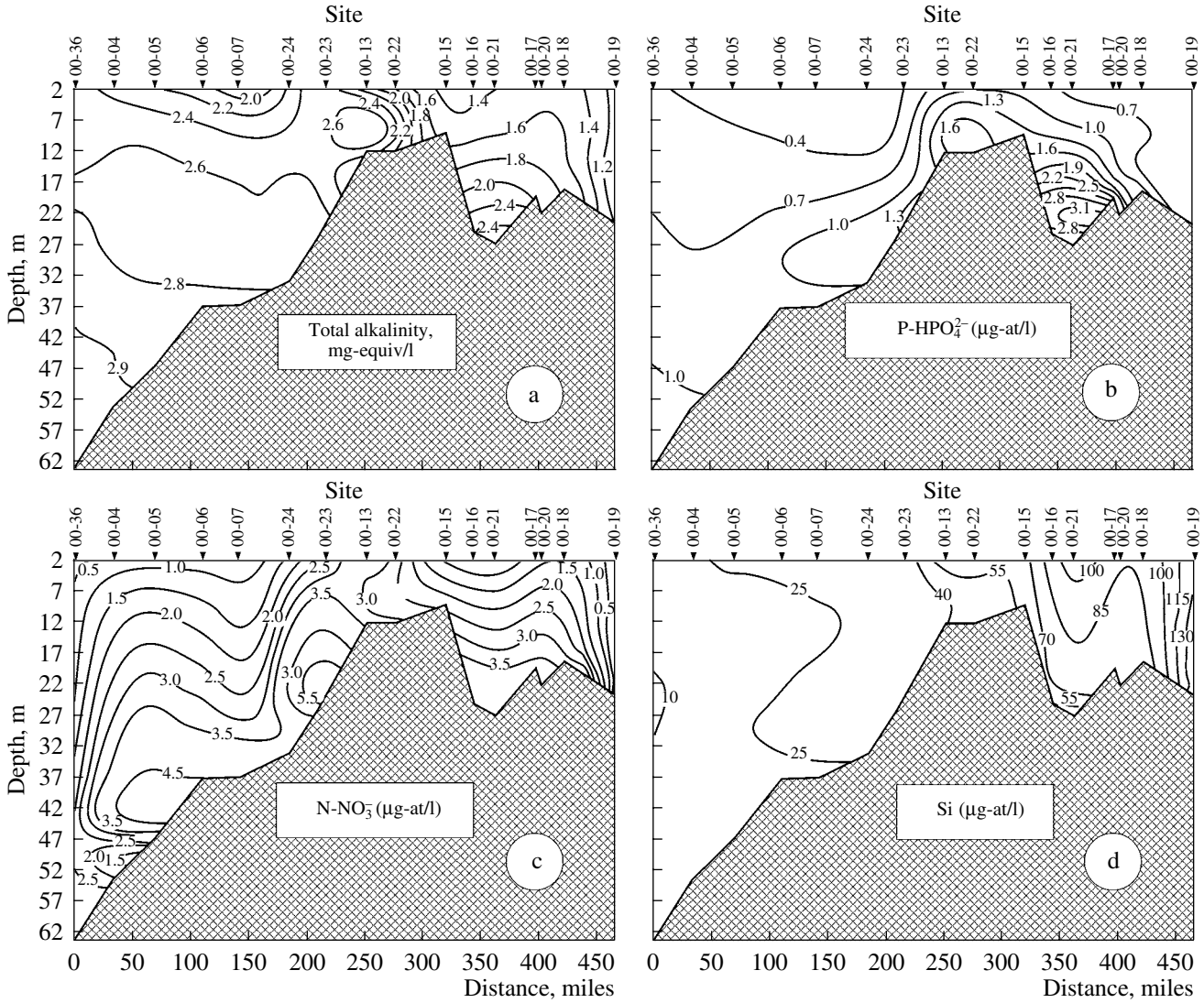

Fig. 4. Hydrochemical characteristics of waters along the Kara Sea–Yenisei estuary profile between Sites 00-36 and 00-19: (a) total alkalinity, mg-at/l; (b) phosphorus concentration; (c) nitrogen concentration; (d) silicon concentration.

of the river mouths. The significant stratification of the water masses hampers the possibility of the arrival of biogenic elements to the biologically active surface water layer.

4. HYDROCHEMISTRY

4.1. Biogenic Elements

The catchment basin area of the Kara Sea is 7.5 times greater than the area of the sea itself, while the analogous ratio for the Arctic Basin as a whole is equal to 1.5 and is 0.5 for the World Ocean. The Ob and Yenisei rivers are characterized by relatively low total concentrations of dissolved inorganic ions: 112 mg/l for the Yenisei and 126 mg/l for the Ob. The predominant ion is HCO_3^-, which accounts for 62 (Ob) and 55% (Yenisei) of the total concentrations of inorganic ions [24].

The rivers of the Arctic Basin typically contain much organic carbon (up to 1000 μg/l, in the dissolved form and as particulate matter). The soils of western Siberia, which is the catchment area of the great Siberian rivers, contain up to 60% of the organic matter concentrated in the soils of our planet [25], and organic carbon (C_{org}) in the rivers consists of 90% dissolved species.

Hydrochemical parameters were obtained along meridional profiles from the Yenisei River to the Kara Sea and from the Ob River to this sea during expeditions in 1999–2002. The longest of these profiles extends from the Yenisei to Kara Sea, from 70°04′ N to 77°53′ N, and intersects various types of water masses (Fig. 4). Data on this profile are presented in Table 1.

The concentrations of biogenic elements in the waters of Arctic rivers vary depending on weather conditions, seasonally, and from year to year. More detailed data

Table 1. Hydrochemical parameters of waters along the Yenisei River–Kara Sea profile

Site	Sea depth (m)	*T*, °C	Salinity (g/l)	Concentration (μg-at/l)					Alkalinity (mg-equiv./l)	pH	O_2	
				phosphorus		nitrogen		Si			mg/l	saturation (%)
				P_{tot}	PO_4^{-3}	NO_2^-	NO_3^-					
01–8	0	14.5	0.0	2.39	1.44	0.12	0.20	66.45	0.9	8.32	–	–
	27	14.3	0.0	2.07	1.44	0.10	0.18	63.70	0.9	8.26	–	–
01–6	0	13.7	0.0	1.23	0.60	0.8	0.12	78.40	0.9	8.36	–	–
	14		0.0	1.65	0.70	0.8	0.12	72.88	0.9	8.35	–	–
01–5	0	–	0.0	3.02	0.86	0.06	0.12	116.52	0.9	8.40	–	–
	13	13.4	0.0	6.28	1.02	0.06	0.22	115.14	0.9	8.34	–	–
01–4	0	13.8	0.0	–	0.91	0.24	0.26	121.39	0.9	8.36	–	–
	19	12.8	0.0	–	0.91	0.24	0.28	125.80	0.9	8.35	–	–
01–16	0	12.9	0.0	1.23	0.65	0.06	0.12	93.09	0.9	8.24	10.14	97.6
	27.8	13.8	0.0	1.44	0.49	0.06	0.08	95.30	0.9	8.24	10.02	95.1
01–14	0	12.8	0.0	1.76	1.55	0.12	0.16	76.56	0.9	8.13	10.25	97.2
	18	12.7	0.0	2.28	1.65	0.12	0.16	94.20	0.9	8.27	9.96	95.4
01–11	0	12.9	0.0	3.75	1.55	0.22	0.24	124.33	0.9	8.14	–	–
	7	11.6	0.5	3.65	1.76	0.30	0.76	99.34	0.9	8.10	–	–
	8.3	7.8	16.4	–	–	0.34	0.60	80.23	1.5	7.53	–	–
01–19	0	9.55	4.1	1.55	0.70	–	–	43.49	1.0	8.20	11.25	99.8
	5	0.5	28.1	1.44	0.70	–	–	20.71	2.2	8.13	11.74	90.2
	23	–1.14	32.5	1.55	1.34	–	–	26.59	2.4	8.03	9.53	68.7
01–23	0	10.15	4.8	2.18	1.34	0.30	0.34	77.00	0.9	8.28	11.14	101.3
	5	9.3	11.7	1.97	1.12	0.30	0.34	34.67	1.2	8.18	11.56	99.8
	8	4.1	28.9	2.39	1.55	0.38	0.76	25.26	2.1	8.08	11.06	83.0
	18	2.2	32.9	3.75	1.55	0.32	0.64	32.32	2.2	8.16	9.73	68.5
01–26	0	7.9	12.3	0.91	0.70	–	–	25.58	1.2	8.33	17.75	110.1
	5.5	5.13	17.5	0.6	0.44	–	–	18.23	1.4	8.31	12.70	102.3
	29	–1.2	33.2	1.76	1.60	–	–	27.87	2.2	8.23	11.07	80.1
01–43	0	5.4	20.5	0.18	0.13	0.04	0.14	5.60	1.9	8.40	12.64	100.1
	10	2.1	24.5	0.34	0.02	0.04	0.14	4.22	2.0	8.44	13.18	102.4
	40	–1.2	33.4	0.7	0.55	0.04	0.28	6.74	2.4	8.34	11.84	83.0

Table 1. (Contd.)

Site	Sea depth (m)	$T°$, C	Salinity (g/l)	Concentration (μg-at/l)					Alkalinity (mg-equiv./l)	pH	O_2	
				phosphorus		nitrogen		Si			mg/l	saturation (%)
				P_{tot}	PO_4^{-3}	NO_2^-	NO_3^-					
0.1–41	0	2.5	23.4	0.23	0.07	0.04	0.08	7.89	1.6	8.40	12.64	100.1
	10	0.2	26.3	0.18	0.07	0.04	0.08	5.83	1.8	8.44	13.18	102.4
	40	–1.1	33.6	0.7	0.60	0.04	0.34	10.65	2.4	8.34	11.84	83.0
01–28	0	2.5	22.6	0.6	0.39	0.28	0.32	9.73	1.8	8.43	13.36	102.5
	17	0.8	30.4	0.91	0.70	0.30	0.40	7.66	2.2	8.38	12.99	89.1
	50	–1.1	33.7	1.34	1.12	0.40	0.62	13.63	2.3	8.39	11.96	82.5
01–30	0	2.5	27.3	0.39	0.28	0.28	0.32	5.83	2.0	8.48	14.80	104.3
	12	–0.8	30.2	1.12	0.07	0.28	0.32	2.38	2.2	8.60	15.61	105.7
	46	–1.3	33.8	1.55	1.23	0.32	0.62	12.26	2.4	8.40	12.33	84.0
01–38	0	2.7	28.9	0.07	0	0.04	0.08	2.15	2.3	8.52	13.36	100.2
	14	2.0	29.7	0.07	0	0.04	0.08	3.99	2.3	8.51	13.36	100.6
	100	–1.4	34.1	0.49	0.28	0.04	0.42	6.28	2.4	8.36	13.31	89.0
01–45	0	3.3	28.7	0	0	0.08	0.14	6.28	2.2	8.46	13.20	100.9
	18	0.8	18.0	0.13	0.07	0.12	0.16	3.53	2.3	8.47	13.93	101.3
	80	–1.4	33.8	0.34	0.28	0.16	0.36	9.04	2.4	8.36	11.32	80.0
01–31	0	2.0	29.1	0.55	0	–	–	2.15	2.2	8.49	13.67	109.5
	15	0.6	30.2	0.65	0.02	–	–	2.15	2.2	8.58	14.19	105.3
	92	–1.4	33.8	1.55	0.70	–	–	8.58	2.3	8.38	9.50	103.1
01–34	0	1.3	29.1	0.07	0	0.04	0.10	4.91	2.1	8.46	14.12	101.6
	19	–0.5	31.5	0.07	0.02	0.04	0.30	2.15	2.2	8.54	14.68	102.3
	90	–1.4	34.2	0.7	0.60	0.04	0.48	4.45	2.4	8.45	13.47	90.6
01–35	0	3.2	28.4	0.18	0.13	0.12	0.32	5.37	2.1	8.53	13.43	101.6
	17	–0.4	31.7	0.18	0	0.12	0.32	3.07	2.2	8.67	14.92	103.0
	150	–1.4	34.3	0.91	0.65	0.28	0.52	7.20	2.4	8.50	13.61	92.5
01–48	0	3.6	26.1	0.28	0.13	0.16	0.20	15.47	2.1	8.56	12.85	99.8
	15	1.9	32.0	0	0	0.04	0.08	2.61	2.1	8.64	13.37	98.7
	187	–1.4	34.5	0.49	0.39	0.16	0.40	12.72	2.4	8.50	12.57	86.7

obtained on the other profiles in different years were published in the reports of the expeditions [3].

The comparison of the concentrations of major biogenic elements in the riverine and marine parts of the long meridional profiles of both rivers indicate that the runoff of these rivers is the source of phosphorus, nitrogen, and silicon for the Kara Sea basin. Table 2 presents averaged values for the concentrations of biogenic elements along the zone of a meridional river–mixing zone–sea profile.

The maximum concentrations of phosphorus (phosphates), nitrogen (nitrates plus nitrites), and silicon were detected in the riverine and estuarine portions of the meridional profiles. The average concentrations of N (NO_3^-) in Yenisei waters are 1 μg-at/l, the analogous value for P (PO_4^{3-}) is 0.3 μg-at/l, and the Si concentrations in the Kara Sea are much higher than the concentrations of other biogenic elements.

The source of Si in riverwaters is the weathering products of rocks and the leaching products of soils. The waters of the Yenisei, which drain mountainous areas in its upper reaches, possess high Si contents, with the weathering products of silicate rocks accounting for approximately 20% of the sum of inorganic components dissolved in the Yenise waters. The concentrations of dissolved Si in the southern riverine site at the Yenisei (Site 00-19) are 125–128 μg-at/l.

The Ob River flows mostly through the lowland areas of western Siberia. The Si concentrations in the riverwaters of the Ob estuary south of the Taz Bay were in 2001 equal to 98 μg-at/l. The right-hand tributaries of the Ob (Taz, Pur, and others) that flow into Taz Bay (an arm of the Ob estuary) drain a lowland boggy territory. Surface water samples were taken in 2001 within Taz Bay (Sites 01-73, 74, 75, 76, and 77) and in the central portion of the Ob current, upstream (Site 01-78) and downstream (Sites 01-79 and 01-72) from Taz Bay down the Ob (Fig. 5). As could be expected, the Si concentration in Taz Bay itself is low: from 12.2 to 4.9 μg-at/l. The marine part of the Ob profile, north of 75° N (starting at Site 01-67) contains Si concentrations gradually decreasing to 19.8 μg-at/l near 78° N. The most probable reason for this tendency is the development of diatomic phytoplankton.

Table 2. Average concentrations (μg-at/l) of biogenic elements and alkalinity (mg-equiv./l) along meridional river–sea profiles (September 2001, R/V *Akademik Boris Petrov*)

Element	River	Mixing zone	Sea
Yenisei River–Kara sea			
Si (SiO_4^{3-})	93.1	81.6	8.5
P (PO_4^{3-})	1.0	1.2	0.2
N ($NO_3^- + NO_2^-$)	0.3	0.5	0.3
Alkalinity	0.9	0.9	1.9
Ob River–Kara Sea			
Si (SiO_4^{3-})	35.5	33.6	4.2
P (PO_4^{3-})	1.7	0.8	0.03
N ($NO_3^- + NO_2^-$)	0.4	0.4	0.2
Alkalinity	0.4	1.0	1.6

4.2. Dissolved Oxygen and pH

The concentrations of dissolved oxygen and pH of waters are sensitive indicators of biogeochemical processes.

As can be seen from the data in Table 1, riverwaters (including the waters of the estuaries, and particularly, bottom and intermediate-depth waters) are undersaturated with oxygen, whereas the marine waters, which are colder and saline in the northern portion of the sea, were oversaturated with this element already in early September. The maximum oxygen concentration (equal to 17.75 mg/l) in the upper water layer and degree of saturation (equal to 110.1%) were detected at the southern boundary of seawaters (Site 01-23, Yenisei profile), where a marine community of microalgae developed in the transparent water with abundant biogenes.

The maximum saturation of water with oxygen (16.42 mg/l, 116%) was detected within the pycnocline at northernmost Site 01-46, largely owing to the free water exchange with the Arctic Basin, the possible inflow of Arctic waters, and the occurrence of thin ice fields in the northeastern part of our study area.

Simultaneously with the increase in the oxygen concentration, the pH of the upper water layer also increased along the Yenisei–sea profile, from 8.14 within the river (71°49′ N) to 8.56 in the north (77°54′N), and along the Ob Sea profile, from 7.65 (68°40′ N) to 8.49 (77°55′N).

The riverwaters differ from seawaters in having lower pH and alkalinity because of the generation of low-molecular acids during the bacterial destruction of organic matter in the waters and the supply of dissolved and colloid humus acids from soils and bogs in the catchment basin (Western Siberian Lowland) that is drained by the Ob and its tributaries. Humus acids account for 60–75% of the organic matter dissolved in the riverwaters of the Ob and Yenisei [19].

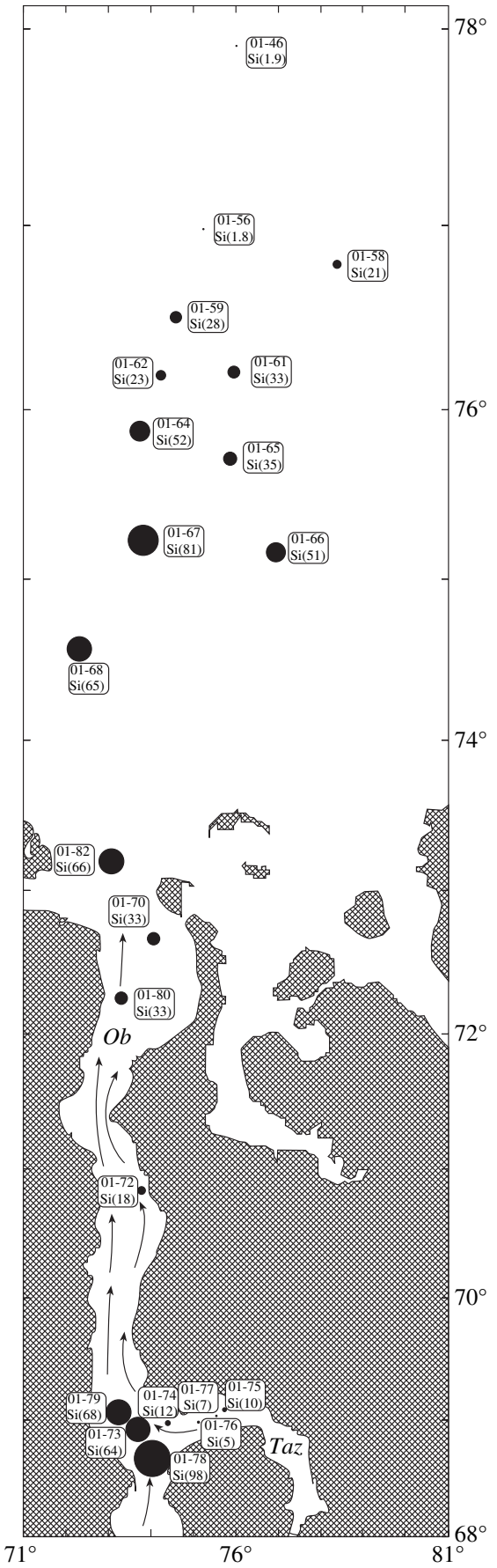

Fig. 5. Concentration of Si in the waters of the Obs Taz Gulf.

The oxygen contained in the waters is consumed by the bacterial decomposition of the organic matter, which is contained in both dissolved and particulate modes in the waters. This process operates mostly where particulate matter and phytoplankton are concentrated within the pycnocline throughout the whole lengths of the meridional profiles and is particularly active in fresh riverwaters at high temperatures. The particulate matter is retained within the region with a density gradient, and plankton migrates there under conditions optimal for photosynthesis. This plankton supplies a substrate for bacterial activity [20]. The oxidative destruction of organic matter, including its proteins and lipid components, is pronounced the most clearly in the aquatic environments along profiles from the estuaries to the northern parts of the sea, where terrigenous organic matter plays a subordinate part, and the bulk of the particulate matter is produced by phytoplankton [26].

4.3. CO_2 –Bicarbonate

The carbon isotopic composition of the dissolved bicarbonates was examined in a vertical cross section through the water mass within the Kara Sea and the Ob and Yenisei estuaries; the data are summarized in Table 3. The riverwaters contain CO_2 depleted in the ^{13}C isotope, and thus, the isotopic composition of bicarbonate from the surface seawaters is an indicator of the distance for which the riverwaters are transported through the sea. Moreover, the carbon isotopic composition of CO_2 contained in the surface layer determines the isotopic complex of the marine plankton.

The area with isotopically light CO_2 is clearly seen in Fig. 6.

It can be seen in Fig. 7 that the isotopic composition of CO_2 in the surface layer of the seawater is correlated with that of CO_2 in the deep seawater, with the latter being isotopically heavier by 3‰ (on average) than the surface bicarbonate.

5. BIOPRODUCTIVITY. ISOTOPIC COMPOSITION OF PHYTOPLANKTON

The primary biological productivity of the Kara Sea is, in recalculation to carbon, 7–10 g/m^2 per year [27, 28], and the analogous values for Obskaya Guba and Yenisei Bay are 3–8 and 13–43 g/m^2 per year, respectively [29]. The ice biota has an annual productivity of 10 g/m^2 [30]. The Central Arctic Basin, whose waters were thought until recently to be lifeless, have an overall productivity of phytoplankton, ice flora, and extracell objects of 1–15 g/m^2 per year. More than half of the production falls to the ice flora [31, 32]. In the open sea

Table 3. Isotopic composition of CO_2 (bicarbonate) dissolved in the water of the Kara Sea (R/V *Akademik Boris Petrov*, years 1995, 1997, 1999, 2000, and 2001)

Site	Latitude N	Longitude E	Depth of sea, m	Depth of sampling	$\delta^{13}C$, ‰ PDB
Sites examined in 1995					
95–34	72°04′	59°58′	110	5	–3.13
				55	–5.44
				250	–
95–36	72°32′	55°47′	66	20	–1.34
				80	–1.55
95–39	73°17′	59°58′	333	10	–1.00
				30	–1.89
				200	–1.68
95–52	75°10′	67°54′	191	5	–3.24
				30	–1.53
				150	–2.03
				186	–1.05
95–63	76°35′	72°35′	59	0	–1.05
				5	–4.34
				45	–2.63
95–75	72° 53′	80°20′	13	5	–8.75
				13	–8.77
95–88	73°11′	72°52′	26	3	–5.95
				25	–9.17
Sites examined in 1997					
97–39	73°32′	79°55′	40	0	–6.01
				12	–5.35
				35	–2.40
97–27	72°53′	80°05′	19	0	–7.58
				8	–6.51
				17	–3.55
97–21	74°00′	81°00′	41	0	–6.21
				10	–4.51
				35	–2.93
97–32	72°05′	81°29′	10	0	–8.31
				5	–7.31
				8	–3.22
97–30	72°30′	80°20′	14	0	–8.16
				5	–8.65
				12	–5.45
Sites examined in 1999					
Ob profile, 1999					
99–01	74°30′	74° 00′	30.1	1.5	–8.19
				24	–5.23
99–36	74°30′	74°00′	30.5	3	–6.28
				28.5	–3.24
99–25	74°00′	74°00′	25	2	–7.16
				9	–6.92
				15	–5.62
				24	–4.37

Site	Latitude, N	Longitude, E	Depth of sea, m	Depth of sampling	$\delta^{13}C$, ‰ PDB
Sites examined in 1999					
Ob profile, 1999					
99–21	73°15′	74°02′	16	5	–6.04
				10	–8.49
				15	–5.74
99–17	72°51′	76°56′	19	0	–11.70
				7	–6.54
				18	–6.14
99–20	72°30′	74°44′	16	3	–11.95
				11.5	–5.57
				15	–5.48
99–18	72°20′	74°00′	13	0	–11.95
				8.7	–12.46
				12	–6.16
99–19	72°11′	74°11′	14	3	–8.38
				10	–8.78
				12	–8.21
99–24	73°26′	74°52′	20	3	–7.63
				12	–7.53
				19	–4.42
Yenisei profile, 1999					
99–6	72°17′	80°02′	7	3	–11.87
99–30	72° 8′	79°18′	13	0	–8.96
99–8	72°56′	79°59′	17	0	–9.90
				12	–7.97
				15	–12.39
99–32	73°08′	79°57′	27.5	2	–8.39
				16	–6.48
				26	–3.28
99–4	73°25′	79°41′	27	0	–10.04
				12	–9.55
				18	–5.66
				27	–4.71
99–11	73°47′	79°59′	40.6	0	–8.51
				7	–7.74
				12	–6.21
				36	–4.01
99–3	74°00′	80°01′	30	0	–11.88
				8	–9.04
				27	–6.93
99–15	74°00′	79°00′	30	3	–7.19
				8	–6.81
				27	–4.05
99–13	74°30′	78°00′	35	2	–6.33
				7	–7.63
				15	–5.87
				32	–4.46

Table 3. (Contd.)

Site	Latitude N, deg	Longitude E, deg	Depth of sea, m	Depth of sampling	$\delta^{13}C$, ‰ PDB	Site	Latitude N, deg	Longitude E, deg	Depth of sea, m	Depth of sampling	$\delta^{13}C$, ‰ PDB
Sites examined in 2000						*Sites examined in 2000*					
00–16	71° 50′	82° 37′	25	0	–13.97	00–25(ice)	74° 30′	80° 32′	59	0	–6.44
				15.5	–10.73	00–26	75° 43′	77° 58′	65	0	–5.66
				23	–10.40					17	–4.33
00–13	72° 56′	80° 33′	11	0	–5.42					63	–4.51
				14.54	–6.85	00–36	76° 58′	81° 58′	66	0	–5.30
				10.185	–3.20					14	–5.25
00–19	70° 00′	83° 27′	22	0	–12.71					17	–4.90
				22	–11.97					63	–4.22
00–17	71° 6′	83° 5′	18	0	–14.80	00–23	73° 29′	79° 51′	33	0	–3.98
				22	–10.79					12	–4.74
00–20	71° 2′	83° 12′	20	0	–13.32					31	–6.07
				17	–12.80	00–15	72° 05′	81° 36′	10	0	–9.74
00–21	71° 41′	83° 29′	20	0	–8.65					7	–8.53
				12	–7.20	00–07	74° 39′	82° 39′	38	0	–5.14
				25	–8.44					12	–4.53
00–08	74° 40′	82° 38′	41	0	–8.53					35	–4.68
				9.5	–7.70	*Sites examined in 2001*					
				39	–5.10	Yenisei profile					
00–09	74° 50′	83° 26′	44	0	–7.75	01–04	71° 05′	83° 06′	22	0	–9.14
				9	–8.65	01–08	70° 04′	83° 04′	28	0	–10.15
				39	–5.56	01–11	72° 02′	81° 42′	9	0	–9.95
00–02	75° 24′	74° 12′	49.6	0	–4.72	01–19	72° 36′	80° 06′	25	0	–4.23
				12	–4.50	01–23	73° 29′	78° 51′	21	0	–7.92
				44	–6.32	01–26	74° 00′	80° 01′	34	0	–3.75
00–03	76° 56′	74° 47′	199	0	–6.33	01–43	75° 23′	85° 50′	46	0	–3.51
00–04	76° 25′	81° 00′	58	0	–4.62	01–28	75° 56′	89° 16′	55	0	–1.51
				12	–5.98	01–45	77° 07′	84° 44′	87	0	–1.25
				50	–4.74	01–31	77° 34′	87° 55′	97	0	–0.88
00–05	75° 50′	81° 00′	50	0	–3.57	01–34	77° 54′	89° 20′	100	0	–0.99
				12	–4.46	01–37	77° 49′	86° 12′	135	0	–2.24
				bottom	–5.82	01–48	77° 53′	81° 30′	192	0	–1.41
00–27	76° 18′	78° 56′	78	0	–6.38	Ob profile					
				12	–4.31	01–46	75° 55′	75° 57′	314	0	–1.58
				74	–6.36	01–51	77° 55′	79° 29′	155	0	–2.20
00–30	75° 59′	83° 02′	52	0	–5.52	01–56	77° 00′	75° 11′	179	0	–2.76
				26	–6.21	01–58	76° 48′	78° 21′	92	0	–2.06
				51	–5.49	01–61	76° 12′	75° 45′	80	0	–2.02
				46		01–67	75° 15′	73° 46′	49	0	–3.63
00–35	75° 21′	83° 48′	46	0	–2.83	01–68	74° 35′	72° 15′	31	0	–4.76
				14	–4.81	01–82	73° 12′	73° 02′	28	0	–3.83
				46	–4.31	01–70	72° 40′	74° 00′	20	0	–11.42
00–24	74° 01′	80° 00′	32	0	–3.62	01–80	72° 15′	73° 15′	16	0	–12.56
				11	–3.52	01–72	70° 50′	73° 44′	26	0	–9.75
				32	–2.08	01–79	69° 03′	73° 14′	13	0	–10.05

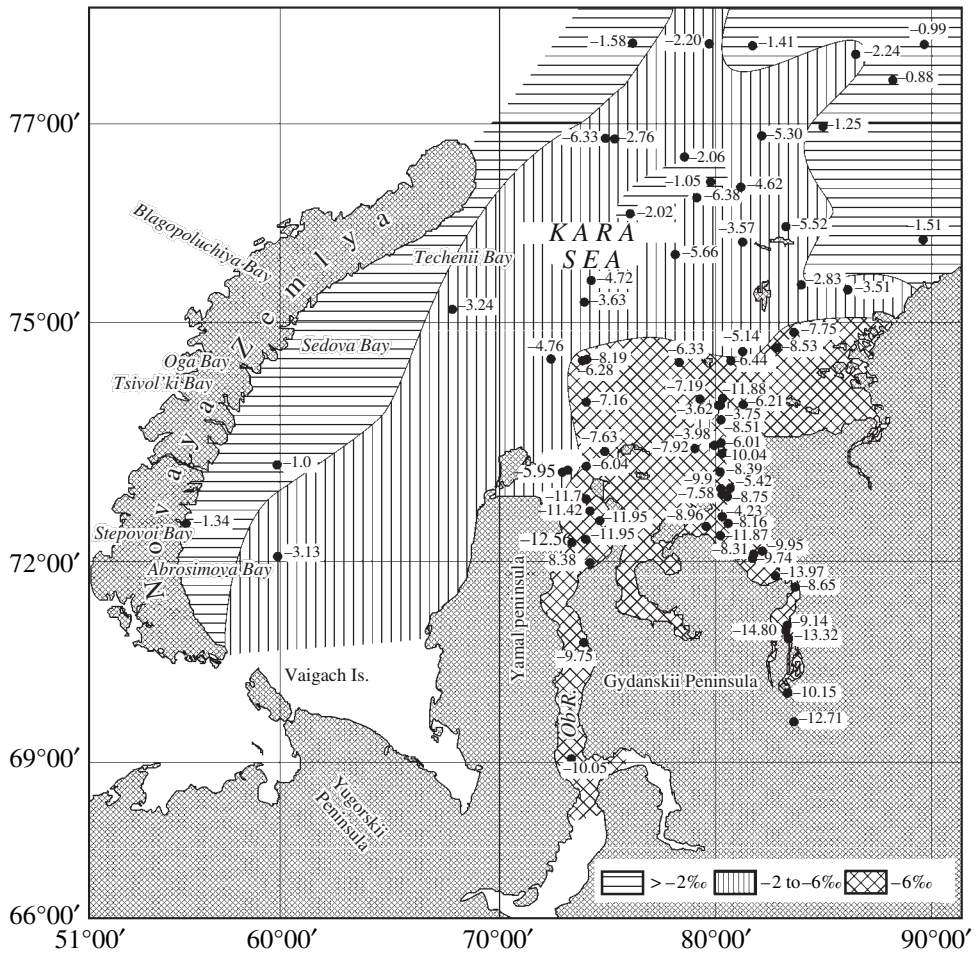

Fig. 6. Distribution of total CO_2 isotopic composition in the surface waters of the Kara Sea.

in the north of our study area, at practically round-the-clock photosynthesis during polar daytime, the waters become >100% saturated with oxygen. The productivity of photosynthesis in the riverwaters is constrained because of the lack of light, which cannot penetrate deep because of the turbidity of these waters. For example, a Secchi disk is visible in Obskaya Guba to depths of no more than 2 m.

The results obtained on the isotopic composition of the plankton and its species composition are presented in Tables 4–8.

Both the Yenisei and Ob are inhabited by freshwater algae, predominantly the diatoms *Melosira granulata* and *M. varians* and the green alga *Chlorophyta*, which occurs as both filamentous (*Oedogonium*, *Ulotrix*) and unicellar (*Pediastrum*, *Scenedesmus*, and others) species, and abound in blue-green algae (predominantly *Oscillatoria*, *Aphanisomenon flos-aquae*).

North of the frontal zone, the contents of biogenic elements decrease because the riverwaters are diluted there by seawaters ($S > 10$ g/l) and marine phytoplankton develops. Upon the deposition of the bulk (>75%)

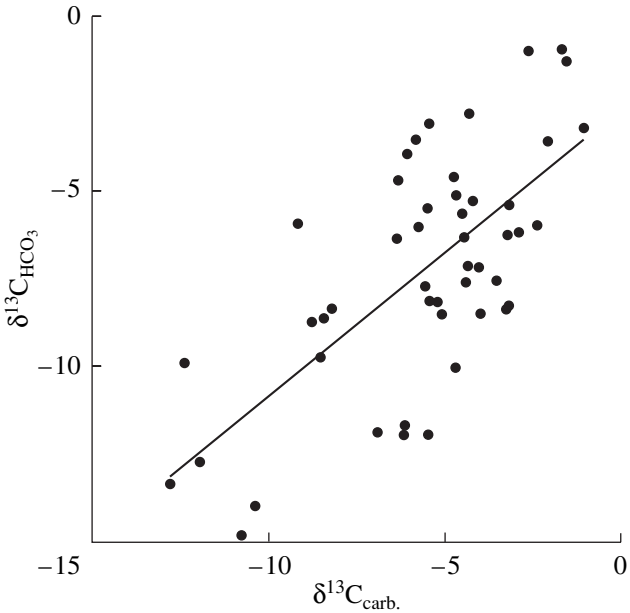

Fig. 7. Comparison of $\delta^{13}C_{CO_2}$ in the surface and deep waters of the Kara sea.

Table 4. Carbon isotopic composition, the floristic composition of phytoplankton samples, and the isotopic composition of dissolved CO_2 (HCO_3^-) in samples taken from the subsurface water layer along the Yenisei River–Kara Sea meridional profile (70–77° N) on September 7–22, 2000, during Cruise of the R/V *Akademik Boris Petrov*

Site	*T*, °C	S (g/l)	Detritus: approximate content and $\delta^{13}C$ (‰)	Predominant species* in the phytoplankton samples, %, %	$\delta^{13}C$, ‰	
					plankton	dissolved HCO_3^-
00 –19	11.7	0.0	<5% –30.6	Freshwater complex: *Melosira granulata* (73), *Asterionella Formosa* (13), blue-green *Flagilaria crotonesis*, green filamentous algae. Sample of *Asterionella formosa* was obtained	–35.6 –37.0 –33.9	–12.7
00–17	10.6	0.0	<5%	Freshwater complex: *Asterionella formosa* (50), *Melosira sp.* (30), green filamentous algae (20), *Fragilaria crotonensis*	–36.2	–14.8
00–16	8.1	2.3	<50% –28.3	Freshwater complex: *M. granulata* (70), *A. formosa* (10), *Synedra sp.* (5), *Chlorophyceae* (15)	–28.3	–14.0
00–15	5.9	6.7	~50%	Freshwater complex: *M. granulata* (50), *Pennatophyceae* (23), *A. formosa* (10), *Synedra* (10), blue-green algae (5), green filamentous algae	–27.8	–9.7
00–22	5.1	6.6	<50%	Predominantly freshwater complex, first occurrence of marine species. *Melosira sp.* (80), *Thalassiosira nordenskioeldii* (5), *Nizschinia grunowii*, *Syndera*, *A. formosa*, green algae	–31.9	–9.1
00–23	0.25	28.5	<5% –25.4	Predominanly marine species. *Chaetoceros socialis* (55), *Nizschinia grunowii* (20), *Thalassiosira sp.* (15), *Melosira sp.* (5), *Dinophyceae*	–24.6	–4.0
00–24	0.62	23.7	5% –26.3	Marine complex *Ch. socialis* (50), *Ch. sp.* (25), *Th. nordenskioeldii* (15), *Dinophyceae* (5), *Nizschinia grunowii*, *A. formosa*	–25.1	–3.6
00–8	0.38	21.1	10%	Marine complex *Nizschinia grunowii* (60), *Th. nordenskioeldii* (30), *Ch. sp.* (10)	–25.9	–8.5
00–9	–0.9	23.8	10%	Marine complex *Nizschinia grunowii* (75), *Th. nordenskioeldii* (15), *Chaetoceros sp.* (5), *Dinophyceae*	–25.9	–5.4
00–26	2.8	19.2	<5%	Marine complex *Ch. decipiens* (35), *Ch. sp.* (50), *Th. nordenskioeldii* (15), *Ceratium arcticum*	–27.5	–5.7
00–28	0.38	25.6	~10% –27.1	Marine complex *Ch. sp.* (95), *Th. nordenskioeldii*, *Nizschinia grunowii*, *Ceratium arcticum*	–27.0	–
00–30	–	24.9	<5% –27.6	Marine complex *Ch. sp.* (85), *Dinophyceae* (10), *Nizschinia grunowii*	–27.9	–5.5
00–35	–0.8	26.6	<5%	Marine complex *Ch. socialis* (90), *Th. nordenskioeldii* (5), *Nizschinia grunowii*, *Dinophyceae*, occasional freshwater species (*Anabaena*)	–24.4	–2.8
00–36	–1.0	27.2	<5%	Marine complex *Ch. decipiens* (>90), *Thalassionema sp.*, *Ceratiu arcticum*	–28.1	–5.3

* Species composition was determined by V.V. Larionov and P.R. Makarevich.

Table 5. Carbon isotopic composition, floristic composition of phytoplankton, and the isotopic composition of dissolved CO_2 (HCO_3^-) in samples from a surface water layer along the Yenisei–Kara Sea profile (70°–78° N). Samples were collected in August 16–30, 2001, R/V *Akademik Boris Petrov*-2001

Site	*T*, °C	S (g/l)	Predominant phytoplankton species * (%)	$\delta^{13}C$, ‰	
				plankton	dissolved HCO_3^-
01–08	14.5	0.0	Freshwater complex with predominant diatoms (80–95) (*Melosira granulata* and *M. varians*, *Fragilaria*, *Rizosolenia*, *Asterionella*, green filamentous alge (*Rhizoclonim*, *Ulotrix*) and unicellar (*Pedistrum*), blue-green (*Anabaena*, *Microcystis*, *Oscillatoria*). Detritus <3%. Three samples were obtained with different proportions of the aforementioned alga classes	–34.5 –32.7 –31.7	–10.1
01–04	13.7	0.0	Same complex: *M. granulata* (80), *Fragilaria*, green (15), blue–green. Detritus 1%	–33.7	–9.1
01–11	12.9	0.0	Same complex: *M. granulata* (60), *Asterionella*, *Fragilaria* (10), *Cyclotella* (5), green (10), blue-green (10). Detritus (zoo) up to 30%	–30.6 –23.5 (zoodetritus)	–9.9
01–19	9.5	6.1	Freshwater complex, first occurrence of marine diatoms (*Chaetoceros*, *Thalassiosira*) and dinoflagellates. major species: *Melosira varians*, *M. granulata*, *Pennatophyceae*. Green and blue-green algae. Detritus up to 10%)	–28.7 –27.0 (detritus)	–4.2
01–23	10.1	5.1	Freshwater complex (up to 70%) with the predominance of *M. varians*, *M. granulata*, *Fragillaria*, *Asterionella*. Less green and blue-green algae. Marine species (30): *Dinophyta*, *Chaetoceros*, *Thalassosira.* Detritus (up to 40%)	–29.1 –28.6 (detritus)	–7.9
01–26	7.8	12.4	Marine complex (90): *Nitzschinia delicatissima* (>80). Various species: *Chaetoceros* (3–5), *Dinophyta* (10–15). Freshwater complex (10): *Melosira.* Detritus 1%	–26.7	–3.7
01–43	5.4	20.9	Marine complex: predominant *Dinophyta* (up to 50–60%), *Chaetoceros* (30), and *Thalassiosira antarctica* (5). Freshwater fragments (5): *Melosira granulata*, *Rhizclonium*, *Scenedesmus*, *Pediastrum*, *Oscillaria*. Detritus (up to 3%).	–27.4	3.5
01–28	2.5	23.4	Marine complex (>90), freshwater (no more than 5%) (*M. granulata*, *Fragilaria*, *Asterionella*). *Dinophyta* (up to 50%), *Chaetoceros diadema* and other species (up to 20), *Coscinodiscus*. Detritus 20%	–27.3	–1.5
01–45	3.3	29.0	Marine complex with the predominance of the diatoms *Chaetoceros decipiens* (60), *Thalassiosira* (5–10), *Coscinodiscus*, *Fragilaria oceanica*. *Dinophyta* (30). Freshwater (1): *M. granulata*, green algae	–26.5	–0.9
01–31	2.0	29.5	Marine complex with the predominance of *Chaetoceros* (40) (five species: *Ch. borealis*, *Ch. decipiens*, and others), *Thakassiosira* (10), *Coscinodiscus*	–26.8 –26.1 (detritus)	–1.2
01–48	3.6	6.1	Predominantly *Chaetocerus diadema* (80), *Ch. convolutes*, *Ch. borealis*, *Ceratium arcticum*, etc. *Dinaphyta* (15–20). Detrutus <5%	–26.2	–1.4

* Species composition was determined by V.V. Larionov.

Table 6. Carbon isotopic composition, floristic composition of phytoplankton, and the isotopic composition of dissolved CO_2 (HCO_3^-) in samples from a surface water layer along the meridional Ob–Kara Sea profile (69°–78° N). Samples were collected in August 31–September 10, 2001, R/V *Akademik Boris Petrov*-2001

Site	*T*, °C	S (g/l)	Predominant phytoplankton species * (%)	$\delta^{13}C$, ‰	
				plankton	dissolved HCO_3^-
01–79	–	0.0	Freshwater complex with the predominant diatoms *Melosira varians* and *M. granulata* (85), *Asterionella*, *Fragilaria*, *Synedra*, green algae (filamentous and *Pedistrum*), blue-green. Detritus 3%	–30.8 –27.0 (detritus)	–10.0
01–72	11.4	0.0	Same complex: *Melosira varians* and *M. granulata* (80), green algae (15). Detritus 1%	–29.5	–9.7
01–80	8.5	1.0	Same complex: *M. granulata* and *M. varians*, *Asterionella*, *Flagilaria*, green algae (10), blue-green algae (10). Detritus up to 30%	–27.6	–
01–70	9.2	0.8	Freshwater complex, first occurrence of marine flagellates. Up to 30% detritus. major species: *Melosira varians*, *M. granulata*) *Pennatophyceae*. Green and blue-green algae	–27.7	–
01–82	6.6	9.8	Freshwater complex with the predominance of *M. varians*, *M. granulata*. Less green and blue-green algae. Occasional marine species *Peridinium*, *Ebria*. Much detritus (40%)	–27.9 –27.4 (detritus)	–3.8
01–68	7.8	9.9	Marine complex: *Nitzschinia delicatissima* (>80). Various species of *Chaetocerus* (3–5). Dinoflaggelates (10–15). Detritus 1%	–27.5	–
01–67	7.4	11.2	*Nitzschinia delicatissima* (>95). Occasional *Chaetocerus* and dinoflagellates. Detritus <3%	–26.6	–3.6
01–61	5.4	18.6	Marine complex: *Chaetoceros diadema* (up to 50), *Ch. convolutes*, and other species (30), dinoflagellates, detritus 20%	–26.0	–2.0
01–56	5.4	21.7	Marine complex with the predominance of dinoflagellates. *Peridinium* (60), *Thalassionema nitzschioides* (20), *Chaetoceros borealis*, *Ch. convolutes*, zooplankton, zoodetritus up to 20%	–26.3	–2.7
01–46	4.2	25.3	Marine complex with the predominance (up to 80%) of diniflaggelates, 30% of which is *Ceratium*. Species of *Chaetoceros* (10). Occasional *Melosira granulata*. Zoodetritus 20%	–25.5	–1.6

* Species composition was determined by V.V. Larionov.

Table 7. Carbon isotopic composition, floristic composition of phytoplankton, and the isotopic composition of dissolved CO_2 (HCO_3^-) in samples from a surface water layer along the meridional Ob–Kara Sea profile (69°–76° N). Samples were collected in September 30–October 8, 2002, R/V *Akademik Boris Petrov*-2002

Site	*T*, °C	S (g/l)	Predominant phytoplankton species (%)	$\delta^{13}C$, ‰	
				plankton	HCO_3^-
02–06	0.7	0.0	A freshwater complex typical of the Ob, with the absolute predominance of diatoms: *Melosira varians* and *M. granulata*. Green (filamentous) and blue-green *Anabaena sp.*, *Microcystis aeruginosa*, *Aphanizomenon flos-aquae*. In addition to general phytoplankton sample (sample 6a), three samples were obtained for determining the isotopic composition: sample 6b pure sample of the blue-green *A. flos-aquae*; sample 6c (major contribution) of *Melosira*, green algae (up to 30%), *Asterionella* (5), detritus (<5%); sample 6d of *Melosira varians* and *M. granulata* (>95)	–30.0(6a) –24.8(6b) –30.5(6c) –29.4(6d)	–8.8
02–12	0.3	8.2	Predominance of the same freshwater complex, but the fractions of green and, particularly, blue-green algae are lower and marine species occur. *Melosira varians* and *M. geanulata* (60), green, blue-green algae, *Ceratium arcticum*, *Peridinium depressum*. Detritus (zoo) up to 30%. Numerous infusoria *Tintinnidae*	–24.9 –27.0 (*Tintinnidae*)	–4.6
02–01	–1.2	26.4	Typically marine complex with the predominance of *Chaetoceros decipiens*, *Ch. borealis*, and *Ch. convolutus* and subordinate *Coscinodiscus oculus-iridis*. The *Dynophyta* are represented by large *Ceratium arcticum*, *C. longipes*, *Peridinium depressum*. Detritus <15%	–24.7	–1.5

of the particulate matter in the estuarine part, the water clears, and, thus, favorable conditions are created for photosynthesis. North of the funnel of the Yenisei estuary, marine phytoplankton biocenosis is formed, along with the still predominant (up to 70%) freshwater species of diatoms and green and blue-green algae; the phytoplankton includes an appreciable number of species of marine Peridiniales and diatoms. Farther northward, the proportions of species in the community shift toward an increase in the amount of marine species, so that already at 74° N, the freshwater species account for no more than 10% of the biomass. Along the Ob profile, whose frontal part is commonly not as clearly pronounced , the marine community of microalgae (mostly dinoflagellates) starts to form much farther southward.

The upper limits for the concentration of biogenic elements that constrain the photosynthesis rate at the low temperatures of the environments are thought to be 3 μg-at/l for nitrogen, 0.5 μg-at/l for phosphorus, and 10 μg-at/l for silicon [29]. It follows from the data of

Table 8. Carbon isotopic composition, floristic composition of phytoplankton, and the isotopic composition of dissolved CO_2 (HCO_3^-) in samples from a surface water layer in the southwestern part of the Kara Sea profile (Novaya Zemlya). Samples were collected in October 20–27, 2002, R/V *Akademik Boris Petrov*-2002

Site	*T,* °C	S (g/l)	Predominant phytoplankton species (%)	$\delta^{13}C$, ‰	
				plankton	dissolved HCO_3^-
Novaya Zemlya, Southern Island; Stepovoi Bay, 02-13	–1.36	27.8	Marine complex, autumn evolutionary stage. The predominant species belong to *Chaetoceros*, the major species is *Ch. borealis* (50)	–27.4	
			Ch. convolutus (10), *Ch. decipiens*, *Thalassionema nitzschioides* (20), *Ceratium*, *Protoperidinium*, and other *Dinophyta* (10). <5%	–27.0 (detritus)	–2.7
			Sample of the diatom *Thalassionema nitzschioides* (>70)	–25.4	
Same place 02–14	–0.24	8–17 (variable due to coastal runoff, creek)	Same oceanic complex but with a lower fraction of *Dinophyta*. The predominant species is *Chaetoceros borealis*, *Ch. convolutus*, *Thalassionema nitzschioides*. Zoodetritus <5%	–26.6	–3.2
			A sample of *Thalassionema* (>90) was obtained. Zoodetritus <5%	–24.1	
Western slope of the Novaya Zemplya Trough 02–16	–1.6	29.0	Predominant *Chaetoceros convolutus* (85), subordinate *Ch. decipiens* + *Ch. borealis* (5), small amounts of *Thalassionema* and *Protoperidinium*. Zoodetritus <5%	–28.2	+1.0
Mouth of Baidaratskaya Guba 02–19	+0.8	29.6	A great diversity of oceanic diatom and dinoflagellate species. Typically, the quantitatively predominate diatoms are *Conscinodiscus oculus-iridis*. Three samples were obtained: 19a—general phytoplankton dominated by *Chaetoceros borealis* and *Ch. decipiens*. *Ceratium arcticum*, *C. longipes*, *Nitzschinia seriata*, *C. oculus-iridis*, zoodetritus <5%	–24.8 (19a)	–1.9
			19b—*Coscinodiscus oculus-iridis* (>90), *Protoperidium depressum*, *P. conicum* (5), zoodetritus <5%;	–23.5 (19b)	
			19c—*Chaetoceros borealis* (80), *Ch. decipiens* (5), *Ceratium* (5–10), *Thalassionema*	–24.5 (19c)	

Table 2 that the contents of nitrates and phosphates in the Kara Sea during our fieldwork were much lower than the limiting values (~0.2 μg-at/l for nitrates and 0.03 μg-at/l for phosphates). Nevertheless, summertime planktonic communities strongly dominated by diatoms and dinoflagellates were observed throughout the whole lengths of the meridional profiles, including the northernmost of them near 78° N.

These observations provide grounds for the conclusion that, in spite of the seawater stratification, periodical water exchange between the surface and bottom waters, a process particularly active and efficient in autumn, maintains the living activity of phytoplankton in the upper part of the water column at the expense of the resource of biogenes in underlying waters. In this context, it is worth noting that the maxima of oxygen concentrations and degrees of saturation occur at several northern sites not in the uppermost water layer but within the pycnocline, in which photosynthesizing phytoplankton is also concentrated.

Available data on the isotopic composition of phytoplankton in the Kara Sea were scarce before our research was launched. These were mostly indirect data, deduced from materials on the carbon isotopic composition of the particulate matter and sediments [33–37].

In the course of studies within the scope of the project, phytoplankton samples from various sites within the Kara Sea were directly analyzed for isotopic composition. Tables 4–8 present data on the carbon isotopic composition of certain biological species. The biological species were described by Makarevich and Larionov [38]. The content of detritus in the samples was estimated visually under a microscope (column 4), and its isotopic composition was determined separately. The reader can find the species composition, bioproductivity, and the distribution of phytoplankton in the Kara Sea in [38–43].

The cold waters in the northern part of the sea are dominated by the diatoms *Chaetoceros*, *Nitzschia*, *Thalassiosira*, and *Thalassionema*. The predominant species in the fresh and brackish waters of the estuaries are *Melosira*, *Asterionella*, and *Fragilaria*. Peridiniales are characteristic of summer phytoplanktonic successions in the cold waters of the northern portions of the river–sea profiles. Their predominant species are *Ceratium* and *Protoperidinium*, with subordinate amounts of green (*Oedogonium*, *Ulotrix*, *Pediastrum*, and *Scenedesmus*) and blue-green (*Oscillatoria*, *Aphanisomenon*, and *Anabaena*) algae (both colonial filamentous and solitary). These alga groups mostly inhabit rivers and estuaries, although they were also found in the saline high-sea waters.

The bulk of the biomass of our samples (1999) from the southern part of shallow Obskaya Guba consisted of freshwater algae, which were dominated by one species of the green filamentous alga *Oedogonium* (*Chlorophyta*), brackish-water *Melosira varians*, *M.granulata*, *Asterionella formosa*, and other small diatom species. The isotopic composition of the freshwater complex from Obskaya Guba varied from –31 to –35.7‰, according to the significant salinity variations over the bay area (from 0.6 to 2). Outside the Ob estuary (73.5° N), the diatom *Thalassiosira*, *Nitzschia* appeared north of the estuary (at 74.5° N) and gradually became predominant in mass in the community (at 80%), and the carbon of their biomass was significantly depleted in the light isotope ($\delta^{13}C$ from –26.2 to –27.6‰).

The green filamentous alga was characterized by record-low values of $\delta^{13}C$ (–37‰), whereas the diatom complex (*Melosira* and *Asterionella*) from the same water sample was isotopically much heavier (–27.4‰). These differences could, perhaps, be partly related to the ability of many diatoms to actively utilize HCO_3^- as a photosynthesis substrate, while the photosynthesis of the green alga *Chlorophyta* is based on CO_2 [44, 45].

The data obtained during the expedition in 2000 on the Yenisei–sea profile are graphically represented in Fig. 8. At an overall increase in the $\delta^{13}C$ of the plankton from south to north, two boundaries can be discerned that are marked by a drastic change in the isotopic composition of plankton between Sites 00–15/00–17 (6–8‰) and 00–22/00–23 (5–7‰). These changes correspond to the changes in the salinity and could be caused by the disappearance of freshwater phytoplankton species that are the most sensitive to salinity from areas where seawater comes into the estuary. At the inner boundary of the hydrological (main) front (Site 00-22), the community was dominated by the diatoms *Melosira granulata*, *Fragilaria crotonensis*, *Asterionella formosa*, and *Fragilaria oceanica*, *Thalassiosira*, with a high percentage (up to 30%) of green and blue-green algae. At the outer boundary of the front (Site 00-23), the plankton complex consists of a marine planktonic species, with the predominance of *Fragilaria oceanica*, and *Thalassiosira* and the first appearance of the typical marine summer-blooming algae *Chaetoceros* and *Protoperodinium*. The freshwater species (*M. granulata* and *Synedra*) are preserved in small amounts and only within the bottom water layer. Farther northward and northeastward, only a marine complex of microalgae occurs, which consists of a few species of *Chaetoceros* and other diatoms, along with numerous *Peridiniales*. Near the ice field (Sites 00-07/00-09), the bulk of the biomass of the community consists of two diatom species: early-spring *Nitzschia grunowii* and late-spring *Chaetoceros socialis*.

As was mentioned above, variations in the $\delta^{13}C$ of the plankton can partly be explained by the character of photosynthesis and, hence, the species composition of the plankton. However, the comparison of the isotopic composition of the plankton and bicarbonate dissolved in the water indicates that these $\delta^{13}C$ values display a fairly strong correlation (Fig. 9). This implies that the isotopic composition of the carbon dioxide contained in the water and utilized in the process of photosynthesis

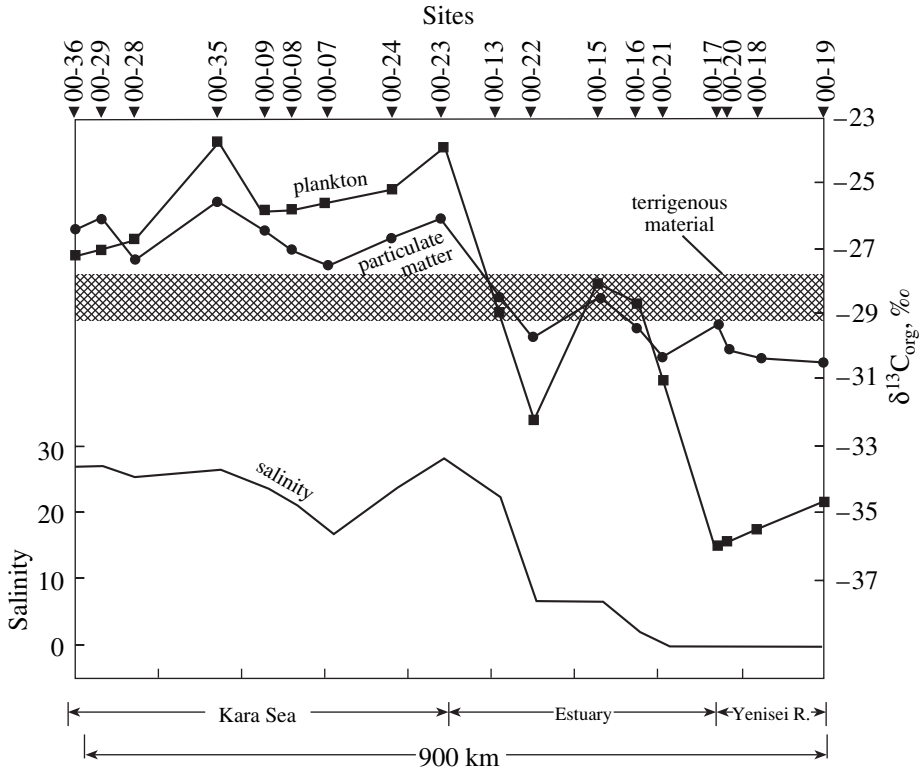

Fig. 8. Variations in the carbon isotopic composition of phytoplankton and organic carbon of particulate matter in waters along the Yenisei River–Kara Sea profile.

predetermines the isotopic composition of the plankton. The isotopic effect of biosynthesis derived from $\delta^{13}C_{CO_2}$ vs. $\delta^{13}C_{plankton}$ dependences in this plot is $\Delta\delta^{13}C_{bio} = \delta^{13}C_{CO_2} - \delta^{13}C_{plankton} \approx 21‰$ on average. The few exceptions are most probably related to the allochthonousness, i.e., inconsistencies between the sites where the organisms were produced and the character of the environment at the sampling site. The high heterogeneity of the carbon background of the environment, including the heterogeneity caused by the mixing of various proportions of CO_2 provided by riverine runoff and marine bicarbonate, seasonal variations in mixing and circulation aureoles, transportation with floating ice, and other factors typical of this part of the Arctic Basin, make this allochthonousness highly probable.

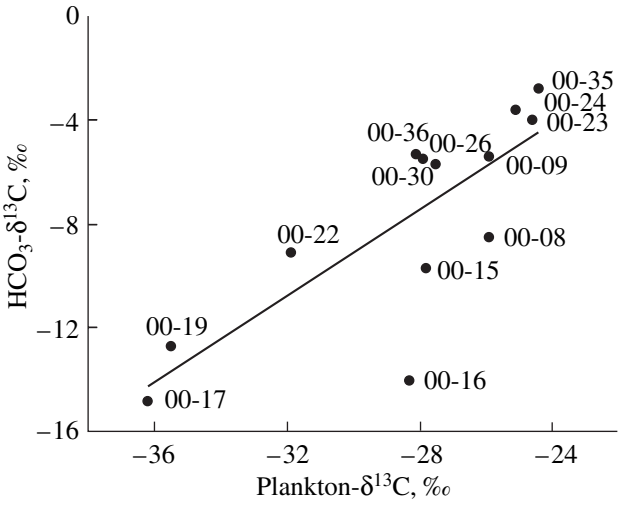

Fig. 9. Comparison of the carbon isotopic composition of phytoplankton $\delta^{13}C_{pl}$ and CO_2 (HCO_3^-) dissolved in the surface water layer.

Another factor that can affect the isotopic composition of the plankton is the coefficient of substrate utilization *f* [46]. If one of the limiting factors is the availability of the substrate (CO_2 and HCO_3^- during photosynthesis), then the isotopic fractionation effect decreases, and the organisms are not as significantly enriched in the light isotope. This takes place, for example, at low CO_2 concentrations in an environment or at high contents of organisms, blooming algae, etc.

For example, one isotopic effect detected in diatoms was related to the ratio of the cell surface to its volume that is unfavorable for CO_2 diffusion and is pronounced in the large cells (60–100 μm) of *Coscinodiscus*. This effect resulted in their additional (by ≈1‰) enrichment in ^{13}C to –23.6‰, which is the highest $\delta^{13}C$ value measured in the Kara Sea plankton in the course of our research. Bloom commonly suppresses the isotopic

effect. For example, a pure sample of the blue-green alga *Aphanisomenon flos-aquae* obtained during the 2002 expedition was characterized by rapid mitosis with the formation of large flake-shaped aggregates of filamentous organisms with a common trichome (outer shell). The alga is typical of the freshwater plankton of the Ob and is transported to the Ob estuary with the waters of Taz Bay. This alga bloom was also noted in the Ob in 2001. The isotopic composition of this alga corresponded to $\delta^{13}C = -24.8‰$, whereas the freshwater complex of the Ob had a composition of $\delta^{13}C = -30.8‰$.

A temperature increase suppresses the CO_2 solubility and, hence, results in an increase in *f* and eventually, diminishes the isotopic effect. However, this correlation is not linear. While the CO_2 concentration is not a limiting factor in this situation, a further increase in this concentration should not enhance the fractionation.

It is pertinent to recall that both the kinetic and thermodynamic isotopic effects during biosynthesis are temperature-dependent. The value of the effect increases by approximately 0.3–0.4‰ with a temperature decrease by 1°C [46], and hence, a decrease in the habitat temperature by 3–5°C can lead to the enrichment of the planktonic carbon in the light isotope by 1–2‰ due to the temperature effect of isotopic fractionation alone, i.e., $\Delta^{13}C_{bio}$ can increase to 23–24‰, which yields, at $\delta^{13}C_{CO_2}$ from –3 to –4‰, a plankton isotopic composition from –26 to –27‰.

These factors should be taken into account in analyzing data on the isotopic composition of plankton from the northern part of the sea (75°–78°N), where the influence of riverwaters is notably weaker but the phytoplankton has, nevertheless, an isotopically light composition ($\delta^{13}C_{pl}$ from –25.5 to –27‰).

The 2002 expedition obtained phytoplankton samples from a bay at Novaya Zemlya and the Novaya Zemlya Trough (2002), none of which is directly affected by riverine runoff. Data on the isotopic composition of the phytoplankton are presented in Table 8. The samples were taken shortly before wintertime, in late October. The seawater in the Novaya Zemlya Trough had a typical marine isotopic composition of its carbonate complex, whereas the typical oceanic complex of the phytoplankton, which contained nearly 95% diatoms (*Ch. convolutes*, *Ch. decipiens*, *Ch. borealis*, and *Thalassionema* sp.) and *Protoperidinium*, were isotopically lighter, as the plankton was sampled in the bay at a negative water temperature.

6. PARTICULATE ORGANIC MATTER IN SEAWATER (POM)

Much organic matter is contained in seawater in the particulate form (suspensions), which is referred to as particulate organic matter (POM). These are remnants of dead organisms, floral and soil detritus, humic compounds, and bio- and geopolymers adsorbed at mineral particles, as well as live plankton. Riverine particulate matter can sometimes contain geologically old organic material borrowed from the weathering products of rocks [47].

Riverwaters annually carry to the Kara Sea >150 mln. tons of dissolved and particulate organic and inorganic material [17, 48]. The peak of the Yenisei runoff falls onto June to August, and the Yenisei runoff volume during its maximum in June reaches 65% of the annual runoff volume. The maximum of the Ob runoff (up to 55% of its annual runoff) corresponds to the three summer months (from June through August), with no more than 15% of the annual runoff emptied into the Arctic Basin during wintertime [17, 49].

The overall annual amount of organic carbon received by the Kara Sea in the form of particulate matter equals 0.3×10^6 tons for the Ob and 0.2×10^6 tons for the Yenisei [50]. More than 90% organic carbon is transported by rivers to the Arctic Basin in the form of soluble organic matter whose particles have various sizes.

The organic matter of seawater is contained in it in the form of particles ranging from submicrometer-sized to readily discernible phytoplankton cells and detrital particles [52]. Our samples of particulate matter examined in the laboratory consisted of integrated material deposited on fiberglass filters, including microphytoplankton (cells <10 μm).

The contents of particulate matter decrease from the river, along the estuary, and farther to the sea. At the southernmost site in the Ob estuary, which was located upstream from the connection of Obskaya Guba and Taz Bay, the content of particulate matter in the water was 17 mg/l, and this content notably decreased farther along the entery course of riverwaters into shallow Obskaya Guba between 71°30′ and 72°20′N, which corresponds to the southern boundary of seawaters according to averaged data of long-term observations [53].

The northern boundary of saline and fresh waters was in 2001 between 73°20 and 72°40' N. The concentration of particulate matter in the water decreases to 4.8 mg/l at the boundary of the marine part and further to 3 mg/l at 74°30 N and 1.7 mg/l at 76° N. A minimum concentration of 0.33 mg/l was detected at northern sampling sites within the sea, at which no immediate effect of riverine runoff can be discerned. This value of 0.3 mg/l can be regarded as the background value for the open sea, because a close value of 0.35 mg/l was also determined for the Yenisei profile.

The content of particulate matter in the Yenisei is lower (3–4.2 mg/l) than in the lower reaches of the Ob, and the concentration decreases to 1.5–1.8 mg/l near the northern boundary of the estuary. North of 75° N, the particulate matter concentration in the seawater is already <1 mg/l and gradually decreases to 0.33 mg/l at 75° N.

The systematic studying of the isotopic composition of particulate matter were initiated in 1997 [4]. The most detailed examination of the particulate matter was carried out during the cruise of the R/V *Akademik Boris Petrov* along the Yenisei–Kara Sea profile in 2000 [9]. During this cruise, the vessel entered into the Yenisei mouth for a few hundred kilometers, to 70° N (Fig. 1).

The distribution of the carbon isotopic composition of the particulate matter along the profile from the Yenisei to Kara Sea is shown in Fig. 10. The structure of the water masses along the profile is characterized by the occurrence of a long (approximately 220 km) freshwater region and a pronounced narrow (approximately 50 km) area where fresh and seawater mix between 72.5 and 73.5°N. The area was subdivided into three zones: (I) fresh riverwaters, (II) brackish estuarine waters, and (III) marine waters, whose salinity was close to normal.

In the vertical section of the water masses, the variations in the $\delta^{13}C$ of the particulate matter are relatively small. In the southern part of the profile, where the depth is shallow and the water mass is not stratified, the isotopic composition of the particulate matter remains practically unchanging with depth (approximately ~ –30‰). Where the water mass becomes stratified, the isotopic composition of the particular matter also displays stratification (at Site 00-21): the most isotopically heavy particulate matter (–24.4‰) was sampled from highly saline bottom high-sea waters.

The variations in the $\delta^{13}C$ of the particulate matter along the meridional profile are quite remarkable. The carbon isotopic composition of the particulate matter varies from –30…–29‰, which is typical of riverwaters, to –27…–28‰ in the estuary and –25…–26‰ in the seawater. It is obvious that this general tendency is complicated by local variations, with drastic changes taking place at the geochemical barrier.

Analogous research was conducted in the Yenisei estuary in 1997, at almost the same sites (Fig. 1). This offered the possibility of comparing the geochemical structures of the profiles studied with a time interval of three years. Figure 11 displays the distribution of the salinity and carbon isotopic composition of the particulate matter in the 1997 profile. It corresponds to the segment of the 2000 profile between Sites 00-24 and 00-15. The comparison of the profiles demonstrates that, although the general tendencies in the distribution of $\delta^{13}C$ coincide, the profiles show certain differences. The 2000 profile demonstrates the expansion of isotopically lighter carbon (up to –29‰) from the mainland. Values of $\delta^{13}C$ close to –25‰ give way to values of about –26‰. It should be mentioned that

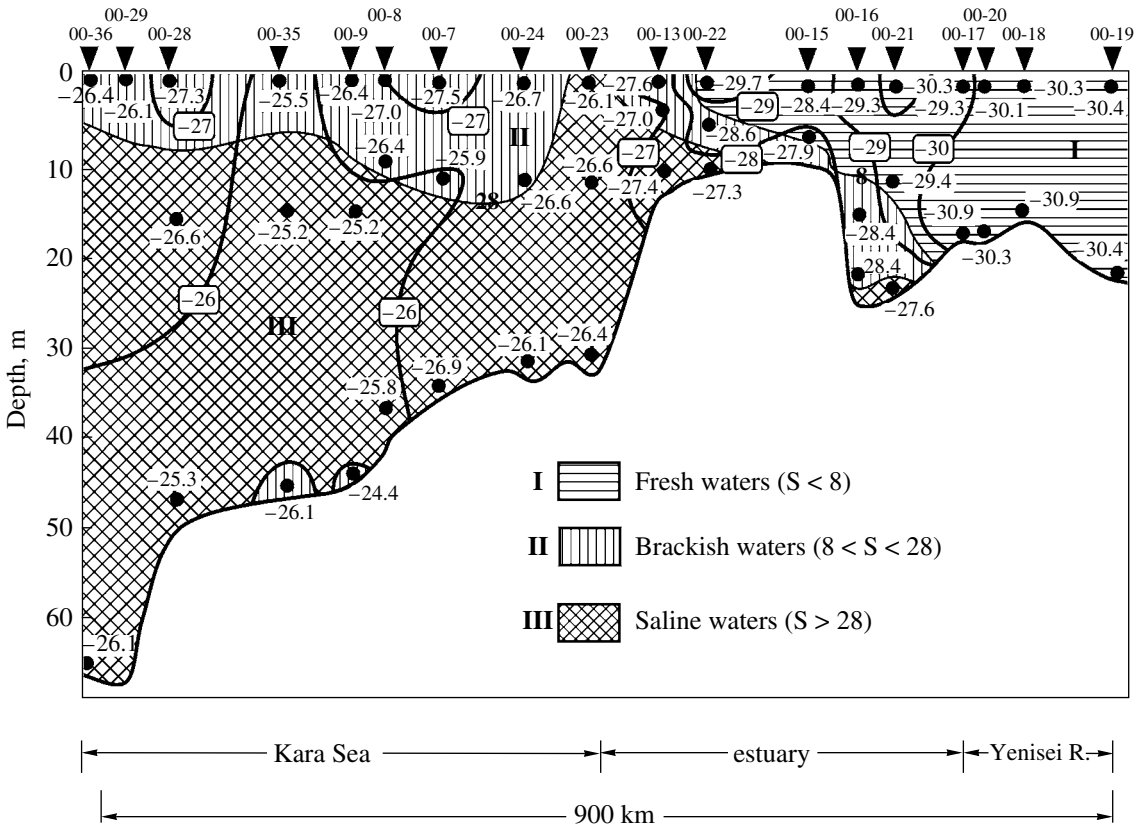

Fig. 10. Distribution of $\delta^{13}C$ values of the organic carbon of particulate matter (POM) in waters along the Kara Sea–estuary–Yenisei River profile. Cruise of the R/V *Akademik Boris Petrov*, 2000

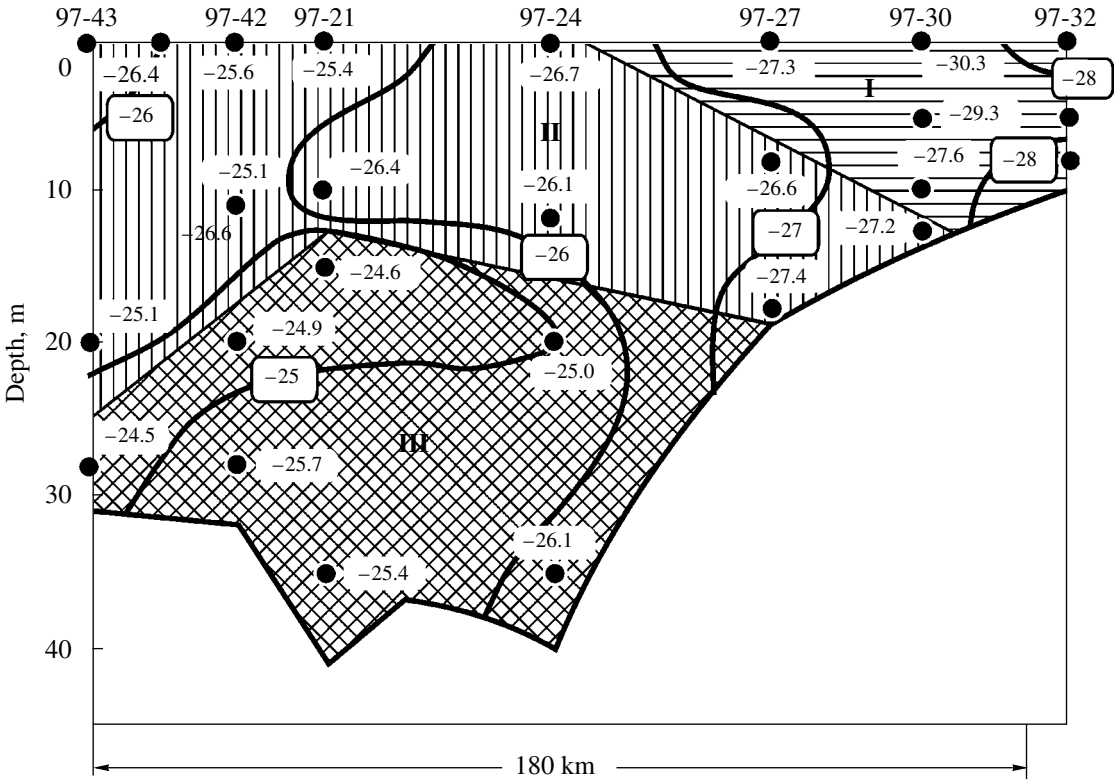

Fig. 11. Same as in Fig. 10 but within a shorter segment of the profile: Site 97-43 is close to Site 00-24, and Site 97-32 is close to Site 00-15. Cruise of the R/V *Akademik Boris Petrov*, 1997.

this zoning can be notably shifted under the effect of storm stirring, variations in the river runoff, depending on the season, etc.

The carbon isotopic composition of the particulate matter in the surface layer can be compared with the isotopic composition of the plankton. These data are presented in Fig. 8.

The organic carbon of particulate matter is a mixture of terrigenous and planktonogenic components. Freshwater plankton is isotopically light, while seawater plankton is isotopically heavier (Table 1), and hence, particulate matter in the marine part is isotopically lighter than the plankton, and this matter in the estuarine–riverine part is, conversely, heavier than the plankton (Fig. 8). The detrital humic material transported from the land obviously should have an isotopic composition varying only insignificantly throughout the whole profile. This composition can be roughly evaluated from the observed relations. The variations should lie within the range of –27.2 to –29.1‰ at an average of –28.0‰, which corresponds to the intersection of the isotopic composition lines of the particulate and planktonogenic organic matter. This implies that the riverwaters contain particulate matter with approximately 70% detrital–humic material and 30% planktonogenic matter. The particulate matter from near-shore seawater contains close to 30% terrigenous material, and the contribution of marine bioproducers is approximately 70%. At sites situated farther away from the shore (for example, at Site 00-58), the contents of terrigenous material becomes insignificant, but the carbon isotopic composition $\delta^{13}C$ of the sediments remains there unusually low for planktonogenic material. Analysis indicates that the enrichment of sediments in this part of the sea in the light isotope is not caused by the contribution of the terrigenous component but is related to the low values of $\delta^{13}C$ of CO_2 utilized in photosynthesis (from –4 to –8‰, instead of common $\delta^{13}C$ from 0 to –2‰; Fig. 6). Its source is isotopically light carbonic acid of continental provenance that is transported into the sea for a long distance.

7. ORGANIC CARBON IN SEDIMENTS

Already the first expedition in 1995 (Cruise 22 of the R/V *Akademik Boris Petrov*) managed to obtain data on the concentrations of carbon and its isotopic composition in the organic matter from bottom sediments. The materials of later cruises made it possible to detail and refine these data (Table 12).

The concentrations of organic carbon in the sediments vary mostly from 0.5 to 2% (Fig. 12). These are not very low contents for an oligotrophic basin. The C_{org} concentrations in the central part of the sea are 0.3–0.9%, and these values increase to 1–1.5% near the shores and to >2% in the estuaries.

Table 9. Contents of particulate matter and dissolved organic carbon and the concentrations and isotopic composition of carbon in particulate matter and dissolved HCO_3^- in the waters of the Ob and Yenisei estuarine zones adjacent to the Kara Sea. Samples were collected in September of 1997, R/V *Akademik Boris Petrov*-1997

Site	Depth, m	S, g/l	Particulate matter content, mg/l	Dissolved carbon content, mg/l	C_{org} concentration		$\delta^{13}C$, ‰	
					in water, μg/l	in particulate matter, %	C_{org} of particulate matter	HCO_3^-
*Kara Sea–Ob River profile**								
97–12	1	3.1	6.23	-	590	9.5	–28.8	–10.7
	8	3.8	7.51	-	691	9.2	–29.0	–6.5
	12	20.1	15.3	-	3160	20.6	–29.7	–9.1
97–10	1	2.4	4.62	5.69	404	8.7	–30.7	–10.7
	10	3.3	4.02	5.64	362	9.0	–29.4	–9.2
	11.5	25.1	7.58	4.42	379	5.0	–29.8	–
	13	25.0	6.45	–	259	4.0	–28.9	–4.7
97–17	1	7.0	7.4	6.11	893	12.1	–28.4	–11.3
	5.1	14.0	5.4	5.11	562	10.4	–27.8	–10.0
	9.0	29.3	7.6	5.11	809	10.6	–28.7	–
	16.0	29.8	5.6	3.00	354	6.3	–28.6	–4.5
97–01	1	12.7	–	6.57	522	–	–26.9	–7.2
	7.4	13.0	–	4.84	312	–	–27.0	–5.2
	9.9	25.7	–	2.32	193	–	–27.4	–
97–47	1	18.9	–	–	141	–	–29.6	–6.4
	10.1	29.4	–	–	244	–	–28.9	–
	16.0	29.6	–	–	244	–	–29.7	–
97–48	1	13.5	1.43	–	228	15.9	–27.6	–
	7.0	16.5	2.33	–	242	10.4	–27.5	–
	10.9	30.3	3.74	–	202	5.4	–27.9	–
	23.9	31.4	5.04	–	248	4.9	–27.3	–
97–49	1	16.4	2.0	–	329	16.5	–28	–5.3
	11.1	22.6	1.53	–	176	11.5	–27.2	–6.3
	15.9	30.5	2.34	–	173	7.4	–25.8	–9.2
	27.0	31.6	13.04	–	379	2.9	–25.6	–
97–50	1	20.8	0.84	–	219	26.0	–26.6	–8.5
	9.4	20.8	1.08	–	256	23.7	–26.7	–
	14.2	31.5	2.34	–	150	6.4	–26.3	–6.9
	26.0	31.8	4.58	–	154	3.4	–26.6	–4.4
97–52	1	18.2	0.64	–	185	29.1	28.2	–
	7.0	22.1	0.64	–	196	30.4	–27.1	–
	10.0	31.0	0.92	–	105	11.4	–27.0	–
	27.0	31.8	9.3	–	360	3.9	–26.4	–
Kara Sea–Yenisei River profile								
97–32	1	1.2	4.42	–	248	5.6	–28.2	–8.3
	5.0	1.2	4.67	–	191	4.1	–27.6	–7.3
	8.0	1.3	4.74	–	157	3.3	–28.8	–
97–30	1	4.0	3.57	–	221	6.2	–27.8	–6.2
	5	4.7	3.84	–	122	3.2	–27.9	–8.6
	10	5.8	2.66	–	186	7.0	–27.6	–

Table 9. (Contd.)

Site	Depth, m	S, g/l	Particulate matter content, mg/l	Dissolved carbon content, mg/l	C_{org} concentration		$\delta^{13}C$, ‰	
					in water, μg/l	in particulate matter, %	C_{org} of particulate matter	HCO_3^-
	13	12.2	2.50	–	–	–	–27.4	–5.4
97–27	1	4.2	1.89	4.4	146	7.7	–27.3	–7.6
	8	8.0	3.78	5.3	377	10.0	–26.6	–6.5
	18	23.0	11.04	2.9	265	2.4	–27.4	–3.5
97–24	112	11.9	1.50	4.3	294	19.6	–26.7	–6.0
	20	16.0	1.04	4.5	181	17.6	–26.1	–5.3
	35	30.3	3.58	2.5	176	4.9	–25.0	–
		31.8	9.23	2.7	397	4.3	–26.1	–2.4
97–21	1	14.8	1.24	4.2	265	21.4	–25.4	–6.2
	10	17.4	1.13	3.9	263	23.2	–26.4	–4.5
	15	30.1	2.80	3.2	221	7.9	–24.6	–
	35	32.6	10.47	3.6	178	1.7	–25.4	–2.9
97–42	1	14.9	–	–	276	–	–25.6	–4.2
	11	15.3	–	–	310	–	–25.1	–3.8
	20	30.8	–	–	204	–	–14.9	–
	28	31.9	–	–	208	–	–25.7	–2.8
97–43	1	10.6	–	–	134	–	–26.4	–6.7
	20	18.2	–	–	–	–	–25.1	–4.1
	28	32.1	–	–	247	–	–24.5	–4.0

* Sites 97-01 through 97–17 were studied on September 13–15, and Sites 97–47 through 97–52 were studied in September 22–24. The time span between these two periods of works in Obskaya Guba was marked by the intensification of the Yamal Current and, consequently, a drastic change in the salinity of the whole water mass.

Table 10. Concentrations and isotopic composition of organic carbon in particulate matter from water samples collected along the Yenisei–Kara sea profile. Samples were collected in September of 2000, R/V *Akademik Boris Petrov*-2000

Site	Sampled level (depth, m)	S, g/l	C_{org} concentration in particulate matter, μg/l	$\delta^{13}C_{org}$ of particulate matter, ‰
00–19	Surface	0.0	282	–30.4
	Bottom (21.7)	0.0	135	–30.4
00–18	Surface	0.0	206	–30.3
	Bottom (15.0)	0.0	171	–30.9
00–20	Surface	0.0	180	–30.1
	Bottom (17.0)	5.7	303	–30.3
00–17	Surface	0.0	207	–29.3
	Bottom (17)	0.4	338	–30.9
00–21	Surface	0.2	374	–30.3
	Pynocline (12.0)	5.6	231	–29.4
	Bottom (24.5)	22.9	705	–27.6
00–16	Surface	2.3	247	–29.3
	Pynocline (15.5)	13.3	209	–28.4
	Bottom (23.0)	20.1	378	–28.4
00–15	Surface	6.7	354	–28.4
	Bottom (6.5)	7.3	144	–27.9
00–22	Surface	6.6	391	–29.7
	Pynocline (3.7)	11.6	169	–28.6
	Bottom (10.0)	29.9	69	–27.3
00–13	Surface	22.8	111	–27.8
	Pynocline (11.5)	25.5	73	–27.0
	Bottom (31.0)	29.6	337	–27.4
00–23	Surface	28.4	144	–26.1
	Pynocline (12.0)	30.7	58	–26.6
	Bottom (24.5)	33.0	63	–26.4
00–24	Surface	23.7	122	–26.7
	Pynocline (11.5)	26.0	35	–26.6
	Bottom (32.0)	32.3	25	–26.1
00–07	Surface	16.5	141	–27.5
	Pynocline (12.0)	25.3	33	–25.9
	Bottom (24.5)	32.8	167	–26.9
00–08	Surface	21.0	166	–27.0
	Pynocline (9.5)	26.4	–	–26.4
	Bottom (37.0)	33.3	78	–25.8
00–09	Surface	23.8	–	–26.4
	Pynocline (14.0)	27.9	81	–25.2
	Bottom (44.0)	33.5	46	–24.4
00–35	Surface	26.6	73	–25.5
	Pynocline (14.5)	30.4	110	–25.2
	Bottom (46.0)	33.5	133	–26.1
00–30	Surface	24.9	–	–26.7
00–28	Surface	25.6	89	–27.3
	Pynocline (16.0)	29.2	23	–26.6
	Bottom (47.0)	34.1	63	–25.3
00–29	Surface	27.3	51	–26.1
00–36	Surface	27.2	–	–26.4
	Pynocline (17.5)	31.2	45	–
	Bottom (64.0)	33.9	60	–26.1

Table 11. Isotopic composition of organic carbon in particulate matter from surface water sampled along the Ob–Kara sea and Yenise–Kara Sea meridional profiles. Samples were collected in 2000, R/V *Akademik Boris Petrov*-2000

Site	Latitude, N	$\delta^{13}C$, ‰
Ob River–Kara Sea profile		
01–78	68°40′	–30.8
01–73/3	68°50′	–29.9
01–73	68°54′	–30.2
01–79	69°03′	–29.2
01–72	70°49′	–29.3
01–80	72°15′	–28.4
01–70	72°40′	–29.4
01–82	73°12′	–28.7
01–68	74°35′	–29.0
01–66	75°10′	–27.4
01–67	75°14′	–28.0
01–64	75°53′	–27.6
01–62	76°12′	–26.2
01–61	76°13′	–27.1
01–59	76°31′	–27.6
01–58	76°48′	–26.4
01–56	76°59′	–25.9
01–46	77°55′	–26.0
Yenisei River–Kara Sea profile		
01–08	70°04′	–32.3
01–05	70°45′	–31.7
01–04	71°05′	–32.1
01–16	71°41′	–31.3
01–11	72°10′	–30.8
01–19	72°35′	–28.9
01–23	73°29′	–29.6
01–26	74°00′	–27.2
01–43	75°23′	–27, 9
01–41	75°41′	–26.7
01–28	75°56′	–27.2
01–30	76°25′	–27.2
01–38	77°05′	–26.6
01–45	77°06′	–26.5
01–31	77°34′	–27.7
01–48	77°53′	–27.3
01–34	77°54′	–25.9
01–35	77°54′	–26.2

Table 12. Isotopic composition of organic carbon in bottom sediments of the Kara Sea

Site	Coordinates		Depth, m	C_{org}, %	$\delta^{13}C$ (‰)	Site	Coordinates		Depth, m	C_{org}, %	$\delta^{13}C$ (‰)
	Latitude, N	Longitude, E					Latitude, N	Longitude, E			
95–30	70°18′	56°33′	87.5	0.43	–22.5	95–78	72°17′	80°18′	8	1.75	–
95–31	71°27′	58°36′	225	1.64	–23.4	95–79	72°17′	80°34′	8.5	1.81	–27.1
95–32	71°23′	56°40′	170	1.32	–24.1	95–80	72°19′	80°49′	9	2.06	–27.1
95–33	72°05′	57°31′	328	0.99	–23.1	95–84	73°45′	75°20′	17	1.22	–26.0
95–34	72°04′	59°58′	110	1.18	–	95–85	73°54′	74°02′	17	0.33	–25.7
95–35	72°18′	56°09′	206	1.10	–23.3	95–86	73°35′	73°12′	24	1.50	–26.3
95–36	72°32′	55°48′	66	0.60	–24.1	95–87	73°20′	72°30′	17	1.65	–
95–37	72°44′	56°00′	60	1.26	–	95–88	73°11′	72°52′	26	0.80	–26.3
95–38	72°38′	57°39′	355	1.20	–	95–89	72°52′	73°45′	23	0.93	–27.1
95–39	73°17′	59°59′	333	1.17	–23.9	95–90	72°52′	73°20′	23	–	–26.6
95–40	73°15′	58°50′	333	1.23	–22.5	95–91	72°52′	72°54′	20	0.78	–27.6
95–41	73°22′	57°47′	242	1.12	–24.4	95–92	73°15′	73°1 8′	19	1.73	–
95–42	73°59′	60°36′	275	1.72	–23.1	95–93	73°30′	73°34′	14	0.49	–
95–43	74°11′	59°44′	285	1.31	–23.4	95–94	73°47′	72°47′	24	0.57	–25.6
95–44	74°25′	60°32′	308	0.99	–23.5	95–95	74°01′	72°10′	18.6	0.25	–25.6
95–45	74°32′	59°34′	72.5	1.44	–23.6	95–96	74°35′	71°49′	26	1.20	–25.2
95–46	74°40′	60°04′	61.5	1.21	–23.7	95–97	74°28′	68°21′	150	0.88	–25.2
95–47	74°38′	61°29′	200	1.32	–23.7	95–98	73°56′	65°23′	177	1.30	–23.4
95–48	75°20′	62°55′	190	1.20	–23.3	95–99	73°27′	62°49′	119	1.19	–23.0
95–49	74°52′	65°43′	219	1.17	–23.2	95–100	73°12′	61° 29′	171	1.41	–23.1
95–50	75°36′	63°40′	134	1.12	–23.9	95–101	72°52′	62°59′	88	0.66	–23.9
95–51	75°30′	65°39′	335	1.18	–23.3	95–102	72°45′	64°18′	49	0.36	–23.4
95–52	75°10′	67°54′	191	0.57	–23.5	95–103	72°29′	65°46′	136	1.58	–23.8
95–53	75°38′	66°50′	306	0.63	–23.2	95–104	72°02′	62°58′	100	1.40	–22.8
95–54	75°57′	66°22′	40	0.84	–	95–105	71°50′	61°43′	148	1.15	–22.4
95–55	76°16′	70°10′	134	0.62	–24.4	95–106	71°34′	63°44′	109	0.81	–
95–56	76°28′	70°26′	216	1.20	–24.5	95–107	72°22′	65°23′	115	1.50	–24.4
95–57	76°55′	69°13′	416	–	–22.6	95–108	71°14′	66°02′	25	0.08	–
95–58	76°58′	70°05′	569	2.12	–22.6	95–109	70°1 8′	65°05′	43	1.07	–24.2
95–59	77°07′	71°40′	272	1.58	–23.4	95–110	69°49′	65°55′	28	0.77	–23.9
95–60	76°59′	74°50′	195	0.96	–23.2	95–111	69°08′	67°03′	28	0.66	–24.7
95–61	76°51′	78°55′	56	0.98	–23.2	95–112	69°44′	65°25′	32	0.94	–24.2
95–62	76°45′	82°00′	53	0.52	–23.6	95–113	69°50′	63°35′	33	0.53	–24.2
95–63	76°35′	79°35′	59–61	0.39	–24.0	95–114	69°55′	61°31′	46	1.25	–24.2
95–64	76°15′	72°30′	62	0.54	–24.0	95–115	70°28′	61°53′	227	1.49	–23.2
95–65	75°46′	74°20′	57	0.63	–24.3	95–116	70°50′	60°31′	139	1.88	–23.8
95–66	75°28′	72°07′	102	1.26	–24.7	95–117	71°04′	59°25′	190	1.00	–24.3
95–67	75°15′	73°43′	44	1.08	–24.7	95–118	70°51′	58°19′	203	1.63	–23.6
95–68	74°22′	74°58′	26	0.41	–25.3	95–119	69°56′	57°60′	40	0.24	–24.6
95–69	74°18′	77°17′	30	0.12	–25.4	95–120	70°15′	57°01′	110	0.58	–22.4
95–70	74°17′	78°43′	28	1.11	–25.6	95–121	70°10′	54°46′	133	–	–22.4
95–71	74°12′	81°36′	33	1.92	–26.4	95–122	70°25′	53°36′	165	–	–22.6
95–72	73°54′	79°11′	26	0.92	–25.4	97–01	73°54′	73°11′	31	–	–25.19
95–73	73°30′	79°50′	34	1.74	–26.6	97–09	72°40′	73°46′	21	–	–27.34
95–74	73°12′	79°50′	29	–	–26.3	97–10	72°30′	74°09′	15	–	–28.70
95–75	72°53′	80°20′	13	2.21	–26.8	97–12	72°10′	74°17′	13	–	–28.16
95–76	72°35′	80°20′	11	2.34	–25.7	97–15	72°38′	73°50′	19	–	–27.68
95–77	72°35′	79°10′	9	1.85	–26.7	97–18	73°57′	76°08′	25	–	–26.42

Table 12. (Contd.)

Site	Coordinates		Depth, m	C_{org}, %	$\delta^{13}C$ (‰)	Site	Coordinates		Depth, m	C_{org}, %	$\delta^{13}C$ (‰)
	Latitude, N	Longitude, E					Latitude, N	Longitude, E			
97–21	74°00′	81°00′	41	–	–24.26	01–19	72°36′	80°06′	28	–	–27.28
97–27	72°53′	80°05′	19	–	–25.83	01–22	73°22′	78°03′	15	0.12	–24.10
97–29	72°41′	80°12′	16	–	–25.97	01–23	73°29′	78°51′	22	–	–26.50
97–30	72°30′	80°20′	14		–25.89	01–25	73°25′	79°40′	28	1.63	–26.80
97–31	72°19′	80°36′	13	–	–26.76	01–26	74°00′	80°01′	33	–	–25.82
97–32	72°05′	81°29′	10		–26.34	01–28	75°56′	89°16′	51	1.50	–22.17
97–34	72°26′	80°24′	12	–	–26.21	01–33	77°30′	87°35′	83	0.42	–22.95
97–37	72°58′	80°05′	20	–	–26.45	01–34	77°54′	89°20′	91	–	–22.21
97–39	73°33′	79°55′	40		–25.84	01–35	77°54′	83°46′	160	0.85	–22.35
97–42	73°54′	81°40′	32	–	–25.50	01–40	76°25′	85°40′	52	1.40	–23.50
97–43	73°42′	82°48′	31	–	–24.82	01–41	75°41′	87°08′	42	–	–23.46
97–46	73°60′	77°12′	27	–	–25.23	01–43	75°23′	85°50′	48	1.40	–24.60
97–47	72°35′	73°44′	18	–	–28.21	01–45	77°07′	84°44′	87	1.23	–22.88
97–48	72°57′	73°09′	29	–	–26.43	01–46	75°55′	75°57′	323	1.19	–22.79
97–49	72°53′	73°12′	29	–	–26.67	01–48	77°53′	81°30′	202	–	–22.71
97–50	72°57′	73°36′	28	–	–25.74	01–49	77°09′	81°05′	198	1.16	–24.90
97–52	72°39′	74°00′	30	–	–25.40	01–51	77°55′	79°29′	158	0.78	–23.64
97–53	73°37′	74°52′	21	–	–27.03	01–52	77°05′	79°09′	75	1.04	–24.16
97–54	73°20′	75°20′	15	–	–25.78	01–57	76°53′	76°36′	113	0.88	–24.41
97–55	73°13′	75°37′	14	–	–26.31	01–58	76°48′	78°21′	94	1.14	–24.58
97–56	72°53′	75°29′	14	–	–27.70	01–59	76°48′	74°31′	176	–	–
97–58	73°39′	74°50′	23	–	–25.66	01–62	76°12′	74°12′	135	–	–24.24
99–19	74°00′	79°01′	30	–	–28.63	01–65	75°43′	75°51′	63	0.75	–23.64
00–06	75°10′	81°00′	38	–	–25.06	01–68	74°35′	72°15′	31	–	–24.46
00–07	74°39′	81°08′	38	–	–25.24	01–64	75°53′	73°39′	99	–	–24.67
00–15	72°01′	81°36′	12	–	–27.03	01–66	75°10′	76°55′	55	1.50	–25.47
00–17	71°06′	83°05′	17	–	–27.97	01–67	75°15′	73°46′	49	–	–25.38
00–22	72°34′	79°55′	15	–	–26.85	01–70	72°40′	74°00′	22	–	–27.44
00–23	73°28′	79°51′	22	–	–26.45	01–71	72°40′	73°18′	23	0.50	–27.82
00–26	75°42′	77°58′	88	–	–27.91	01–72	70°50′	73°44′	26	0.45	–27.20
01–11	72°02′	81°42′	12	–	–26.11	01–73	68°50′	73° 43′	8	–	–30.31
01–13	71°53′	82°33′	11	1.14	–26.49	01–80	72°15′	73°15′	16	–	–28.91
01–18	72°05′	79°03′	13	1.77	–	01–82	73°12′	73° 02′	29	–	–27.46

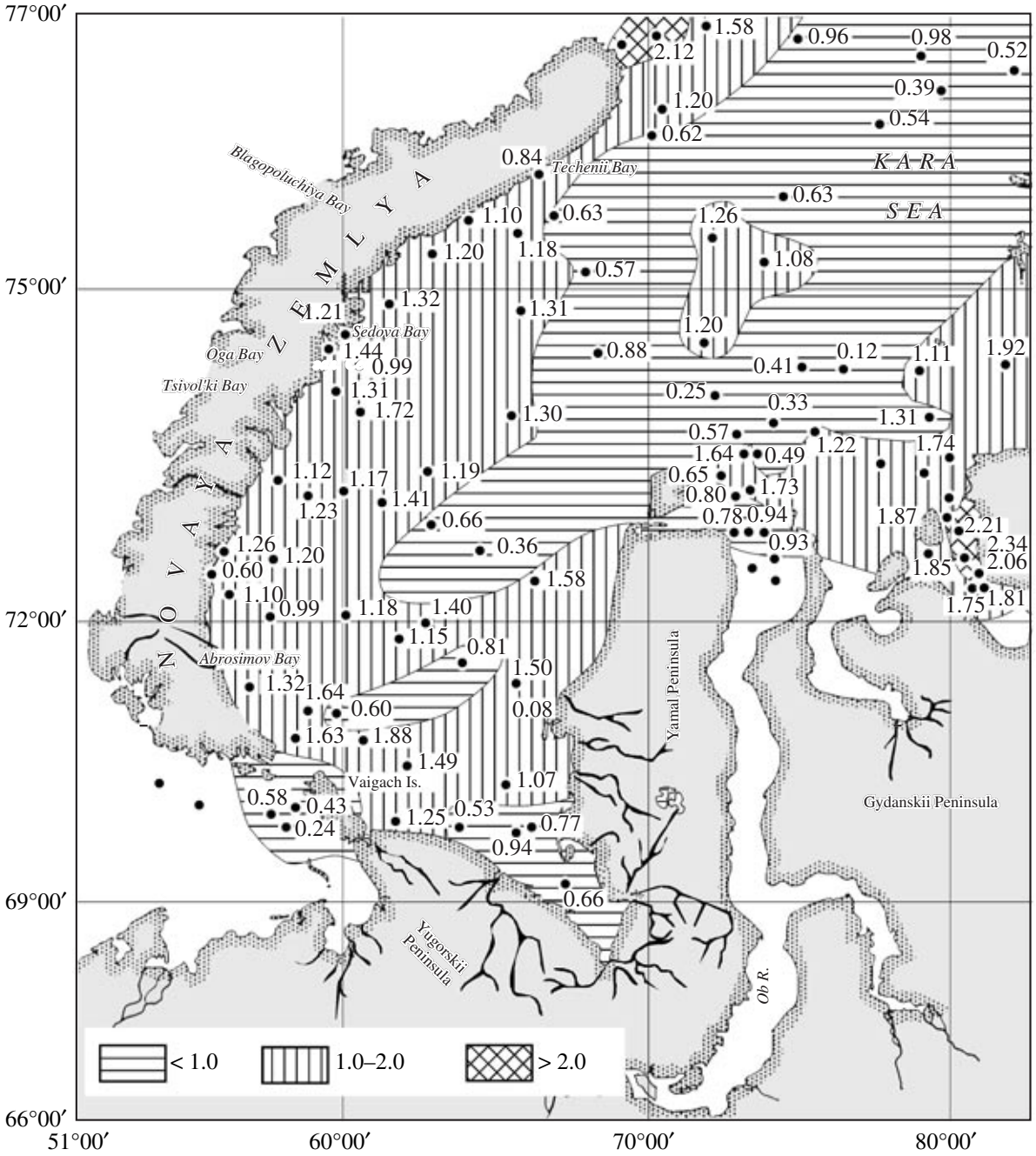

Fig. 12. Organic carbon concentrations C_{org} (%) in the upper layer of bottom sediments in the Kara Sea.

The carbon isotopic composition broadly varies (Fig. 13). The lowest values (from –27 to –30‰) characterize organic carbon in the mouths of the Ob and Yenisei rivers. The highest $\delta^{13}C$ values (from –22.5 to –23.5‰) typically occur where Atlantic waters enter the Kara Sea: at the northern tip of Novaya Zemplya and in the Kara Strait in the south as well as in the northen and north-eastern marginal part of the sea. The observed zoning is in principle quite trivial: marine planktonogenic material is isotopically heavy, and rivers provide isotopically light terrigenous organic carbon.

The utilization of other parameters characterizing biogenic carbon allowed us to reveal additional details. For example, some samples were analyzed (together with researchers from the Institute of Oceanology) for lignin monomers and the relative concentrations of individual normal alkanes [54].

Lignin is typically contained in terrestrial plants and was not found in plankton. Because of this, this com-

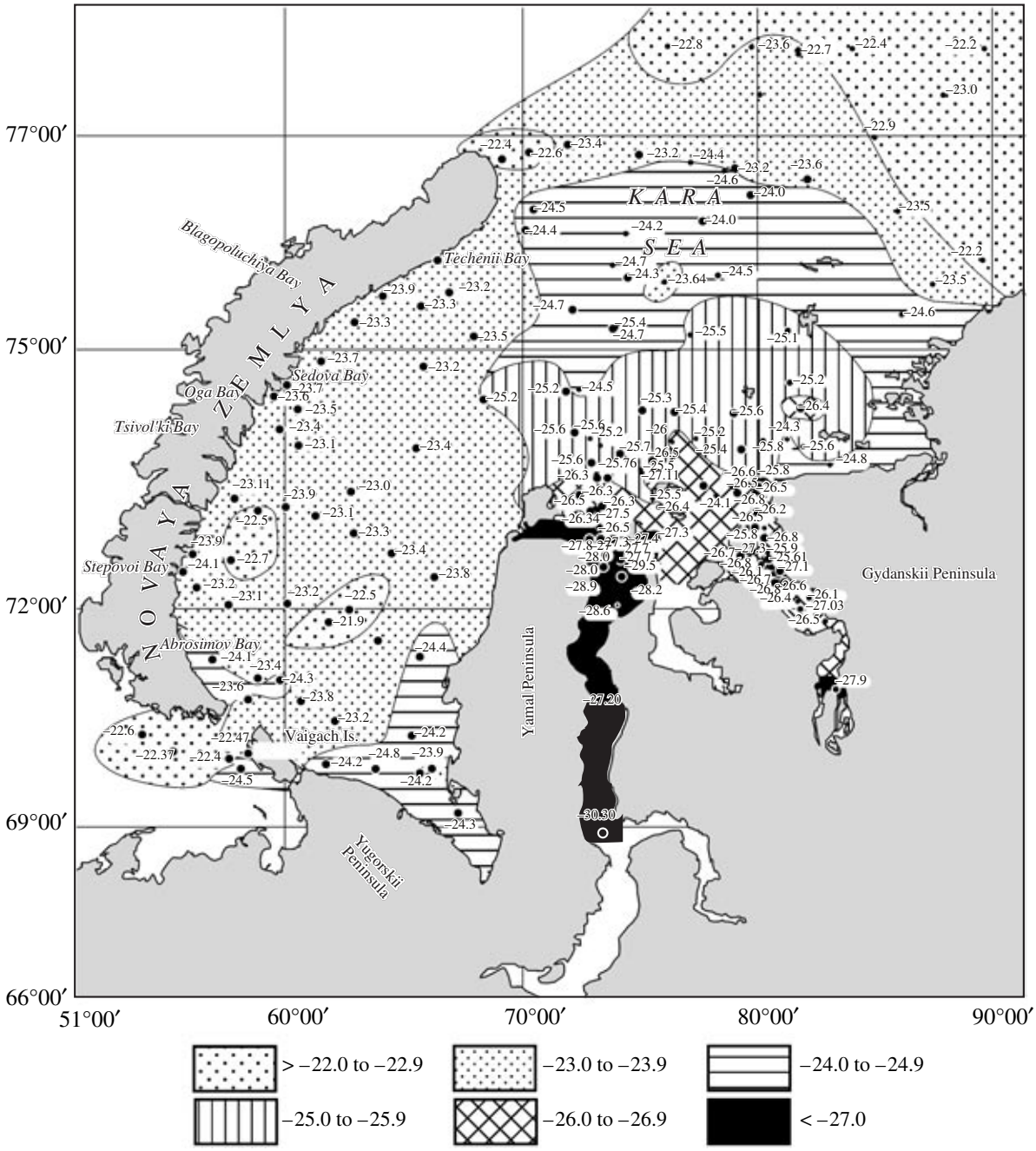

Fig. 13. Isotopic composition of organic carbon ($\delta^{13}C_{org}$) in the upper layer of bottom sediments in the Kara Sea.

pound is a good indicator of the contribution of the terrigenous component. Another parameter is the distribution of normal alkanes. Terrigenous organic matter is characterized by elevated concentrations of high-molecular alkanes C_{25}–C_{31}, with a pronounced difference between the concentrations of even and odd alkanes. The concentrations of high-molecular alkanes in planktonogenic matter are insignificant, whereas the concentrations of alkanes within the molecular-mass range of C_{14}–C_{19} strongly increase. Figure 14 schematically represents the distribution character of normal alkanes and the lignin concentration. The sides of the rectangles are proportional to the concentrations of vanillin-guaiacyl monomer of lignin (in μg/g).

As could be expected, in the Ob and Yenisei mouths, all of the three parameters consistently point to a predominantly terrigenous source of the organic carbon, and one can readily discern areas with the predominant contribution of planktonogenic material in the northern and northwestern parts of the Kara Sea. These waters

contain isotopically heavy carbon and practically no lignin and are characterized by the corresponding distribution of normal alkanes.

The organic matter is often of intermediate character, particularly at sites relatively close to the sources of terrigenous material. The mixed nature of material at these sites is quite natural, but the combinations are in places more complicated.

Unexpectedly high concentrations of the aromatic lignin monomer were detected in seemingly typical marine samples with relatively high concentrations of the ^{13}C isotope ($\delta^{13}C$ from –22.4 to –22.5‰) of Novaya Zemlya to the North. In other words, these two correlated parameters are in conflict. The possible reason for this is that terrigenous material at high latitudes can contain admixtures of remnants of primitive plants: mosses and lichens, which often have an isotopic composition unusual for terrestrial plants. For example, Antarctic lichens have $\delta^{13}C$ from –22 to ‰ at an average of –22.5‰ [55]. An admixture of such terrigenous material should not result in the enrichment of C_{org} in the light isotope relative to the planktonogenic material.

In contrast to other oceanic areas, an important factor affecting the biogeochemistry of Arctic seas is the ice cover and its dynamics. The Kara Sea is an area where drift ice is formed, with about 230 000 km^2 of ice annually transferred from there to the Laptev and Barents seas. The ice carries significant amounts of organic and finely dispersed mineral material. The ice-transported organic matter can account for a significant fraction of marine particulate material in the sediments. For instance, the frequent enrichment of the organic carbon of particulate matter in the light isotope in areas remote from sources of terrigenous material can be explained by this phenomenon.

It is hard to expect that a basin such as the Kara Sea with a heterogeneous composition of carbon sources can have similar isotopic compositions of organic carbon in the sediments, plankton, and particulate matter that simultaneously occur at a given moment of time at the sea surface, although this consistency can be observed in more stable environments, with an insignificant (within1–2‰) shift in the isotopic composition due to isotopic fractionation during the transformations of organic matter from biopolymers to geopolymers [56].

Table 13 summarizes data characterizing the changes in the organic carbon isotopic composition in the vertical section of the water column from plankton to sediments at some sites in the Yenisei and Ob meridional profiles, from the estuaries toward open sea. As can be seen from this table, the isotopic composition of the near-bottom particulate matter is practically identical with the isotopic composition of

Table 13. Variations in the isotopic composition of organic carbon in the vertical section of waters, from plankton to sediment, along the Yenisei River–Kara Sea and Ob River–Kara Sea profiles

Site (latitude)	Plankton	Particulate matter in water			Near-bottom particulate matter	Sediment (0–1 cm)
		surface	pycnoline	bottom		
Yenisei River–Kara Sea						
01–11 (72° N)	–30.64	–30.20	–29.58	–28.60	–26.78	–26.10
01–26 (74° N)	–	–26.73	–27.09	–24.25	–25.83	–26.20
01–43 (75.4° N)	–27.38	–	–25.50	–23.71	–24.79	–24.60
01–45 (77.2° N)	–27.06	–25.30	–24.20	–25.57	–23.69	–22.88
01–45 (77.2° N)	–27.06	–25.30	–24.20	–25.57	–23.69	–22.88
Ob River–Kara Sea						
01–72 (70.72° N)	–29.77	–29.36	–	–29.18	–	–26.50
01–80 (72.2° N)	–27.8	–28.72	–29.04	–29.53	–29.68	–28.92
01–70 (72.7° N)	–27.7	–29.4	–28.18	–29.03	–28.57	–27.44
01–68 (74.6° N)	–27.57	–28.98	–28.15	–27.75	–24.79	–24.07
01–66 (75.2° N)	–	–27.44	–26.86	–27.30	–25.03	–25.77
01–46 (77.9° N)	–25.49	–26.0	–26.03	–26.23	–23.12	–22.79

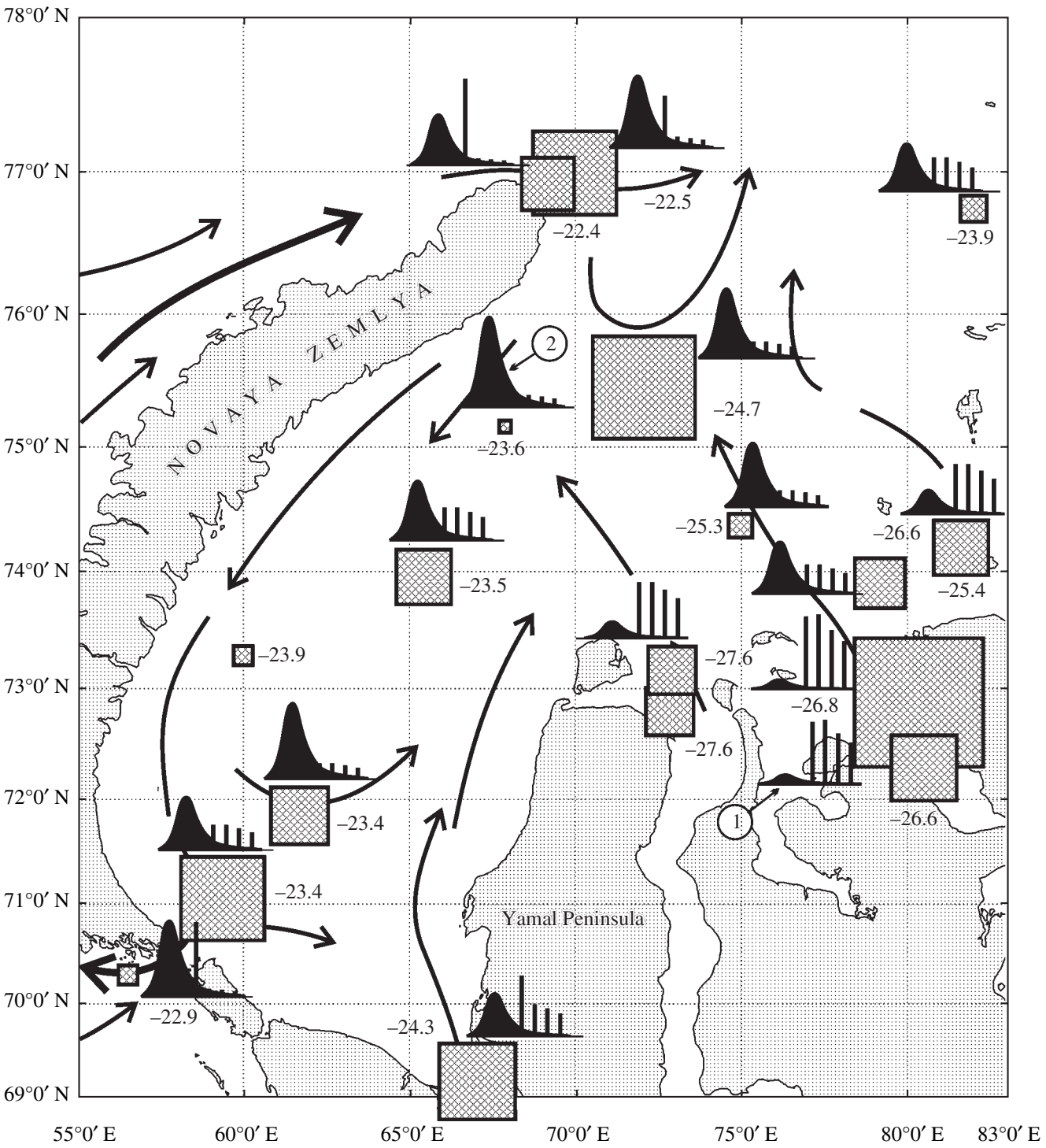

Fig. 14. Relative contents of lignin (shaded square whose side is proportional to the concentration of the vanillin component, μg/g) and C_{14}–C_{19} (black areas) and C_{25}–C_{31} (bars) alkanes in comparison with the $\delta^{13}C_{opr}$ of the corresponding sediments.

organic carbon in the uppermost 1-cm layer of the sediments. Conceivably, the near-bottom particulate matter resulted from the roiling of the sediment. The isotopic composition of the plankton from the profiles in question is 3–4‰ isotopically lighter than the isotopic composition of the sediment, a fact suggesting that the phytoplanktonic carbon is not the immediate and predominant precursor of the organic carbon of the sediments. A fairly stable correlation was detected between the isotopic composition of organic carbon in

the pycnocline and organic carbon in the sediment, with a discrepancy of approximately 1–2‰.

8. HYDROCARBONS

8.1. Hydrocarbon Gases in Water

In contrast to earlier studies [57], which were constrained to measuring the methane concentrations, we separated the whole complex of hydrocarbon gases from the waters, including methane homologues up to C_5 inclusive, as well as unsaturated hydrocarbons and isoalkanes. We also examined the molecular composition of the gases in the vertical profile of the river and seawater. Moreover, a complex of hydrocarbon gases was separated from the Holocene sediments. The water and sediments were determined to contain, along with methane C_1, also ethane C_2, ethylene $C_{2=}$, propane C_3, propylene $C_{3=}$, *n*-butane C_4, isobutane *i*-C_4, butylene $C_{4=}$, pentane C_5, and isopentane *i*-C_5. The results of these studies are summarized in Tables 14–17. Details of the methods used in this research were published in [8].

The methane concentrations in the waters are commonly relatively low. With a few exceptions, including instances for which it is reasonable to suggest methane inflow from sediments, its concentrations in the waters vary from 0.5 to 3 μl/l. The concentrations in the estuarine waters (3–4 μl/l) are a little bit higher than in the marine waters (0.5–2 μl/l). The concentration slightly increases at the geochemical barrier (to 6–8 μl/l) and in the pynocline waters, where destruction processes intensify (tables). Figure 15 illustrates the CH_4 distribution in the waters along the meridional profile from the Yenisei to Kara Sea.

An analogous methane distribution in the Ob–Kara Sea profile was detected in 2001. The methane concentration varied in 2001 from 0.3 to 6.6 μl/l in the riverine and estuarine parts of the profile and from 0.1 to 1.1 μl/l in its marine part (Table 17). Elevated methane concentrations were spatially restricted to shallow-water sites in Taz Bay. In this situation, the elevated C_1 concentration in the bottom water could be caused by the vertical gas inflow from the sediments. The sediments of this site at the seafloor surface (0–2 cm) contained 1.9 ml/l methane, and this concentration reached 13 ml/l at a depth of 40 cm. The methane is biogenic, as follows from its isotopically light composition in the surface sediment layer ($\delta^{13}C = -105‰$). The water mixing zone in the Ob estuary during our expedition covered virtually the whole Obskaya Guba, the hydrological front area is pronounced unclearly at the surface and extended from 72°N (Site 01-80) to 73° (Suite 01-82), and the water of the bottom layer extended upstream and was detected south of 71°N. The methane concentration in the surface and bottom waters decreases to 0.3–0.5 μl/l south of 73°N (Sites 01-80 through 01-70)

Table 14. Concentrations of hydrocarbon gases in waters along the Yenisei–Kara sea meridional profile. Samples were collected by the 1997 expedition aboard the R/V *Akademik Boris Petrov*

Site	Sampling depth, m	*T*, °C	S, g/l	$C_{part.}$, μg/l	Concentration ml/l × 10^{-4}			
					CH_4	$C_2 - C_4$	$C_{2=} - C_{4=}$	C_5
97–32	0	7.8	1.2	248	18.4	1.1	0.8	2.8
	5	7.8	1.2	191	19.1	0.7	0.5	1.4
	8	7.8	1.2	157	16.0	0.2	0.2	0.5
97–30	0	7.3	4.0	221	3.0	0.5	0.7	2.8
	5	7.1	4.7	122	15.1	0.3	0.2	0.8
	12	4.9	12.2	–	9.5	0.3	0.2	0.4
97–27	0	6.6	4.9	146	16.1	0.7	0.4	0.9
	8	6.1	8.0	877	0.5	0.2	0.5	5.5
	14	2.4	23.1	265	0.5	0.4	0.4	0.9
97–24	0	6.1	11.9	294	7.4	0.5	0.5	2.2
	12	5.2	16.0	181	4.2	0.8	0.6	0.9
	20	–0.3	30.3	176	5.6	0.6	0.1	1.2
	35	–1.2	31.8	397	6.4	traces	traces	0.0
97–21	0	5.6	15.3	265	6.7	0.4	0.4	0.9

Table 15. Distribution of hydrocarbon gases in the vertical section of waters in the Yenisei–Kara Sea system, September of 2000, R/V *Akademik Boris Petrov*

Site	Sampling depth, m	Concentration µl/l	
		CH_4	$C_4 + C_5$
00–19	0	3.12	1.33
	21.5 (bottom)	2.94	
00–18	0	2.28	0.7
	17 (bottom)	3.78	0.7
00–20	0	3.85	1.3
	19 (pycnocline)	2.85	–
00–17	0	4.37	1.96
00–21	11 (pycnocline)	4.38	1.5
00–15	6.5 (pycnocline)	4.20	1.0
00–22	0	0.82	0.5
	3.5	8.52	1.0
	10 (bottom)	5.92	1.3
00–13	0	0.94	0.57
	13 (bottom)	0.69	2.47
00–23	0	0.51	–
	30 (bottom)	1.7	1.0
00–24	0	0.51	0.43
	11	0.42	0.12
	30 (bottom)	0.71	0.27
00–07	0	1.49	1.15
	11	2.11	–
	35	2.11	2.73
00–08	0	0.58	–
	–	–	0.98
	39	2.47	–
00–35	–	–	–
	16 (pycnocline)	0.75	0.22
00–30	0	0.89	0.19
	27	1.05	0.24
	50	0.70	0.27
00–36	0	0.85	0.7
	15	1.15	0.69
	63	1.82	0.43

Table 16. Distribution of methane and its higher homologues in the waters of the Yenisei–Kara Sea profile as of August 14 to September 11, 2001, R/V *Akademik Boris Petrov*-2001

Site	Depth, m	S(g/l)	Concentration µl/l		
			CH_4	$C_2 – C_5$	$C_4 + C_5$
01–14	0	0.0	1.7	1.4	1.1
	18	0.0	1.8	1.1	0.8
01–11	0	0.0	1.5	2.1	1.9
	pycnocline	0.5	0.8	0.6	0.4
	bottom	16.4	0.9	2.0	1.9
01–19	0	4.1	0.5	0.8	0.7
	5	28.1	0.6	0.7	0.6
	23	32.5	0.4	0.9	0.7
01–23	0	4.8	1.0	2.7	2.2
	5	11.7	1.0	2.7	2.1
	18	32.9	0.8	1.4	1.1
01–26	0	–	0.8	3.5	2.7
	5.5	12.3	0.2	1.7	1.4
	29	17.5	0.5	3.4	1.3
	bottom	33.2	0.6	2.3	1.8
01–43	0	–	0.8	4.1	3.3
	10	20.5	0.5	2.3	2.0
	40	24.5	0.7	1.6	1.3
	bottom	33.4	0.7	2.0	1.5
01–28	0	–	0.4	2.6	2.0
	17	22.6	0.5	1.7	1.2
	50	30.4	0.5	2.3	1.7
	bottom	33.4	0.4	1.5	1.1
01–30	12	27.3	0.2	0.6	0.5
	46	30.2	0.5	1.1	0.8
	bottom	33.8	0.6	1.5	1.2
01–38	0	28.9	0.3	1.4	1.1
	14	29.7	0.8	5.4	4.2
	100	34.1	1.0	5.5	4.2
01–31	0	29.1	0.2	2.7	2.1
	15	30.2	0.2	0.5	0.4
	bottom	33.8	0.2	0.6	0.4
01–34	0	–	0.6	2.7	2.1
	19	29.1	0.6	3.1	2.6
	90	31.5	0.4	1.5	1.1
	bottom	34.0	0.8	2.0	1.4
01–35	0	28.4	0.3	1.2	0.9
	17	31.7	0.5	1.2	0.9
	bottom	34.3	0.7	3.1	2.2
01–48	0	26.1	0.5	1.5	1.2
	15	32.0	0.5	1.6	1.3
	187	34.5	0.4	1.6	1.3

and remains at this level throughout the whole northern part of the profile at salinity variations from 10 to 25.

The concentrations of saturated C_2–C_4 hydrocarbons (ethane, propane, i-butane, and n-butane) in the hydrocarbons dissolved in seawater varies from 0.3 to 13.0%. A close proportions (from 0.3 to 100%) in the gases are typical of alkenes $C_{2=}$–$C_{4=}$ (ethylene, propylene, and butylene). The concentration of C_5 in the water varies from 0 to 0.5 μl/l, which sometimes amounts to 40% of the overall concentration of hydrocarbon gases. The variations in the contents of C_2–C_5 hydrocarbons along the Yenisei–Kara Sea profile are displayed in Fig. 16.

The geochemistry of hydrocarbon gases in surface freshwater is characterized by comparable contents of methane and heavier hydrocarbons, including unsaturated ones. The total concentration of C_2–C_5 hydrocarbons in the sea waters is comparable with the methane concentration or is sometimes higher than it.

This is obviously explained by the fact that methane, like other low-molecular hydrocarbons, is produced by the destruction of organic compounds early in the course of their transformations. It is known that C_2–C_4 and C_2–$C_{4=}$ hydrocarbons are produced by the biochemical destruction of the dead material of higher plants and phytoplankton [58]. Another possible product of this process is destructive methane, which is not in this situation a synthesis product of methane-generating bacteria.

The isotopic composition of methane generated by bacteria by means of both the reduction of CO_2 ($CO_2 + 4H_2 \longrightarrow CH_4 + 2H_2O$) and the fermentation of acetate ($CH_3COOH \longrightarrow CH_4 + CO_2$) and other methyl-compounds is enriched in the light isotope up to $\delta^{13}C$ from –110 to –90‰ in the first portions. Regretfully, we failed to measure the carbon isotopic composition of the gases dissolved in water. If the isotopic composition of catagenetic methane during the earliest transformation stages of organic matter in the sediments is extrapolated to the initial stage ($\delta^{13}C$ from 55 to –65‰ [59]), then, based on isotopic–kinetic considerations, it is reasonable to expect a $\delta^{13}C$ value from –70 to –85‰ for the early destruction methane. The situation can be further complicated by the overprinted fractionation of isotopes during methane oxidation.

8.2. Hydrocarbons in Sediments

Data on the distribution of hydrocarbon gases in sediment samples from the Yenisei–Kara Sea profile are presented in Table 18.

In the upper part of the sedimentary column, the ratios of the concentrations of methane and its heavier homologues are roughly the same as in the water. The concentrations of C_2–C_5 and $C_{2=}$–$C_{4=}$ hydrocarbons

Table 17. Distribution of methane and its higher homologues in the waters of the Ob–Kara Sea profile as of August 14–September 11, 2001, R/V *Akademik Boris Petrov*-2001

Site	Depth, m	S (g/l)	Concentration μl/l		
			CH_4	C_2–C_5	$\Sigma C_4 + C_5$
01–78	0	0.0	2.0	3.6	2.8
01–77	0	0.0	2.7	3.1	2.2
01–73	9	0.0	2.6	2.8	2.2
	bottom	0.0	6.6	2.2	1.6
01–74	0	0.0	1.0	1.3	1.0
01–76	0	0.0	2.6	2.8	2.2
01–75	0	0.0	3.2	2.5	2.0
01–79	0	0.0	1.7	1.9	1.5
01–80	0	0.7	0.4	1.0	0.8
	7	6.8	1.0	0.7	0.6
	bottom	21.9	2.4	0.6	0.5
01–70	0	0.9	0.3	0.8	0.7
	7	13.2	1.4	2.8	2.2
	15	–	1.3	2.6	2.0
	bottom	30.6	1.0	1.9	1.5
01–82	0	9.8	0.5	0.8	0.5
	7	23.8	0.7	1.0	0.7
	20	31.3	0.7	0.6	0.4
01–68	0	9.9	0.4	1.9	1.5
	6	22.9	0.3	1.0	0.8
	45	31.0	0.4	0.8	0.7
01–66	0	0.3	0.3	1.1	0.8
	10	0.5	0.5	1.9	1.5
	45	0.5	0.5	1.4	1.0
	bottom	0.3	0.3	1.1	0.8
01–67	6	25.1	0.5	1.5	1.1
	40	31.6	0.9	2.9	2.5
01–65	0	19.2	0.6	2.3	1.8
01–64	0	15.4	0.4	2.8	2.2
	10	26.1	0.3	3.4	3.0
	23	29.3	1.1	2.2	1.7
	40	33.3	0.4	2.1	1.7
	95	–	0.4	1.4	1.1
	bottom	–	0.2	0.8	0.7
01–62	0	23.1	0.3	1.9	1.6
	12	29.1	0.5	1.3	1.0
	120	33.3	0.4	1.7	1.4
	bottom	–	0.2	0.9	0.7
01–61	0	18.7	0.7	1.6	1.3
	20	28.3	0.8	1.8	1.3
	100	34.0	0.8	2.2	1.8
01–59	0	18.7	0.7	1.5	1.2
	16	28.3	0.6	2.0	1.6
	bottom	34.0	0.5	1.4	1.1
01–56	0	21.5	0.4	0.6	0.4
	16	32.3	0.1	0.8	0.6
	95	–	0.5	1.4	1.1
	bottom	34.4	0.3	1.3	1.0
01–46	0	25.4	0.3	1.8	1.4
	20	34.1	0.2	0.6	0.5
	290	34.7	0.1	1.2	1.0
	bottom	–	0.4	4.1	3.8

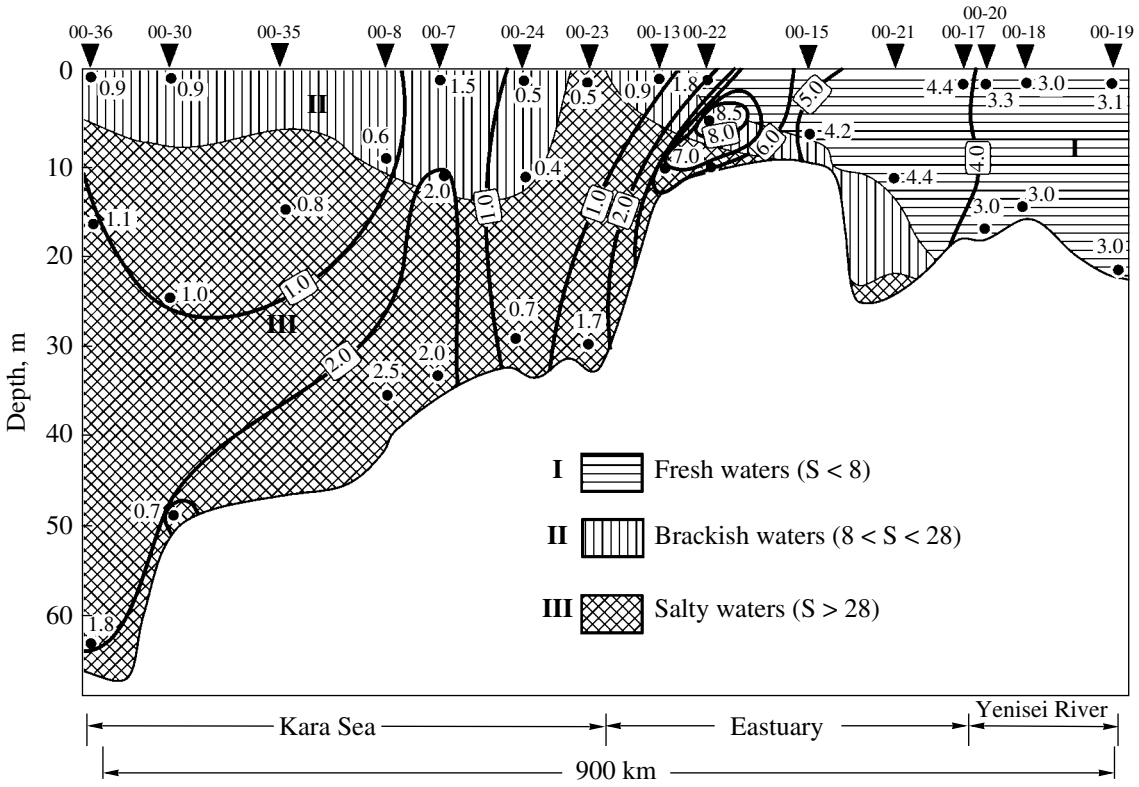

Fig. 15. Methane concentrations (μl/l) in waters along the Kara Sea–estuary–Yenisei River profile. 2000 expedition of the R/V *Akademik Boris Petrov.*

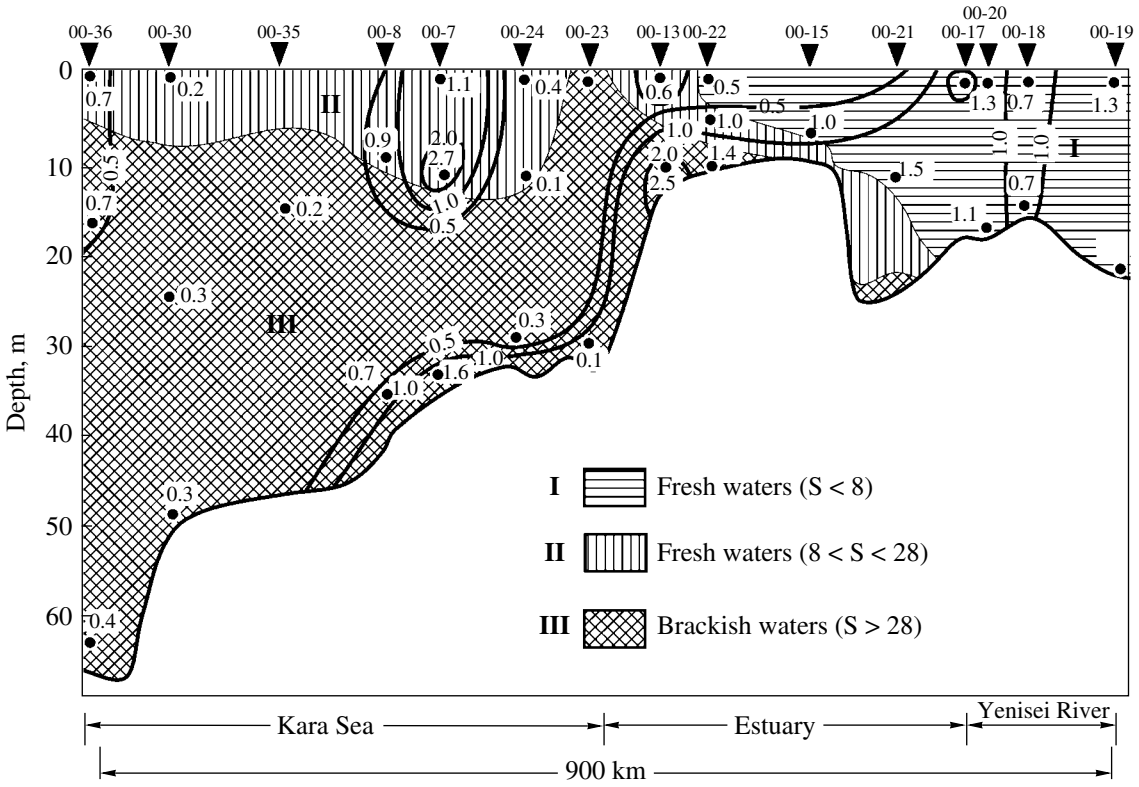

Fig. 16. Concentrations of C_2–C_5 hydrocarbons (as in Fig. 15).

Table 18. Concentration of methane (ml/l) and higher hydrocarbons (μl/l ×10^{-4}) in sediments at sites along the Yenisei–Kara Sea profile. Samples were collected during the 2000 and 2001 cruises of the R/V *Akademik Boris Petrov*

Site	Sampling depth, m	C_1	C_2	$C_{2=}$	C_3	$C_{3=}$	*i*-C_4	*n*-C_4	$C_{4=}$	*i*-C_5	*n*-C_5	$C_2/C_{2=}$	$C_1/C2_2 + C_3$
00–15	0–2	30	5	2	5	0.2	3	3	0.3	7	3	2.5	3
	7–10	500	8	7	10	1	4	4	0.8	10	4	1.1	28
	30–40	10900	4	4	4	0.4	2	2	0.6	5	3	1	1366
	120–130	86600	9	7	14	1	9	7	–	18	9	1.3	3765
	210–230	288000	11	9	17	2	8	5	0.5	21	7	1.2	10285
	310–330	121600	6	5	8	0.5	4	2	0.8	22	9	1.2	8686
	410–430	169600	10	6	12	1	8	6	1	18	6	1.7	7709
00–14	0–2	30	8	2	10	0.4	2	2	0.6	15	5	4	2
	3–8	30	5	1	7	0.1	4	3	–	18	6	5	3
	45–50	70	3	0.5	0.7	0.1	2	1	0.6	7	2	6	19
	56–76	180	6	1	7	0.2	5	3	0.2	19	6	6	14
	96–100	30	1	10	–	0.2	–	–	0.2	–	–	0.1	–
	206–220	1190	20	3	19	0.7	11	10	0.6	34	16	7	31
00–23	0–2	130	19	17	25	7	15	15	9	37	15	1.1	3
	5–10	230	28	33	70	22	42	45	14	130	46	0.8	2
	30–40	130	4	6	8	0.9	3	3	2	7	2	0.7	11
	52–72	160	1	6	3	1	0.9	1	–	2	1	0.2	40
	120–130	130	2	3	4	0.4	1	1	–	3	1	0.7	23
	160–180	60	0.4	2	1	0.3	0.1	0.2	0.3	–	–	0.2	46
	250–280	750	4	38	3	1	0.1	0.3	0.7	–	–	0.1	108
	337–365	140	0.3	1	1	0.2	–	0.1	–	–	–	0.3	111
	390–414	70	0.6	2	1	0.5	–	0.2	–	–	–	0.3	44
00–7	0–2	120	14	10	17	5	11	10	14	27	14	1.4	4
	3–8	200	21	32	29	9	18	19	31	51	21	0.6	4
	10–18	170	17	10	21	0.1	12	10	0.5	27	4	1.7	5
	40–50	110	9	3	10	1	16	5	3	18	6	3	6
	98–127	240	5	0.9	6	0.3	4	4	0.5	12	4	5.5	22
	297–322	1090	13	1	12	0.7	4	3	0.9	13	4	13	44
	508–538	412900	22	2	24	3	16	14	4	40	20	11	8976
	637–665	124900	5	1	6	0.4	4	3	0.3	10	4	5	11354
00–37	0–2	10	2	1	2	1	0.9	0.9	–	4	4	2	2
	4–7	50	6	5	7	3	4	3	0.4	3	7	1.2	4
	9–14	40	4	4	5	2	3	3	0.3	10	5	1	3
	22–27	30	5	2	4	0.9	3	4	0.4	25	7	2.5	10
	45–55	370	5	2	7	1	2	2	–	15	5	2.5	31
	73–81	880	9	3	9	2	3	3	–	9	5	3	49
	90–103	1300	15	5	14	2	5	4	2	14	6	3	45
	113–130	730	14	4	14	2	3	3	–	27	9	3.5	26
	173–183	1400	14	3	15	1	1	3	2	5	–	4.7	48
	220–223	1800	16	3	13	1	1	2	3	3	1	5.3	62
	268–283	930	9	2	10	1	0.6	0.6	1	–	–	4.5	42
	298–333	68600	2	1	8	–	–	–	–	–	–	2	6860
	347–362	225200	6	1	6	–	0.3	0.3	–	–	–	6	18767
	387–400	168300	10	2	10	0.6	0.6	0.6	–	–	–	5	8415
	400–413	472000	5	3	8	2	0.6	0.8	–	–	–	1.7	36307

Table 18. (Contd.)

Site	Sampling depth, m	C_1	C_2	$C_{2=}$	C_3	$C_{3=}$	*i*-C_4	*n*-C_4	$C_{4=}$	*i*-C_5	*n*-C_5	$C_2/C_{2=}$	$C_1/C2_2 + C_3$
01–38	0–2	45	25	27	28	2	13	27	0	73	28	9	0.8
	4–7	37	17	1.2	18	0	7	14	0	37	12	14	1.0
	29–34	73	19	1.2	21	0	10	19	0	45	17	16	1.8
	70–100	162	17	0.9	17	0.1	5	11	0	30	12	19	4.8
	190–220	249	13	0.5	12	0	5	9	0	17	5	26	10.0
	233–270	469	23	1.6	3	0.2	11	18	0	31	7	15	18.0
	333–370	360	6	0.5	5	0.1	3	6	0	21	14	12	33.0
	435–460	1680	30	1.8	25	0.3	13	23	0	43	12	17	30.5
	480–510	15500	9	0.8	5	0.1	3	4	0	13	6	11	1107
	510–530	26700	20	1.0	3	0	2	3	0	9	4	20	1160
	600–630	127700	86	2.8	11	0.3	5	10	0	30	7	30	1316
01–34	24–29	4	0.5	0.04	1	0	0.2	0.4	0.0	4	0	12.5	2.7
	55–87	244	30	2	37	1.0	23	47	0.0	49	17	15	3.6
	150–180	150	24	1	24	0.02	15	22	0.0	43	15	24	3.1
	250–280	284	40	25	50	0.4	29	54	0.0	144	58	1.6	3.2
	280–380	974	28	2	21	0.2	8	12	0.0	42	37	14	19.9
	450–480	218	25	2	31	0.4	20	29	0.0	77	133	12.5	3.9
01–47	0–3	328	24	2	31	1.0	17	31	1.3	86	39	12	6
	6–10	298	25	2	29	0.5	17	28	0.0	64	59	12.5	5.5
	20–24	94	18	1	21	0.1	14	20	0.0	53	23	18	2.4
	34–38	310	7	0.2	18	0.04	9	15	0.0	43	14	35	12.4
	97–127	260	23	2	27	0.4	15	24	0.3	65	28	11.5	5.2
	170–192	531	20	1	25	0.6	11	22	0.3	68	26	20	11.8
	202–225	659	26	1	31	0.3	18	30	0.4	83	25	26	11.6

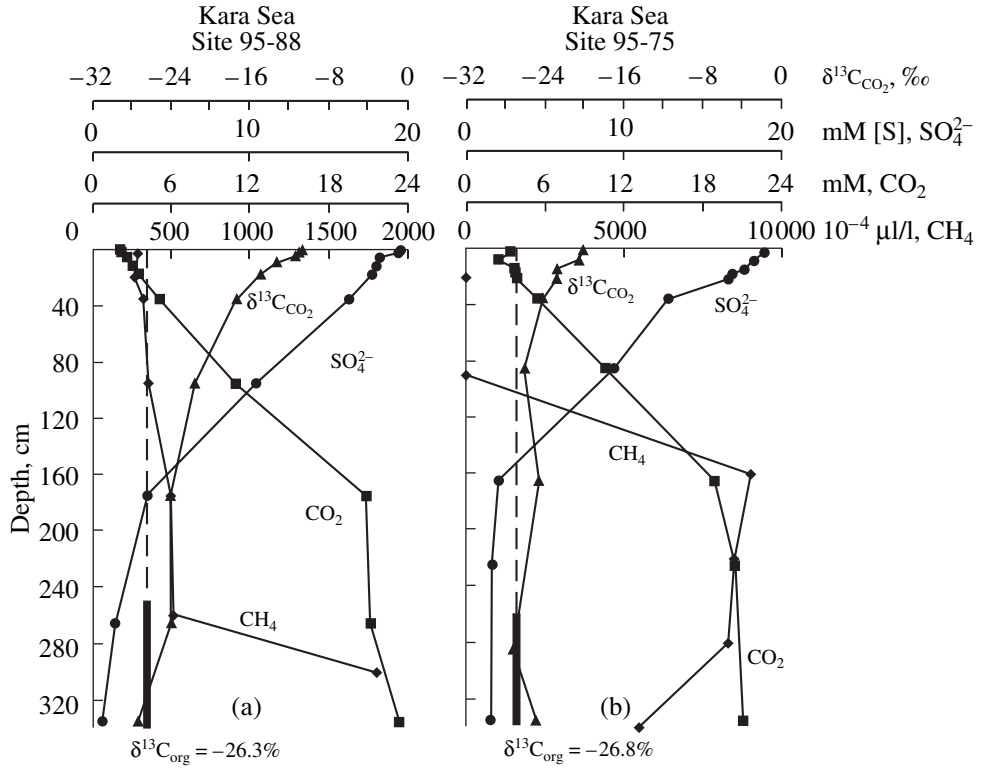

Fig. 17. Zoning of biogeochemical processes in a sedimentary section with a normal redox regime: (a) Site 95-88 in the southern part of the Kara Sea, (b) Site 95-75 in the Yenisei estuary.

unsystematically vary with depth within a range of 0.01 to 2–3 ml/l $\times 10^{-4}$, and this concentration increases to 13–14 ml/l $\times 10^{-4}$ at some intervals. Obviously, these hydrocarbons are the products of destructive geochemical processes that continue in the sediment. The process of the microbiological generation of methane is "switched on" at a certain depth, as can be seen in the last column of Table 18 from the drastic (by two orders of magnitude) increase in the $C_1(C_2 + C_3)$ ratio.

Marine sediments are known to be characterized by geochemical zoning, which also occurs in the sediments of the Arctic Basin. Examples are Site 95-88 in the southern part of the Kara Sea and Site 95-75 in the norther part of the Yenisei Estuary (Figs. 17a, 17b). The sites show evidence of a decrease in the SO_4^{2-} concentrations due to the sulfate-reduction process. The CO_2 concentration increases simultaneously with CO_2 enrichment in the light isotope from the initial value of $\delta^{13}C$ of –7 to –9 to values typical of organic carbon (close to –25‰). The exhaustion of sulfate and the termination of sulfate reduction opens the way to the methane generating process.

Table 19 presents data on the isotopic composition of methane studied in sediments at sites examined during the 1999, 2000, and 2001 expeditions. The methane isotopic composition varied from –105 to –75‰.

The section of sediments at site 00-37 (Table 18) is interesting because the drastic increase in the $C_1(C_2 + C_3)$ proportion with depth is also associated (within the depth interval of 280–300 cm) with a discontinuity in the systematic trend in the methane isotopic composition with depth (Fig. 18). Obviously, this depth interval is characterized by a conflict between processes that control the isotopic composition of methane. The lower branch of the variations in the methane isotopic composition with $\delta^{13}C$ from –102 to –93.3‰ is definitely related to the onset of microbiological methane generation. The upper branch can either characterize destruction methane or result from the oxidation of methane diffusing into the upper layers from its generation zone. Inasmuch as methane generation is characterized by a notable kinetic isotopic effect, the methane that was not oxidized is depleted in the light isotope.

8.3. Oxidation of Methane and Formation of Ikaite

Methane generation in marine sediments results in the accumulation of huge reserves of natural gas in the oceanic sedimentary shell. Some methane is oxidized

Table 19. Methane isotopic composition in sediments from the Kara sea

Site	Interval	Concentration, ml/l	$\delta^{13}C$ (‰)
00–37	220–223	0.180	–83.3
	268–283	0.093	–91.8
	298–333	6.86	–102.3
	347–362	22.52	–97.7
	387–400	16.83	–96.3
	400–413	47.20	–93.3
00–22	190–205	2.0	–91.6
	428–438	–	–86.4
00–15	410–430	16.96	–86.6
99–31	100	–	–79.4
	150	–	–78.8
	200	–	77.4
01–26	26–50	0.145	–98.4
	75–95	0.028	–82.5
	126–146	0.042	–79.7
	175–195	0.051	–79.9
	200–220	0.199	–77.4
	226–246	0.194	–78.2
	305–325	4.29	–93.5
	350–370	10.60	–90.2
	400–420	6.77	–89.5
	495–515	7.80	–85.5
01–55	16–36	0.107	–100.9
	36–60	0.217	–104.4
	105–125	0.315	–99.4
	135–165	4.33	–86.0
	180–217	11.27	–81.5
	270–285	10.84	–80.7
01–73	0–2	1.92	–105.0
	34–39	13.12	–75.0

[60], and this has important geochemical and mineralogical consequences.

Methane oxidation and the related generation of CO_2 and carbonate result in isotopically anomalously light carbonates (with $\delta^{13}C$ up to –60‰) in the bottom sediments.

An interesting manifestation of biogeochemical processes coupled with methane oxidation is the origin of ikaite, a fairly rare mineral (Fig. 19). Ikaite was found during Cruise 35 of the R/V *Akademik Boris Petrov* in 2001 in the Kara Sea [10, 11, 14]. Ikaite is hexahydrate of calcium carbonate $CaCO_3 \cdot 6H_2O$. It is metastable under normal conditions and can be formed at temperatures close to 0°C in the presence of ions inhibiting calcite crystallization. One of these effective inhibitors is the phosphate ion. Another necessary condition is a high concentration of CO_2, which can be maintained, for example, by the microbiological oxidation of methane in the process of sulfate reduction. The carbon dioxide produced during the oxidation of biogenic methane is enriched in the light isotope, which is responsible for the low $\delta^{13}C$ values of the ikaite.

The carbon isotopic composition of ikaite and nodules samples from the Kara sediments varies from –60.1 to –23.3‰ (Table 20).

Figure 20 shows the variations of some hydrochemical parameters in the vertical section of sediments at Site 01-26, where ikaite was found. The sediments are characterized by an active process of sulfate reduction. Biogenic methane generation via the mechanism of microbiological CO_2 reduction starts at a depth of 250 cm and below. Correspondingly, the CO_2 concentration decreases (Fig. 20a). The methane thus generated ascends and is consumed in the process of anaerobic oxidation The newly generated CO_2 is mineralized in the form of ikaite.

The realism of this mechanism is confirmed by isotopic data (Fig. 20b). Methane is enriched in the light isotope in the oxidation zone, a fact demonstrating that the methane is formed from isotopically light biogenic methane. The shift in the methane isotopic composition toward higher $\delta^{13}C$ values points to the process of its oxidation. Moreover, hydrochemical analyses indicate that the concentration of the phosphate ion in the zone where ikaite is formed is at a maximum.

9. REDOX REGIME IN SEDIMENTS

Figure 21 exhibits the degree of oxidation of the bottom sediments measured in the Kara Sea during Cruise 22 of the R/V *Akademik Boris Perov* in 1995. As the measure of this parameter, we provisionally used the thickness of the oxidized uppermost layer (in centime-

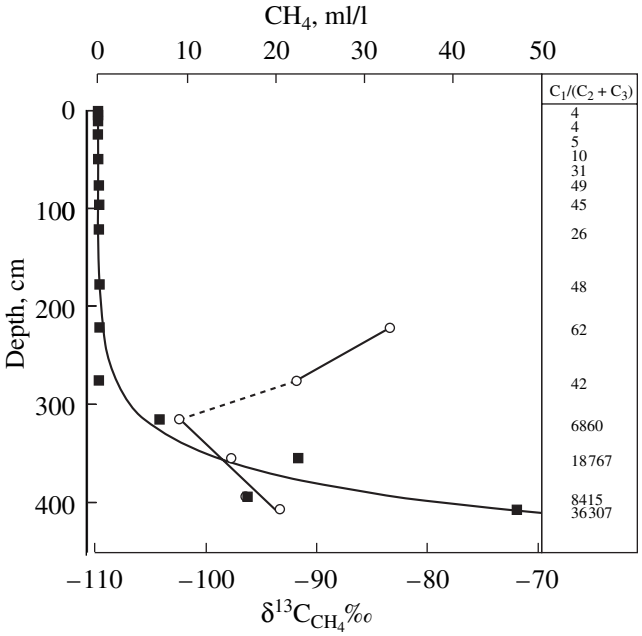

Fig. 18. Variations in the CH_4 concentration and isotopic composition in the profile of sediments at Site 00-37, Kara Sea, 2000 expedition of the R/V *Akademik Boris Petrov.*

ters), i.e., the depth range where the Eh changes its sign from positive to negative. Elevated oxidation of sediments is characteristic of the zone adjacent to the eastern shore of Novaya Zemlya.

Organic geochemistry offers a technique for the pyrolitic determination of the hydrogen (HI) and oxygen (OI) indexes. The (HI/OI) parameter is determined by the ratio of oxygen and hydrogen atoms in organic matter. Planktonogenic material is usually characterized by a high hydrogen index HI, and terrigenous material contains much oxygen-bearing functional groups and, hence, shows low HI/OI ratios. Inasmuch as terrigenous organic matter has $\delta^{13}C$ values lower than those of planktonogenic organic matter, the values of the HI/OI ratio and $\delta^{13}C$ should be correlated.

Indeed, as can be seen from Fig. 22, the bottom sediments of the Kara Sea do display such a dependence. At the same time, a great number of points in the lower part of the diagram plot away from this dependence and are characterized by low HI/OI ratios, as is the case with oxygen-rich terrigenous detritus. At the same time, they show elevated $\delta^{13}C$ values, which are typical of planktonogenic carbon. Analysis of this situation indicates that all anomalous points characterize the highly oxidized zone.

This problem finds its explanation under the assumption that planktonogenic material in the western part of the Kara Sea was affected by oxidation during

Fig. 19. Ikaite samples and clay–carbonate nodules extracted from Holocene sediments in the Kara Sea.

diagenesis and acquired a high oxygen index already in the inert form [61].

The scheme in Fig. 23 illustrates this situation. Normally the $\delta^{13}C$ and HI/OI parameters vary synchronously, and this synchronism can be disturbed by oxidation diagenesis. It is interesting to note that we have documented the opposite situation in the sediments of the Black Sea in 1995–1997 [62]. In contrast to the Kara Sea, the isotopic anomaly in the Black Sea was related to the notable contribution of chemosynthetic bacteria to bioproduction in the zone rich in H_2S. These bacteria have a biochemical composition and, hence, an HI/OI index similar to those of plankton but are different from plankton in being relatively enriched in the light isotope.

The oxidation of organic matter notably modifies its properties. Above we presented examples of normal geochemical zoning and methane genesis in the sediments of the Kara Sea (Fig. 17).

Table 20. Carbon isotopic composition of authigenic carbonates (minerals, nodules, and crusts) in the sediments of the Kara Sea

Site	Sample		$\delta^{13}C$, ‰ PDB
97–24	Small (<2 cm) platy and acicular ikaite crystals from modern bottom deposits, depth 10–25 cm below bottom surface		–29.2
			–28.8
			–30.0
			–28.0
00–37	Aggregates of pyramidal ikaite crystals from Holocene sediments; length 6 cm, depth 103–113 cm		–49.0
	Ikaite (glendonite ?) crystals, length ~2.5 cm		–36.5
	Sampling depth 223–233 cm		–37.6
	Clayey–carbonate nodules replacing mollusk shells:		
	Sampling depths (cm): 25–35		–60.1
	38–40		–58.9
	58–68		–55.4
	158–173		–59.9
	Sampling depths (cm): 38–40		–4.6
01–26	Small (<1 cm) aggregates of platy ikaite crystals composing a spherical cluster ~5 cm in diameter		–24.0
			–23.8
			–24.5
	Sampling depth 226–230 cm		–23.3
01–55	Large single pyramidal crystals of ikaite, length >12 cm, sampling depth 165 cm	Pyramid top	–41.6
		Outer part	–42.3
		Inner part	–42.3
	Aggregates of ikaite crystals (single crystals and aggregates of 2–3 crystals); crystals 4–6 cm long; sampling depth 135 cm		–41.7
			–42.7
			–40.94
			–42.00
01–45	Carbonate crust at the sediment surface		–14.4
03–07	Numerous pyramidal ikaite crystals (2–4 cm long) disseminated within the interval of 170–320 cm of Holocene sediments.		
	Sampling depth, cm: 175		–57.1; –57.3
	191		–43.8; –43.3
	199		–45.3; –45.1
	200		–41.8; –42.0
	215		–41.8; –42.0
	260–270		–30.6; –30.4
	280–285		–30.6; –30.5
	300–305		–28.8; –29.1
	315		–37.0; –37.1
	320		–33.7; –33.5

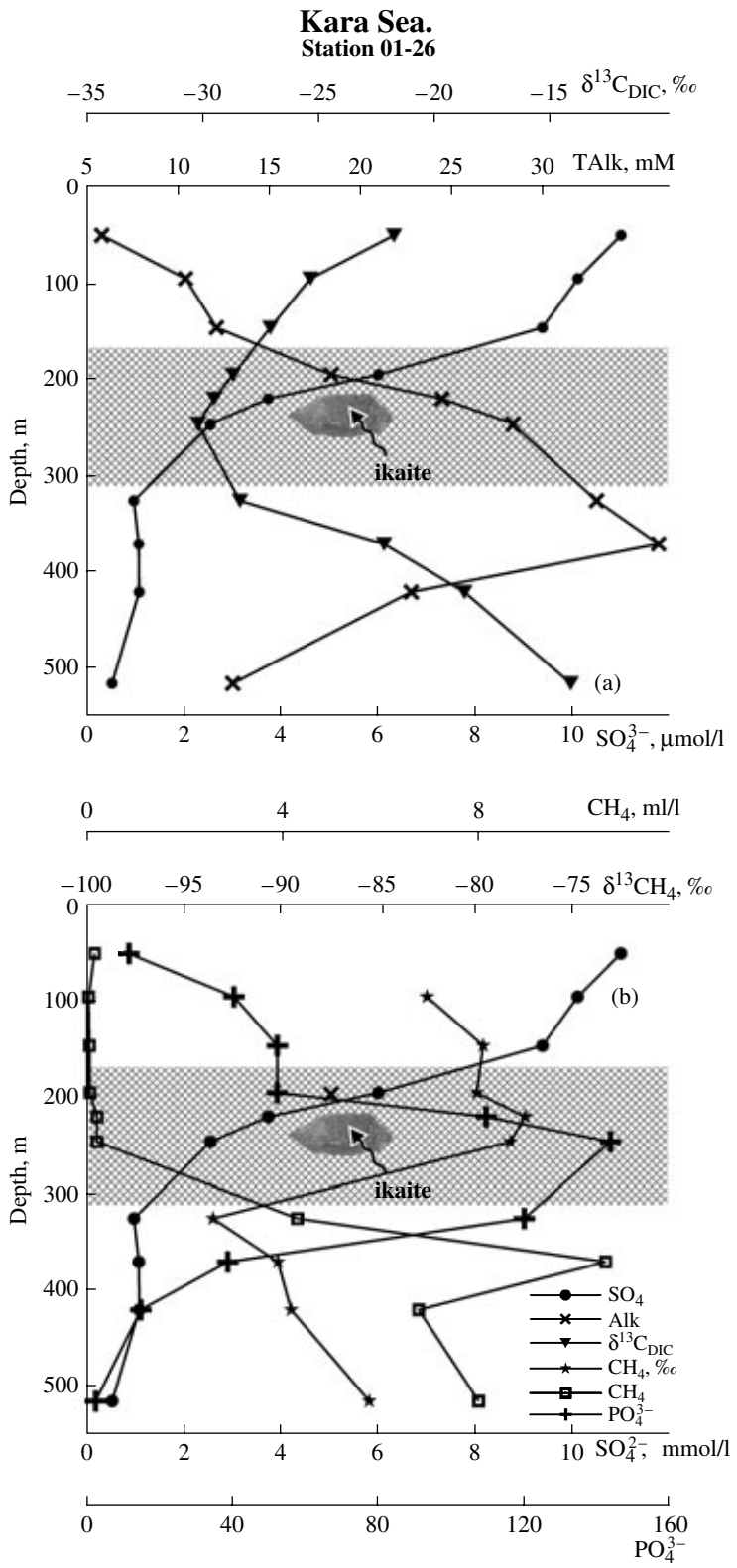

Fig. 20. Variations in geochemical parameters: (a) SO_4^{2-} concentration, $\delta^{13}C_{CO_2}$ isotopic composition, and the concentration of CO_2 dissolved in the pore waters; (b) P concentration, CH_4 isotopic composition $\delta^{13}C_{CH_4}$, and CH_4 concentration in the vertical section of sediments at Site 01-26, at the finding site of ikaite.

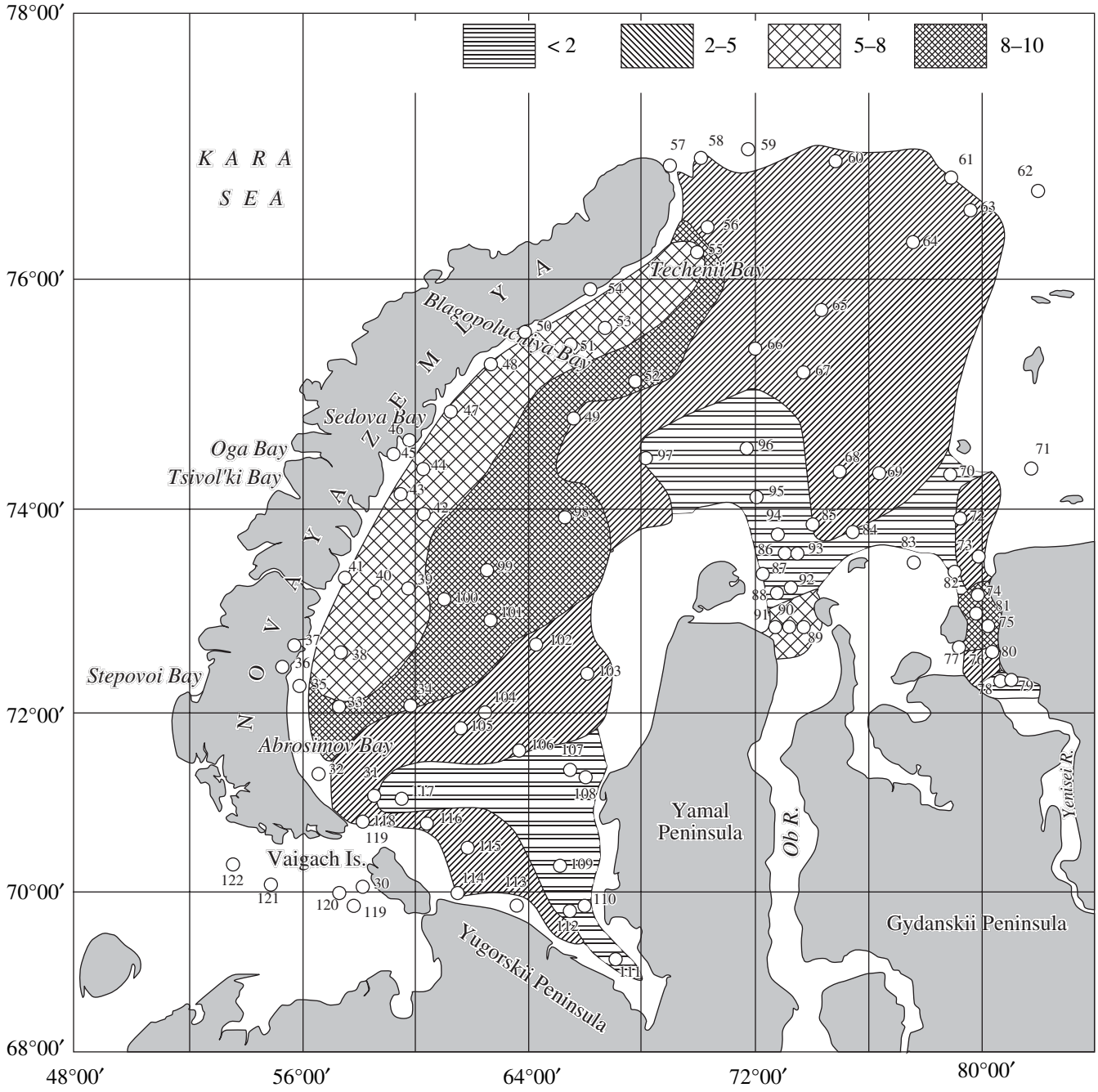

Fig. 21. Redox regime in the bottom sediments of the Kara Sea. The degree of oxidation of the samples was provisionally assayed by the thickness of the bottom sediment layer with Eh ≥ 0.

The processes in the zone of deep oxidation in the Kara Sea are of principally different character (Fig. 24). For example, the process of sulfate reduction is pronounced only weakly in the vertical section of sediments at Site within the Novaya Zemlya Trench. The isotopic composition of pore CO_2 varies insignificantly and does not approach the value typical of organic carbon. Methane generation is suppressed, an indication of the inertness of the organic matter, which cannot serve any more as a favorable substrate for the development of microorganisms and the maintaining of their biochemical activity. This organic matter becomes, for example, nonproductive in terms of the processes of microbiological methane generation.

Hence, a combination of isotopic and pyrolitic analyses of organic matter in sediments provides a tool for assaying the redox regime in a sea basin, and these data can be further used for paleofacies reconstructions.

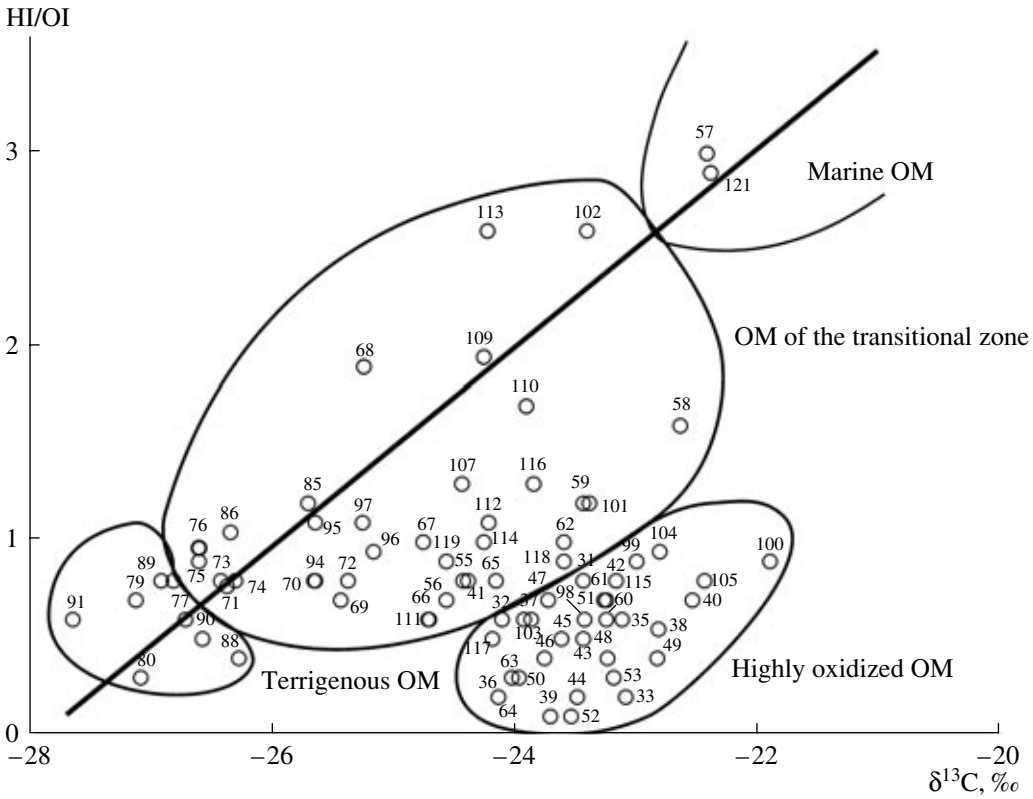

Fig. 22. Correlation between the HI/OI ratio (ratio of the hydrogen index to the oxygen index) and δ^{13}Corg in the bottom sediments from the central part of the Kara Sea. Numerals correspond to the sites where the measurements were conducted (during the 1995 cruise).

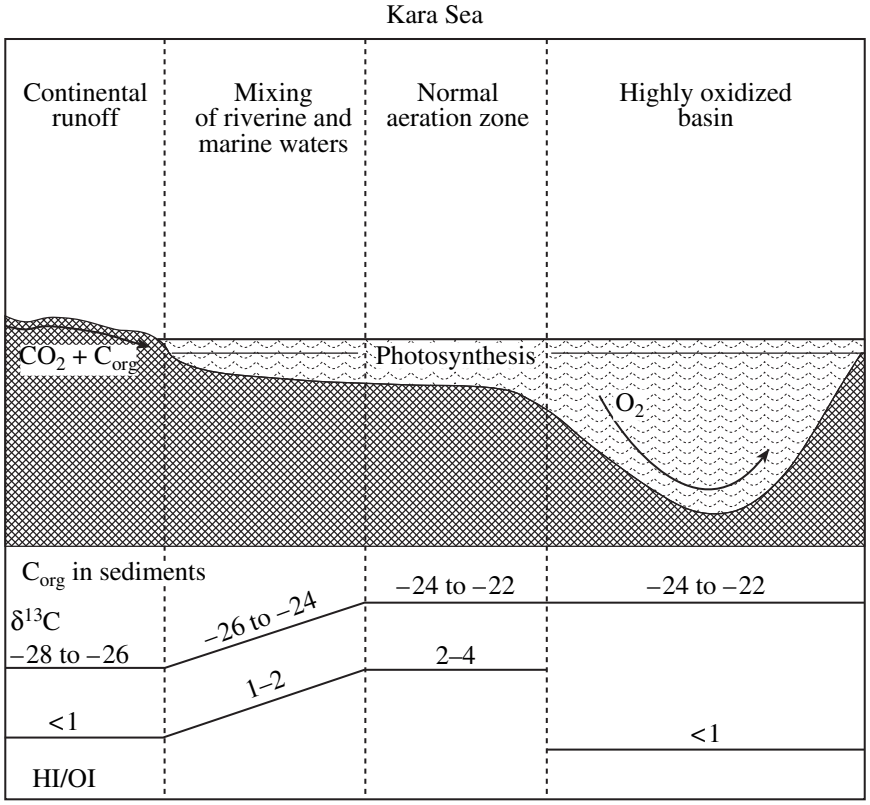

Fig. 23. Model illustrating the disturbance of correlations between the HI/OI ratio and $\delta^{13}C_{org}$ in the zone of oxidative diagenesis.

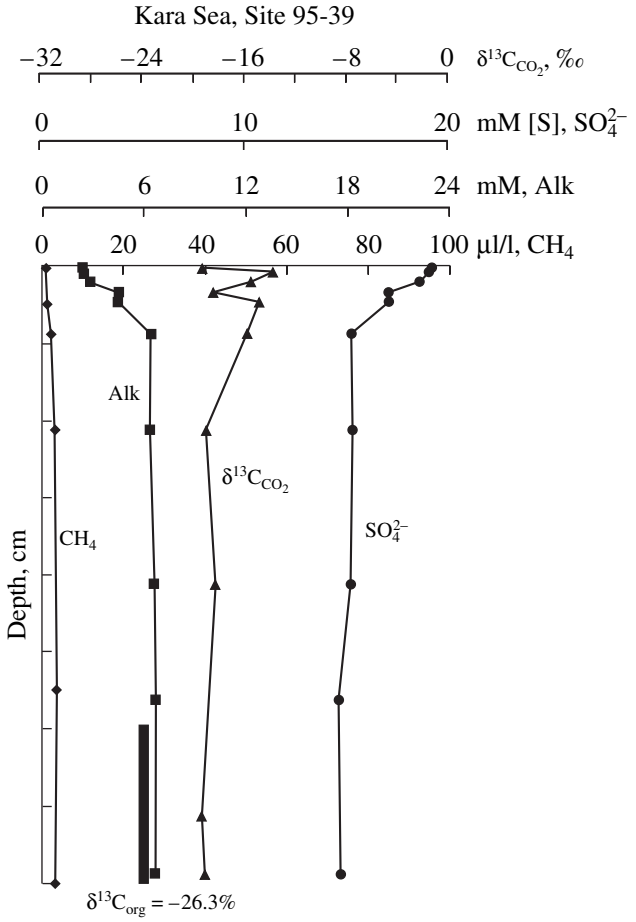

Fig. 24. Suppression of biochemical processes in the vertical section of sediments at Site 95-39, where the organic matter was affected by oxidative diagenesis.

10. RADIOECOLOGY

The distribution and behavior of radionuclides ($^{134, 137}$Cs, ^{90}Sr, and $^{239, 240}$Pu) in the water and sediments of the Kara Sea was examined in much detail during the expedition aboard the R/V *Akademik Boris Petrov* in 1995 [1]. The data then obtained provided a general idea of the radioecological situation in the basin, which was an important problem because of the occurrence of significant potential pollution sources and the vulnerability of the Arctic ecosystem. In this publication, we will not characterize all data obtained during that expedition and limit ourselves only to some addenda that are important for refining the situation with the distribution of radionuclides as described in [1].

Data on the moisture of the sediments provide insight into the distribution of lithologically contrasting constituents of the sediment: clay and sand. Figure 25 presents data on the moisture and the distribution of radioactive Cs in the surface layer. High Cs concentrations were noted in two major regions: the northern part of the Yenisei estuary and the Kara Strait. Separate areas of high concentrations were also detected within the Novaya Zemlya Trough and in the central part of the sea, along the course of the Ob–Yenisei Current. The radioactive component of the Kara Sea is notably affected by the Yenisei runoff. This is obviously related, first, to the influence of an integrated radiochemichal plant situated within the catchment area of the Yenisei and, second, to the precipitation of the bulk of the particulate matter within the water mixing zone in the estuary. The clayey oozes of this area are characterized by a high sorption capacity with respect to Cs.

A source of radionuclides is also present in the Ob drainage basin: this is the Mayak plant. However, the sand-rich sediments of Obskaya Guba adsorb only an insignificant fraction of radioactive Cs, which is proportional to the clay contents in the sediments.

An analogous situation takes place in the Kara Strait area. Barents Sea waters carry there radiochemical wastes from Cellafield, Great Britain. Radioactive Cs coming to the Kara Sea becomes involved in the system of cyclonic currents and is locally deposited at favorable sites of natural morphological (topographic deeps in the seafloor) or natural geochemical traps.

Thus, in the presence of a localized radioactivity source, the principal factor controlling the distribution of radioactive Cs is the clay contents in the sediments.

An insignificant part of the riverine runoff comes to the open sea bypassing the sedimentation deposition center and, gradually mixing with the saline waters of the Arctic Basin, is transferred to high latitudes. Figure 26 shows the correlation of the isotopic composition of C_{org} and the activity of radioactive Cs in the sediments. This correlation is sometimes thought to be related to the hypothetic relations between Cs and terrigenous organic matter [63]. However, the results of experiments with the use of ultrafiltration did not confirm the existence of these relations (Table 21). This is an indirect consequence of the actually existing relations between radioactive Cs and adsorption on clay minerals.

The experiments involved the analysis of the concentrations of ^{137}Cs and other radionuclides in the filtrates after the filtration stage (0.2 µm) and then, ultrafiltration with the use of organic membranes of the DK type. This made it possible to assay the contents of radionuclides in fractions of the dissolved organic matter (DOM) with various molecular masses. When ^{137}Cs was determined on filtrates passed through organic membranes, we did not detect any differences between the concentrations of radioactive Cs in the original sample and filtrates, a fact suggesting that Cs insignificantly participates in complexation with the dissolved organic matter. It was determined that much ^{90}Sr and $^{239, 240}$Pu can be bound with dissolved species of organic matter.

It was also demonstrated that the sorption activity of the sediments with respect to ^{137}Cs also depends on

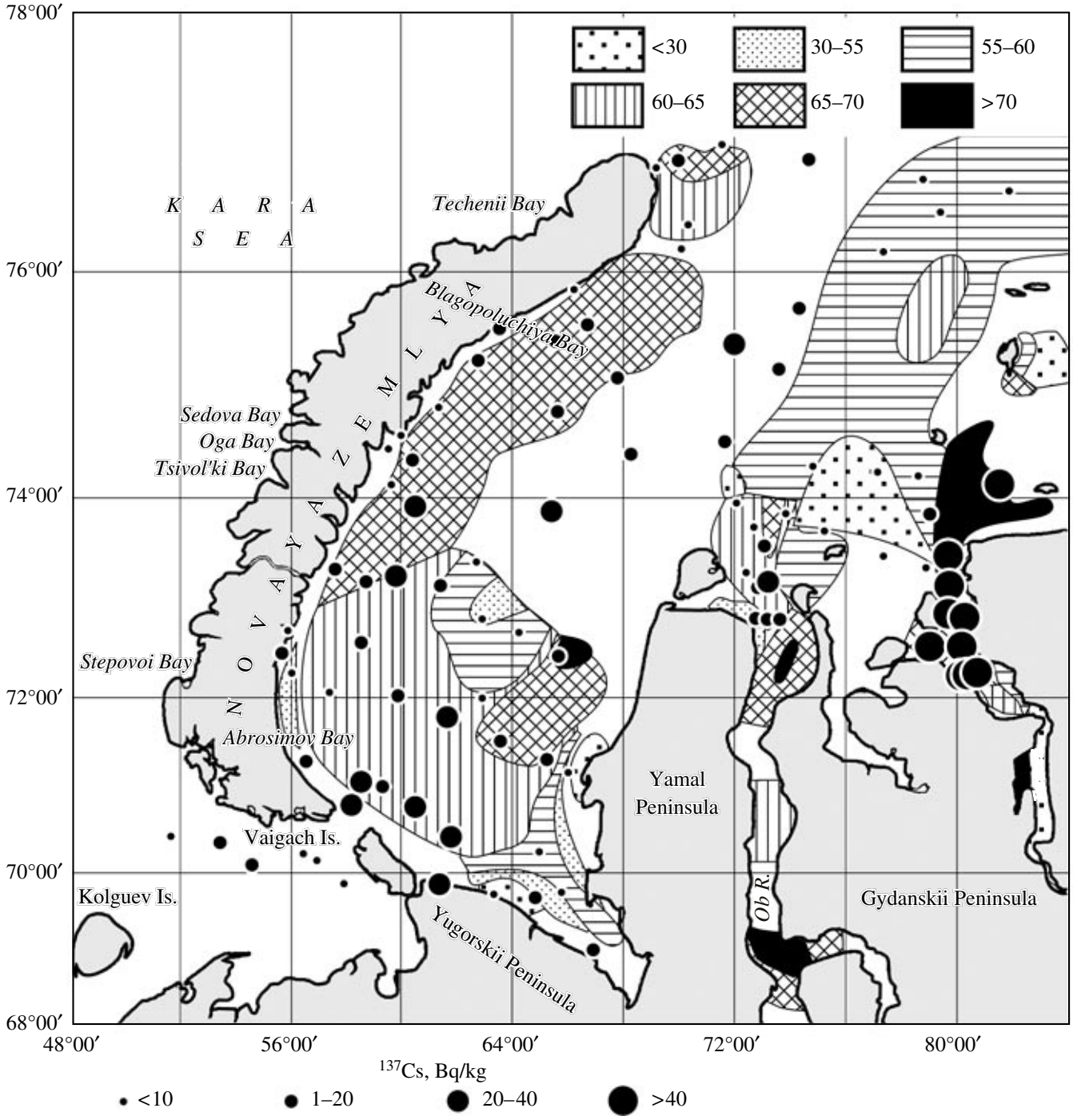

Fig. 25. Distribution of ^{137}Cs in the bottom sediments in correlation with their moisture.

their lithological composition. Samples of bottom sediments taken from areas where solid radioactive wastes were dumped in shallow bays of the Novaya Zemlya Archipelago, at sites with the maximum pollution of the bottom sediments, in Stepovoi and Abrosimov bays, were examined for the sorption activity of the bottom sediments with respect to various radionuclides. It was demonstrated that the distribution coefficients for the kinetic adsorption profiles of radioactive ^{137}Cs by sediments are different for these two bays (Fig. 27). Higher distribution coefficients were determined in sediment samples from Abrosimov Bay, although the sediments from Stepovoi Bay were dominated by clay particles of smaller sizes (Table 22).

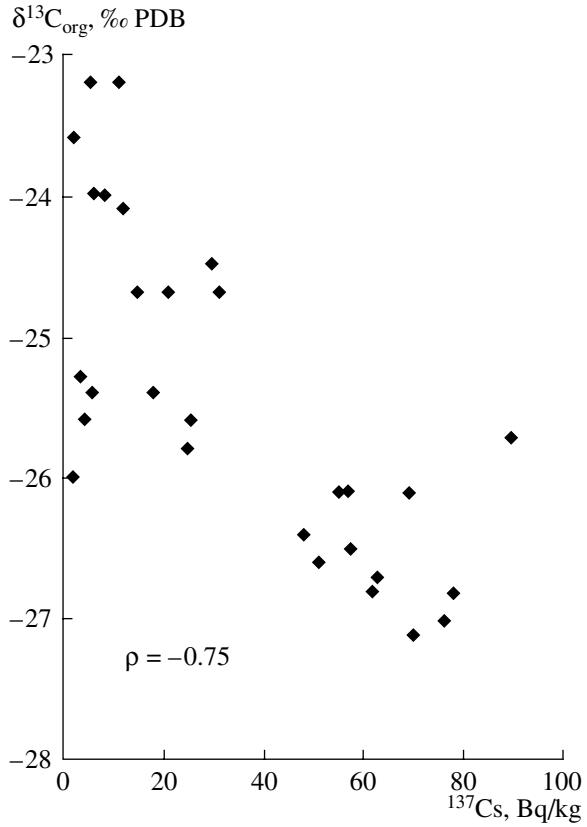

Fig. 26. Concentration of ^{137}Cs in the bottom sediments of the Kara Sea.

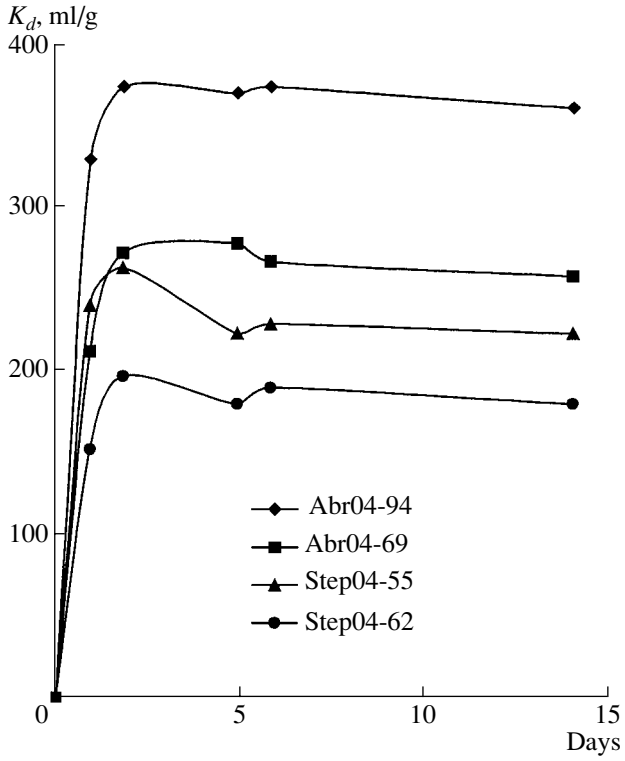

Fig. 27. Kinetic curves of the ^{137}Cs distribution coefficients for sediment from Stepovoi and Abrosimov bays.

Inasmuch as the maximum of Cs activity corresponds to intermediate particle sizes, it is evident, in this situation, that the differences between the lithological compositions of sediments from these bays more significantly affected the equilibrium distribution coefficients. In contrast to other radionuclides, ^{137}Cs participates not only in ion-exchange and sorption interactions with clay particles but is also able to selectively

Table 21. Concentrations of radionuclides in water after filtration and ultrafiltration

Site	Depth level, m	Salinity, ‰	^{137}Cs activity, Bq/m^3		
			original water	water after filtration (0.2 μm)	water after ultrafiltration (2000 Da)
01–70	3	1.5	2.2 ± 0.4	2.0 ± 0.2	2.0 ± 0.2
01–25	3	17.0	4.8 ± 0.9	4.6 ± 0.4	4.5 ± 0.4
01–11	3	<0.1	6.0 ± 0.5	5.1 ± 0.5	5.2 ± 0.5
01–46	3	24.5	4.9 ± 0.5	4.6 ± 0.5	4.6 ± 0.5
Site	Depth level, m	Salinity, ‰	^{90}Sr activity, Bq/m^3		
			original water	water after filtration (0.2 μm)	water after ultrafiltration (2000 Da)
01–72	3	<0.1	9.7 ± 1.9	8.0 ± 1.6	5.9 ± 1.2
00–40	3	9.3	6.0 ± 1.2	5.7 ± 1.1	2.6 ± 0.5
00–19	3	<0.1		4.2 ± 0.8	1.9 ± 0.4
00–05	3	33	0.9 ± 0.2	1.0 ± 0.2	0.6 ± 0.1
Site	Depth level, m	Salinity, ‰	^{239}Pu, ^{240}Pu activity, mBq/m^3		
			original water	water after filtration (0.2 μm)	water after ultrafiltration (2000 Da)
01–08	28	<0.1	31.6 ± 6.3	24.2 ± 4.5	22.6 ± 4.5
01–72	3	<0.1	32.0 ± 6.4	29.2 ± 6.0	28.3 ± 5.6 <

Table 22. Granulometric composition (%) of the surface layer (0–2 cm) of bottom deposits

no. (Site)	Fraction (mm) contents, %					
	1–0.25	0.25–0.05	0.05–0.01	0.01–0.005	0.005–0.001	<0.001
1	1.17	6.40	16.28	34.21	24.43	17.51
2	1.66	8.83	22.98	13.71	35.68	17.14
3	0.64	10.88	43.03	13.53	19.40	12.52
4	1.60	0.10	41.00	12.80	26.42	18.08

Note: (1, 2) Stepovoi Bay; (3, 4) Abrosimov Bay.

enter the interlayer space of clay phyllosilicates (illite, smectite, and montmorillonite). The bonds of Cs within the crystal are the strongest, and thus, sediments containing mica minerals are traps for ^{137}Cs.

In practice, the difference revealed between the equilibrium distribution coefficients of radioactive Cs in sediments from Abrosimov and Stepovoi bays may imply that, at the equality of all other factors, some ^{137}Cs can spread from the source of radioactive contamination at dumping areas for longer distances within Stepovoi Bay than in Abrosimov Bay.

A complex approach to studying the anthropogenic pollution of aqueous environments coupled with the determination of certain parameters of the natural geochemical background make it possible to reveal the distribution of anthropogenic pollutants in the study water areas. In general, carbon geochemistry is the most important factor controlling the overall geochemical background of a sea basin, the redox regime of its bottom sediments and waters and, consequently, the migration modes of elements in the dynamic sediment–water system.

CONCLUSIONS

—In spite of the harsh environment of the Arctic Basin, active biogeochemical processes occur in both the waters and the sediments of the Kara Sea.

—Efficient transformations in the composition and migration modes and concentrations of compounds occur at geochemical barriers that separate the marine and continental zone of the hydrosphere.

—The concentrations of organic carbon in the sediments reaches 2.5%, which is higher than could be expected for an oligotrophic basin such as the Kara Sea.

—Organic carbon of this basin has an extremely heterogeneous genesis. The carbon isotopic composition of the organic matter varies within the range from –22 to –24‰ (where the Kara waters mixed with those from the Atlantic near the northern and southern tips of Novaya Zemlya) to –27 …–30‰ in the Yenisei and Ob estuaries.

—The distribution of the isotopic composition of CO_2 dissolved in the surface waters suggests that river waters penetrate far into the sea.

—The relative enrichment of the plankton in the light carbon isotope is caused by the temperature effect and the long-distance transportation of continental CO_2 in the sea. A certain role (which is still not completely understood) in the transport and production of organic matter in arctic seas is played by drift ice.

—Data obtained on the relations between the carbon isotopic compositions of the plankton and particulate matter along river–estuary–sea profiles indicate that the material carried by riverwaters consists of 70% detrital–humic material and 30% planktonogenic matter, and the offshore marine waters contain 20% terrigenous material and 70% bioproducers.

—The concentration of particulate matter in the waters decreases from 15–20 mg/l in the riverwaters to 1.5–2.0 mg/l in seawaters in the central part of the Kara Sea and no more than 0.3–0.35 mg/l in waters at the northernmost sites. The latter value can be regarded as the background value for open sea.

—The geochemistry of the hydrocarbon gases is characterized by comparable concentrations of methane and heavier hydrocarbons, including unsaturated ones. Methane obviously is not synthesized in these environments by methane-producing bacteria but is generated, along with other low-molecular hydrocarbons, by the biochemical destruction floral material.

—Microbiological methane with δ^{13}C from –105 to –90‰ first appears in the sediments at depths from 40 to 200 cm. These sediments virtually always show traces of methane oxidation in the form of a shift of the δ^{13}C of the methane toward higher values and the appearance of authigenic carbonate material, including ikaite, that is enriched in the light isotope. Ikaite (δ^{13}C from –25 to –60‰) was found and examined in several profiles.

—The redox conditions in the sediments vary from normal in the southern part of the sea to highly oxidized in the Novaya Zemlya Trough. The diagenetic oxidation of organic matter completely suppresses the biochemical activity of microorganisms in the respective sections of sediments.

—The comparison of the HI/OI and δ^{13}C parameters of organic carbon in sediments is an efficient tool for the identification of the predominant redox regime in the marine basin.

—Our data provide insight into the biogeochemistry of the Kara Sea and constrain the background values of geochemical parameters necessary for ecological monitoring in view of future exploration for hydrocarbons in the Kara Sea and their possible extraction.

ACKNOWLEDGMENTS

The authors thank the Vice President of the Russian Academy of Sciences Acad. N.P. Laverov for constant support of marine research conducted at the Vernadsky Institute of Geochemistry and Analytical Chemistry, Russian Academy of Sciences. We also thank our German colleagues Prof. J. Tide, D. Futerer, and R. Stein for organizing the fruitful cooperation of Russian and German researchers. We are grateful to M.P. Bogacheva, L.N. Vlasova, V.G. Tokarev, and E.V. Kul'bachevskaya, and V. S. Sevastyanov participants of the expeditions, for help with laboratory studies. This research was financially supported by the following grants: Grant NSh-1590.2006.5 "Support for the Leading Research Schools" no. 00-15-98482; the Russian Foundation for Basic Research, project no. 02-05-64343, 00-05-64574, 00-05-64575; State Program of the Ministry of Industry and Science of the Russian Federation; International Program for Cooperation in Marine Research, State Contract no. 43.700.12.0043; INCO: International Scientific Cooperation Project. Estuarine Specific Transport and Biogeochemically Linked Interactions for Selected Heavy Metals and Radionuclides (Project ICA-CT-2000-10008 "ESTABLISH") (2000–2006); Federal Research Program "World Ocean" of the Ministry of Industry and Science of the Russian Federation, Project no. 5 "Complex Study of Processes, Characteristics, and Resources of Russian Arctic Seas and the Arctic Ocean; Program no. 14 of the Presidium of the Russian Academy of Sciences "Fundamental Problems of Oceanology: Physics, Geology, Biology, and Ecology", 2004, Theme "Biogeochemical Cycles and the Pollution Problem of Russia's Seas and Selected Areas of the World Ocean"; Program 13 of the Presidium of the Russian Academy of Sciences (2004) Variability of the Environment and Climate: Natural Catastrophes", Branch 5; grant from the Vernadsky Nongovernmental Foundation "Ecological Problems of Russian Arctic and the Role of Geochemical Studies in Their Solution" (1998).

REFERENCES

1. E. M. Galimov, N. R. Laverov, O. V. Stepanets, and L. A. Kodina, "Preliminary Results of Ecological and Geochemical Investigations of the Russian Arctic Seas (Data obtained from Cruise 22 of the R/V Academik Boris Petrov)," Geokhimiya, No. 7, 579–597 (1996) [Geochem. Int. **34**, 521–538 (1996)].
2. *Siberian River Run-off in the Kara Sea. Characterization, Quantification, Variability and Environmental Significance. Proceedings in Marine Science,*" Ed. by R. Stein, K. Fahl, D. Fuetterer, E. M. Galimov, and O. V. Stepanets (Elsevier, Amsterdam, 2003), Vol. 6.
3. Rep. Polar Mar. Res. **266**, 266 (1988); **300**, 239 (1999); **360** 141 (2000); **393**, 287 (2001); **419**, 278 (2002); **450**, 109 (2003).
4. L. A. Kodina, M. P. Bogacheva, L. N. Vlasova, and E. M. Galimov, "Particulate Organic Matter from the Yenisei Estuary: Isotopic Composition, Distribution, and Genesis," Geokhimiya, No. 11, 1206–1217 (1999) [Geochem. Int. **37**, 1087–1096 (1999)].
5. L. A. Kodina, S. V. Lyutsarev, and M. P. Bogacheva, "Sources of the Sedimentary Material in Drift Ice of the Arctic Basin According to Isotope Data on Organic Carbon from an Ice-Related Suspension," Dokl. Earth Sci. **371**, 526–530 (2000) [Dokl. Akad. Nauk **371** (4), 511–515 (2000)].
6. M. P. Bogacheva, S. V. Lyutsarev, and L. A. Kodina, "Particulate Organic Carbon in River and Sea Waters: Concentration and Stable Isotope Ratio," Rep. Polar Mar. Res. **393**, 161–164 (2001).
7. L. A. Kodina, S. V. Lyutsarev, and M. P. Bogacheva, "Isotopic Composition of Organic Carbon of Ice Suspension as an Indicator of the Source of the Sedimentary Material of Drifting Arctic Ice: Evidence from Particulate Matter in the Drifting Ice of the Barents Sea," in *Experience of System Oceanological Studies in Arctic*, Ed. by A.P. Lisitsyn, M. E. Vonogradov, and E. A. Romankevich (Nauchnyi Mir, Moscow, 2001), 244-255 [in Russian].
8. G. S. Korobeinik, V. G. Tokarev, T. I. Vaisman, and L. A. Kodina, "Distribution of Hydrocarbon Gases in the Water Sequence along the Yenisei River–Kara Sea Profile," in *Experience of System Oceanological Studies in Arctic*, Ed. by A. P. Lisitsyn, M. E. Vinogradov, and E. A. Romankevich (Nauchnyi Mir, Moscow, 2001), [in Russian].
9. L. A. Kodina, "Carbon Isotope Composition of Phytoplankton on the Yenisei River-Estuary–Open Sea System and the Application of Isotopic Approach for Evaluation of Phytoplankton Contribution to the Yenisei POC Load," Rep. Polar Mar. Res. **419**, 143–149 (2002).
10. L. A. Kodina, V. G. Tokarev, L. N. Vlasova, et al., "New Findings of Ikaite in the Kara Sea During RV "Akademik Boris Petrov" Cruise 36, September 2001," Rep. Polar Mar. Res. **419**, 164–172 (2002).
11. L. A. Kodina and E. M. Galimov, "Authigenic Carbonate Mineral Ikaite Originated from Biogenic Methane in the Kara Sea Sediments," in *Proceedings of 12th Annual V. M. Goldschmidt Conference, Davos Switzerland, 2002* Geochim. Cosmochim. Acta, Spec. Suppl. A409 (2002).
12. L. A. Kodina and M. P. Bogacheva, "POC Isotope Composition in the Ob Estuary as Compared with the Yenisei System," Rep. Polar Mar. Res. **419**, 151–157 (2002).
13. G. S. Korobeinik, V. G. Tokarev, and T. I. Vaisman, "Geochemistry of Hydrocarbon Gases in the Kara Sea Sediments," Rep. Polar Mar. Res. **419**, 158–164 (2002).
14. L. A. Kodina, V. G. Tokarev, L. N. Vlasova, and G. S. Korobeinik, "Contribution of Biogenic Methane to Ikaite Formation in the Kara Sea: Evidence from the Stable Carbon Isotope Geochemistry," in *Siberian River Run-Off in the Kara Sea. Characterization, Quantification, Variability, and Environmental Significance. Proceedings in Marine Science*, Ed. by R. Stein K. Fahl, D. Fuetterer, E. M. Galimov, and O. V. Stepanets (Elsevier, Amsterdam, 2003), Vol. 6, 349–375.
15. S. V. Lyutsarev and S. S. Shanin, "Characteristic Features of Particulate Organic Carbon Distribution in the Water Column of the Black Sea," Okeanologiya **36** (4) (1996) [Oceanology **36**, 504–508 (1996)].

16. S. Opsahl and R. Benne, "Distribution and Cycling of Terrigenous Dissolved Organic Matter in the Ocean," Nature **386**, 480–482 (1977).
17. V. V. Gordeev, J. M. Martin, S. I. Sidorov, and M. V. Sidorova, "A Reassessment of the Eurasian River Input of Water, Sediment, Major Elements, and Nutrients to the Arctic Ocean," Am. J. Sci. **296**, 664–691 (1996).
18. H. Kohler, B. Meon, V. V. Gordeev et al., "Dissolved Organic Matter (DOM) in the Estuaries of Ob and Yenisei and Adjacent Kara Sea, Russia" in *Siberian River Run-off in the Kara Sea. Characterization, Quantification, Variability, and Environmental Significance. Proceedings in Marine Science*, Ed. by R. Stein, K. Fahl, D. Fuetterer, E. M. Galimov, and O. V. Stepanets (Elsevier, Amsterdam, 2003), Vol. 6, 281–308.
19. M. J. Kärcher, M. Kulakov, S. Pivovarov et al., "Atlantic Water Flow to the Kara Sea: Comparing Model Results with Observations," in *Siberian River Run-Off in the Kara Sea. Characterization, Quantification, Variability, and Environmental Significance. Proceedings in Marine Science*, Ed. by R. Stein, K. Fahl, D. Fuetterer, E. M. Galimov, and O. V. Stepanets (Elsevier, Amsterdam, 2003), Vol. 6, pp. 47–73.
20. B. Meon and R. M. W. Amon, "Heterotrophic Bacterial Activity and Fluxes of Dissolved Free Amino Acids and Glucose in the Arctic Rivers Ob, Yenisei and the Adjacent Kara Sea," Aquatic Microb. Ecol. **37**, 121–135 (2004).
21. I. H. Harms and M. J. Karcher, "Kara Sea Freshwater Dispersion and Export in the Late 1990s," J. Geophys. Res. **110**, C08007 (2005).
22. V. K. Pavlov and S. I. Pfirman, "Hydrographic Structure and Variability of the Kara Sea: Implications for Pollutant Distribution," Deep-Sea Res. II **42**, (6)1369–1390 (1995).
23. *Ecology and Bioresources of the Kara Sea*, Ed. by G. G. Matishov (AN SSSR, Apatity, 1989) [in Russian].
24. J. Gaillardet, B. Dupre, P. Louvat, and S. J. Allegre, "Global Silicate Weathering and CO_2 Consumption Rates Deduced from the Chemistry of Large Rivers," Chem. Geol. **159**, 3–30 (1999).
25. R. K. Dixon, S. Brown, R. A. Houghton, et al., "Carbon Pools and Flux of Global Forest Ecosystems," Science **263**, 185–190 (1994).
26. D. Unger and B. Gaye-Haake, K Neuman et al., "Biogeochemistry of Suspended and Sedimentary Material in the Ob and Yenisei Rivers and Kara Sea: Amino Acids and Amino Sugars," Cont. Shelf Res. **25**, 437–470 (2005).
27. A. P. Lisitsyn, V. P. Shevchenko, M. E. Vinogradov, et al., "Flux of Sedimentary Material in the Kara Sea and in the Ob and Yenisei Estuaries," Okeanologiya **34**, (5) 748–758 (1994).
28. E. A. Romankevich and A. A. Vetrov, *Carbon Cycle in Arctic Seas* (Nauka, Moscow, 2001) [in Russian].
29. V. I. Vedernikov, A. B. Demidov, and A. I. Sud'bin, "Primary Production and Chlorophyll in the Kara Sea in September, 1993," Okeanologiya **34**, (5) 693–703 (1994).
30. R. A. Hörner, "Ecology of Sea Ice Microalga," in *Sea Ice Biota* Ed. by R. A. Hörner (CRC Press, Boca Raton, Florida, 1985), pp. 84–103.
31. M. Gösselin, M. Lewasseur, P. A. Wheeler, et al., "New Measurements of Phytoplankton and Algal Production in the Arctic Ocean," in *Deep Sea Res. Part II: Topical Studies in Oceanography*, **44**, (8) 1633–1625 (1997).
32. P. A. Wheeler, M. Gösselin, E. Sherr, et al., "Active Cycling of Organic Carbon in the Central Arctic Ocean," Nature **380**, 697–699 (1996).
33. D. Hebbeln and H. Berner, "Surface Sediment Distribution in the Fram Strait," Deep-Sea Res. I **40** (9), 1731–1745 (1993).
34. R. Goerike and B. Ery, "Variations of Marine Plankton $\delta^{13}C$ with Latitude, Temperature, and Dissolved CO_2 in the World Ocean," Glob. Biogeochem. Cycles **8** (1), 85–90 (1994).
35. W. O. Smith, I. D. Walsh, D. C. Booth, and J.W. Deming, "Particulate Matter and Phytoplankton and Bacterial Biomass Distributions in the Northeast Water Polynya During Summer 1992," J. Geophys. Res. **100** (C3), 4341–4356 (1995).
36. C. J. Schubert and R. Stein, "Lipid Distribution in Surface Sediments from the Eastern Central Arctic Ocean," Mar. Geol. **138** (1–2), 11–25 (1997).
37. H. Notholt, "Die Auswirkungen der 'NorthEastWater'—Polynya auf die Sedimentation vor NO Gronland und Untersuchungen zur Paleo-Ozeanographie seit dem Mittelwechsel," Ber. Polarforsch. **275**, 120 (1998).
38. V. V. Larionov and P. R. Makarevich, "The Taxonomic and Ecological Descriptions of the Phytoplankton Assemblages from the Yenisei Bay and Adjacent Waters of the Kara Sea in September 2000," Rep. Polar Mar. Res. **393**, 48–62 (2001).
39. V. V. Larionov and L. A. Kodina, "Phytoplankton of the Ob–Yenisei Transects," Rep. Polar Mar. Res. **393**, 48–62 (2000).
40. V. V. Larionov, "Phytoplankton of the Ob–Yenisei Shallows in the Autumn," Rep. Polar Mar. Res. **450**, 20–21 (2003).
41. V. V. Larionov, "Phytoplankton Distribution in the Ob and Yenisei Estuaries and Adjacent Kara Sea," Rep. Polar Mar. Res **419**, 41–43 (2002).
42. E.–M. Nöthig, Y. Okolodkov, V. V. larionov, and P. R. Makarevich, " Phytoplankton distribution in the Inner Kara Sea: A Comparizon of Three Summer Investigations, " in *Siberian River Run-off in the Kara sea. Characterization, Quantification, Variability, and Environmental Significance.Proceedings in Marine Science*, Ed by R. Stein, K. Fahl, D. Fuetterer, E. M. Galimov, and O. V. Stepanets (Elsevier, Amsterdam, 2003), Vol. 6, pp. 173–183.
43. P. R. Makarevich, N. V. Druzhkov, V, V, Larionov, and E. I. Druzhnikova, "The Freshwater Phytoplankton Biomass and Its Role in the Formation of a Highly Productive Zone of the Ob–Yenisei Shallows (Southern Kara Sea)," in *Siberian River Run-Off in the Kara Sea. Characterization, Quantification, Variability, and Environmental Significance. Proceedings in Marine Science*, Ed. by R. Stein, K. Fahl, D. Fuetterer, E. M. Galimov, and O. V. Stepanets (Elsevier, Amsterdam, 2003), Vol. 6, pp. 181–185.
44. P. D. Tortell, J. R. Reinfelder, and F. M. M. Morel, "Active Uptake of Bicarbonate by Diatoms," Nature **390**, 243–244 (1997).

45. B. Fry and S. C. Wainright, "Diatom Sources of ^{13}C-Rich Carbon in Marine Food Webs," Mar. Ecol. Progress Ser. **76**, 149–157 (1991).

46. E. M. Galimov, *Biological Isotope Fractionation* (Academic Press, New York–Toronto–Orlando, 1984).

47. M. A. *Goňi*, M. B. Yunker, R. W. MacDonald, and T. I. Eglinton, "The Supply and Preservation of Ancient and Modern Components of Organic Carbon in the Canadian Beaufort Shelf of the Arctic Ocean," Mar. Chem., No. 93, 53–73 (2005).

48. S. Pivovarov, R. Schlitzer, and A. Novikhin, "Modern Discharge: Data and Modeling," in *Siberian River Run-off in the Kara Sea. Characterization, Quantification, Variability, and Environmental Significance. Proceedings in Marine Science*, Ed. by R. Stein, K. Fahl, D. Fuetterer, E. M. Galimov, and O. V. Stepanets (Elsevier, Amsterdam, 2003), Vol. 6, pp. 9–27.

49. R. M. Holmes, B. J. Peterson, A. V. Zhulidov, et al., "Nutrient Chemistry of the Ob and Yenisei Rivers, Siberia: Results from June 2000 Expedition and Evaluation of Long-Term Data Set," Mar. Chem. **75**, 219–227 (2001).

50. K. Fahl, R. Stein, B. Gaye-Haake et al., "Biomarkers in Surface Sediments from the Ob and Yenisei Estuaries and the Southern Kara Sea: Evidence for Particulate Organic Carbon Sources, Pathways, and degradation," in *Siberian River Run-off in the Kara Sea. Characterization, Quantification, Variability, and Environmental Significance. Proceedings in Marine Science*, Ed. by R. Stein, K. Fahl, D. Fuetterer, E. M. Galimov, and O. V. Stepanets (Elsevier, Amsterdam, 2003), Vol. 6, pp. 329–349.

51. H. Köhler, B. Meon, V. V. Gordeev et al., "Dissolved Organic Matter (DOM) in the Estuaries of Ob and Yenisei and Adjacent Kara Sea, Russia," in *Siberian River Run-off in the Kara Sea. Characterization, Quantification, Variability, and Environmental Significance. Proceedings in Marine Science*, Ed. by R. Stein, K. Fahl, D. Fuetterer, E. M. Galimov, and O. V. Stepanets (Elsevier, Amsterdam, 2003), Vol. 6, pp. 281–308.

52. R. Benner, B. Biddanda, B. Black, and M. McCarthy, "Abundance, Size Distribution, and Stable Carbon and Nitrogen Isotopic Composition of Marine Organic Mater Isolated by Tangential Ultrafiltration," Mar. Chem. **57**, 343–363 (1997).

53. V. Stanovoy and N. Schmelkov, "Water Temperature Fluctuations in the Marginal Zones in the Svjataja Anna and Voronin Troughs," Rep. Polar Mar. Res. **419**, 22–28 (2002).

54. L. A. Kodina and V. I. Peresypkin, "Stable Carbon Isotope ($\delta^{13}C_{org}$) Ratio and Lignin-Derived Phenol Distribution in Surface Sediments of the Inner Kara Sea," in *Scientific Cruise Report of the Kara-Sea Expedition 2001 of R/V Akademik Boris Petrov,* Ed. by R. Stein, and O. V. Stepanets, Ber. Polarforsch. Meeresforsch. **419**, 134–141 (2002).

55. E. M. Galimov, "Carbon Isotope Composition of Antarctic Plants," Geochim. Cosmochim. Acta, No. 64, 1737–1739 (2000).

56. E. M. Galimov, "Fractionation of Carbon Isotope in the Way from Living to Fossil Organic Matter," in *Stable Isotope in Biosphere,* Ed. by E. Wada et al. (Kyoto Univ., Kyoto, 1995), 133–170.

57. A. M. Bol'shakov and A. V. Egorov, "Results of Gasometry in the Kara Sea," Okeanologiya **35** (3), 399–404 (1995).

58. A. N. Belyaeva and G. Eglinton, "Lipid Biomarker Accumulation in the Kara Sea Sediments," Okeanologiya **37** (5), 705–714 (1997) [Oceanology **37**, 634–642 (1997)].

59. E. M. Galimov, "Sources and Mechanisms of Formation of Gaseous Hydrocarbons in Sedimentary Rocks," Chem. Geol. **71**, 77–95 (1988).

60. B. B. Namsaraev, I. I. Rusanov, A. S. Savichev, et al., "Bacterial Oxidation of Methane in the Estuary of the Yenisei River and Kara Sea," Okeanologiya **35** (1), 88–93 (1995).

61. E. M. Galimov, "The Pattern $\delta^{13}C_{org}$ Versus HI/OI Relation in Recent Sediments as an Indicator of Geochemical Regime in Marine Basing: Comparison of the Black Sea, Kara Sea and Cariaco Trench," Chem. Geol. **204**, 287–301 (2004).

62. E. M. Galimov, L. A. Kodina, L. I. Zhiltsova, et al., "Organic Carbon Geochemistry in the North Western Black Sea Danube River System," Estuar. Coast. Shelf Sci., No. 54, 631–641 (2002).

63. R. V. Krishnamurthy, M. Machavaram, M. Baskaran, et al., "Organic Carbon Flow in the Ob, Yenisey and Kara Sea of the Arctic Region," Mar. Poll. Bull. **42** (9), 726–732 (2001).

View publication stats